SANDIA REPORT

SAND92–2537 • UC–705
Unlimited Release
Printed January 1993

Stability Analysis and Modeling of Rotating Flexible Structures

Clark R. Dohrmann

Prepared by
Sandia National Laboratories
Albuquerque, New Mexico 87185 and Livermore, California 94550
for the United States Department of Energy
under Contract DE-AC04-76DP00789

Issued by Sandia National Laboratories, operated for the United States Department of Energy by Sandia Corporation.

Available to DOE and DOE contractors from
Office of Scientific and Technical Information
PO Box 62
Oak Ridge, TN 37831

Prices available from (615) 576-8401, FTS 626-8401

Available to the public from
National Technical Information Service
US Department of Commerce
5285 Port Royal Rd
Springfield, VA 22161

NTIS price codes
Printed copy: A05
Microfiche copy: A01

SAND92-2537
Unlimited Release
Printed January 1993

Distribution
Category UC-705

Stability Analysis and Modeling of Rotating Flexible Structures

Clark R. Dohrmann
Structural Dynamics Department
Sandia National Laboratories
Albuquerque, New Mexico 87185

Abstract

A method is presented for determining the nonlinear stability of undamped flexible structures spinning about a principal axis of inertia. Equations of motion are developed for structures that are free of applied forces and moments. The development makes use of a floating reference frame which follows the overall rigid body motion. Within this frame, elastic deformations are assumed to be given functions of n generalized coordinates. A transformation of variables is devised which shows the equivalence of the equations of motion to a Hamiltonian system with $n + 1$ degrees of freedom. Using this equivalence, stability criteria are developed based upon the normal form of the Hamiltonian. It is shown that a motion which is spin stable in the linear approximation may be unstable when nonlinear terms are included. A stability analysis of a simple flexible structure is provided to demonstrate the application of the stability criteria. Results from numerical integration of the equations of motion are shown to be consistent with the predictions of the stability analysis.

A new method for modeling the dynamics of rotating flexible structures is developed and investigated. The method is similar to conventional assumed displacement (modal) approaches with the addition that quadratic terms are retained in the kinematics of deformation. Retention of these terms is shown to account for the geometric stiffening effects which occur in rotating structures. Computational techniques are developed for the practical implementation of the method. The techniques make use of finite element analysis results, and thus are applicable to a wide variety of structures. Motion studies of specific problems are provided to demonstrate the validity of the method. Excellent agreement is found both with simulations presented in the literature for different approaches and with results from a commercial finite element analysis code. The computational advantages of the method are demonstrated.

Contents

Figures

1. Introduction

The analysis of rotating flexible structures is an active area of research having applications in a variety of engineering disciplines. A thorough and accurate dynamic analysis is often critical to the success of structural designs that involve rotating members. Examples of fields requiring such analysis include robotics, rotating machinery, flexible space structures, helicopter blades, and wind turbines.

The design of a vertical axis wind turbine is one example which highlights the importance of dynamic analysis in the design of rotating structures. During its operation, the turbine is subjected to wind loads with frequency content primarily at integer multiples of the rotation rate. Successful design of the wind turbine depends heavily on the ability to accurately predict the natural frequencies of the structure so to avoid any resonances. Failure to do so can result in designs having unacceptably short lifetimes.

Analysis of the motion of rotating flexible structures presents many challenges. Much care must be taken in forming the equations of motion to correctly account for the coupling between the flexible and overall rigid body motions. In contrast to the motion of fixed structures, small strains can be accompanied by large displacements and rotations. The equations of motion are inherently nonlinear, even when the effects of flexibility are absent.

1.1 Focus of Report

The focus of this report is on the stability analysis and modeling of rotating flexible structures. Two fundamental areas are entailed in the study. The first one deals with determining the stability of motion based upon the equations of motion. Of particular interest is the stability of unrestrained bodies rotating about an axis of principal moment of inertia. The second area involves the development of mathematical models for rotating structures. It is upon these models and basic physical laws that the equations of motion are based.

1.1.1 Stability Analysis

A great deal of information is available in the technical literature on the stability analysis of rotating flexible structures. A classical result for rigid bodies states that a motion of simple spin is stable about either the axis of minimum or maximum moment of inertia in the absence of external moments. Stability criteria obtained to date for flexible structures require spin to occur about the axis of *maximum* moment of inertia. Such criteria generally hold either in the presence or absence of internal energy dissipation. The

principal contribution of the present work is the development of a method to assess the stability of spin about the axis of *minimum* moment of inertia for undamped structures.

1.1.2 Modeling

The modeling of rotating flexible structures is another area which is represented well in the literature. Recent approaches for modeling often involve use of the finite element method in one form or another. Commercially available finite element analysis codes are capable of simulating the motion of rotating structures, but the computational requirements can be excessive even for simple problems. In addition, simulation provides only a part of the picture as far as stability is concerned. The contribution of the present work in this area is towards the practical application and verification of a recently proposed modeling technique based on finite elements. This modeling technique can be used along with the method developed for stability analysis to assess the attitude stability of a rotating flexible structure.

1.2 Literature Review

A review is made of the relevant literature in this section. The first part is concerned primarily with the topic of stability analysis, but involves certain aspects of modeling as well. In many instances, a combined discussion of stability and modeling is justified by the strong link between the two. The second part of the review deals exclusively with modeling techniques. In the light of the scope of the present work, attention is restricted to single-body, flexible structures. Papers dealing with multi-body configurations and dual-spin satellites are not discussed.

1.2.1 Stability Analysis

Much of the interest in the unrestrained motion of rotating flexible structures has its origins with America's first satellite, Explorer I. The configuration of Explorer I consisted of a long cylindrical core body with radially attached flexible antennas [1]. The satellite was initially put into a spinning motion about its longitudinal axis of symmetry (minimum moment of inertia). After only one complete orbit, radio signals indicated that the satellite was in a tumbling motion.

The explanation for the unexpected motion of Explorer I is attributed to Bracewell and Garriott [2]. For fixed angular momentum, one can show that the kinetic energy of a rigid body is maximized for spin about the axis of minimum moment of inertia. In contrast, spin about the axis of maximum moment of inertia corresponds to the minimum energy state. It was concluded that the nominal spinning motion of Explorer I about its axis of minimum moment of inertia could not be maintained because of hysteretic energy losses caused by motion of the flexible antennas.

Thomson and Reiter [3] quantitatively examined the effects of energy dissipation on the attitude of a spinning body. Expressions were obtained for the time rate of change of a body's precession cone angle in terms of a hysteretic damping factor and other parameters for two simple models. Flexible deformations were expressed in one of the models using a modal expansion technique, a practice used subsequently by many other authors.

A solid mathematical basis for the stability analysis of rotating bodies was provided by the work of Pringle [4]. Using the direct method of Liapunov, basic theorems were established on the stability of damped mechanical systems with connected moving parts. Among these was the so-called maximum axis rule which states that for a completely damped system[1] a motion of simple spin can only be stable about the axis of maximum moment of inertia. The stability of an unconstrained, nongyroscopic system with damping was shown to depend on the positive definiteness of a potential function.

A linear stability analysis of a spin-stabilized satellite with flexible antennas along its axis of rotation was performed by Meirovitch and Nelson [5]. Both spring-mass and continuous beam models of the antennas were used in the analysis and yielded similar results. In addition to the requirement of spin about the axis of maximum moment of inertia, other relations involving the spin velocity and dynamic properties of the antennas were needed to establish stability. A similar analysis of a slightly more general model with antennas transverse to the axis of rotation was given by Dokuchaev [6].

Nonlinear stability analyses of torque-free motions invariably made use of the conservation of angular momentum. Conserved momentum quantities along with the total system energy allowed authors to construct Liapunov functions for stability considerations. A common result of such analyses was the maximum axis rule. Other conditions specific to the given problem were also required to establish sufficient conditions for stability.

Hughes and Fung [7] studied the stability of a satellite consisting of a central rigid body with flexible, radial beams. Implicit in their analysis was the assumption that the central body mass center remains fixed in an inertial frame. Centrifugal stiffening was accounted for by including second-order terms associated with the foreshortening effect in the radial beams [8]. Deformations of the radial beams were described in terms of a modal expansion. Remarkably, the authors obtained sufficient conditions for stability which did not depend on truncation of the modal expansion.

Nelson and Meirovitch [9, 10] applied Liapunov's direct method to the analysis of gravity-gradient stabilized satellites for both discrete mass and continuous system models. In the second of these two works, bounding properties of Rayleigh's quotient were exploited to establish stability criteria. Interestingly, the method did not require

[1] A completely damped system dissipates energy for all motions except "rigid body" spin about a principal axis.

the solution of the complete eigenproblem associated with elastic motions, but only the first eigenvalue. The work in [9] was extended by Meirovitch [11] to incorporate angular momentum integrals and was applied to the torque-free spinning motion of a satellite modeled as a rigid body with two flexible attachments.

Meirovitch [12] later introduced the notion of integral coordinates to accomodate situations where density functions could not be readily defined. The method of integral coordinates was applied to the problem of a torque-free satellite modeled as a rigid central body with up to three pairs of flexible rods. The stability criteria compared favorably with ones from another analysis based on a modal approach with series truncation. A comparative study of stability analysis methods based upon density functions, integral coordinates, and modal analysis was given in [13].

Teixeira-Filho and Kane [14] developed a method to construct stability criteria for spinning, torque-free, elastic, dissipative systems. Unique to their analysis was the use of a floating reference frame always aligned with the principal axes of the body. As a consequence, stability criteria decoupled directly into external (maximum axis rule) and internal stability conditions. The method was applied to a rigid satellite carrying four elastically mounted antennas in [15]. Levinson and Kane [16] later used this method along with a finite element approach to analyze the attitude stability of a spinning satellite equipped with four elastic booms.

Numerous other works on stability similar to the ones just described were provided by a host of authors [17, 18, 19, 20, 21, 22, 23, 24]. In most instances, stability criteria were based upon the direct method of Liapunov and involved the maximum axis rule.

More recently, Holm et al. [25] applied the so-called Energy-Casimir Method to study the stability of spinning motions of a torque-free rigid body and a Lagrange top. The method involves inferring stability from the sign-definiteness of a function composed of the total system energy and a Casimir(s). The stability conditions obtained were consistent with classical results. For discrete problems having a finite number of degrees of freedom, this method does not appear to offer any advantages over earlier approaches based on Liapunov's direct method.

Krishnaprasad and Marsden [26] applied the Energy-Casimir Method in an infinite-dimensional setting to the stability analysis of an undamped, unrestrained rigid body with an attached shear beam. In this case, the Casimir was simply a function of the angular momentum magnitude, a conserved quantity. Sufficient conditions for stability involved inequalities similar to the maximum axis rule as well as an upper bound on the spin velocity. A related analysis for a disk-beam system rotating about a fixed axis was given by Baillieul and Levi [27].

Simo et al. [28] developed a nonlinear stability analysis technique called the Energy-Momentum Method and applied it to coupled rigid body and elastic rods. The method is a generalization of the classical energy method of Lagrange and makes use of both the

energy and other conserved quantities such as the components of angular momentum. In this particular sense, the method is quite similar to others described earlier. The major difference with the method is its applicability to infinite-dimensional systems. Use of a block diagonalization technique leads to a division of rigid body and internal vibration stability criteria analogous to that found in [14]. A simpler application of the Energy-Momentum Method to the planar motions of a rotating beam was given by Bloch [29].

Liu [30] made a stability analysis of a rotating system consisting of two rigid bodies connected together by a frictionless spherical joint. Both bodies were assumed to be axisymmetric and the spherical joint connecting the two was located at the intersection of their axes of symmetry. Two cyclic integrals were shown to exist in addition to the integrals of angular momentum and energy. Using the four constants of motion, a Liapunov function was constructed which inferred stability for spin about either the axis of maximum or minimum moment of inertia of the combined bodies. As an aside, it is noted that the system examined was not flexible in the sense that relative motion of the two rigid bodies causes changes in strain energy. That is, the spherical joint provided no restoring torque.

1.2.2 Modeling

Since the period of the late 1960's, a large number of publications appeared on the modeling and analysis of rotating space structures. A key element common to many of the analyses was the use of a floating reference frame which follows the overall "rigid body" motion (see, e.g., [31, 32, 33, 34, 35]). Expression of elastic deformations with respect to such a frame often obviated the need for large displacement elasticity theory. It is noted, however, that although strains within a rotating structure may remain small, some form of nonlinear analysis is required to capture the effects of geometric (centrifugal) stiffening [8].

Laskin et al. [36] studied the unrestrained motion of a free-free beam subject to large overall motions. A description of the beam kinematics was given in terms of the motion of a floating reference frame along with a modal expansion for elastic deformations. Kane's equations [37] were used to derive the governing dynamical equations. Centrifugal stiffening effects were accounted for by generalized active forces derived from the nonlinear theory of elasticity.

In recent years, a renewed interest has emerged in the modeling of rotating flexible structures. An often cited reference dealing with this subject is by Kane et al. [38]. Here, the authors developed a comprehensive theory for small vibrations of a general beam attached to a base undergoing arbitrary, prescribed motion. Perhaps more important was the attention they drew to certain deficiencies of existing multibody computer programs.

To illustrate these deficiencies, simulations for a spin-up maneuver of a cantilever beam attached to a rotating base were carried out using both the new approach and the

conventional approach upon which the multibody codes were based. Results from the conventional approach indicated that the beam tip displacement grows without bound. In contrast, results based on the new approach predicted the expected bounded motion of the beam.

The cause for the unrealistic predictions of the multibody codes was attributed ultimately to the omission of centrifugal stiffening. Such an omission is somewhat surprising, considering the wealth of knowledge on the subject at the time. Evidently, though, the belief was commonly held in the aerospace industry that these multibody codes could be used to correctly simulate the motion of systems containing flexible bodies [39].

Lee and Christensen [40] developed a finite element method applicable to the motion of unrestrained flexible structures undergoing large elastic deformations. Equations of motion were derived from momentum principles and the principle of virtual work. A three-noded, eighteen degree of freedom beam element was developed and applied to motion studies of a simple spacecraft.

Simo and Vu-Quoc [41] used finite strain rod theories in a treatment of the planar motion of beams undergoing large overall motions. A distinguishing feature of their approach was the use of an inertial frame as opposed to a floating frame for the description of beam motion. As a consequence, the inertia operator was linear and uncoupled, while the stiffness operator was nonlinear. The method was applied to several example problems in [42] and later extended to the three dimensional case in [43].

Simo and Vu-Quoc stressed the advantages of their approach over ones which employ a floating reference frame. Key to one of their arguments was the assertion that introduction of a floating frame leads to a system of differential equations involving a nonlinear algebraic constraint. Examples are presented in Chapter 4 which show that this assertion is certainly not true for all such formulations.

The analysis of plate-like structures has also received due consideration in the literature. As with beams, care must be taken to account for geometric nonlinearities such as centrifugal stiffening. Examples of formulations specific to rotating plates include the work in [44, 45, 46, 47].

Application of a commercial finite element analysis code to the dynamic analysis of rotating beams was reported by Peterson [48]. Simulations were carried out for three different problems which were modeled using ten geometrically nonlinear beam elements. Results of the simulations indicated that the finite element analysis code accounted for various geometric nonlinearities.

In theory, one should be able to use any one of several existing finite element analysis codes to simulate the motion of rotating flexible structures. Although this may be true in some instances, the computational requirements often become excessive even for relatively simple problems. A specific example which illustrates this observation is provided in

Chapter 4.

Zeiler and Buttrill [49] presented a method of analysis providing a compromise between fully nonlinear theories and others that assume rotation about a fixed axis. The method involved a floating reference frame and the calculation of geometric stiffness matrices for six sets of centrifugal loads. The effects of centrifugal stiffening were accounted for approximately by including the geometric stiffness matrices in the analysis. Computational requirements of the method were reduced by expressing elastic deformations as a modal expansion of a structure's free-free modes.

A method quite similar to that in [49] was given by Banerjee and Dickens [50]. Simulations of spinning motions for a cantilevered beam and a cantilevered plate were performed. Results of the simulations were shown to be in good agreement with the predictions of special-purpose theories developed earlier.

The methods presented in the two previously cited works made a significant contribution to the state of the art for motion simulation of rotating flexible structures. Both of the methods have the advantage of being applicable to general structures. Another important advantage is that of computational efficiency. By employing a floating reference frame and modal expansions for elastic deformations, the computational requirements for motion simulations are reduced significantly.

A recently proposed method possessing all of the advantages just mentioned was given by Segalman and Dohrmann [51]. Their approach makes use of a floating reference frame and a reduced set of degrees of freedom, but does not explicity involve the calculation of geometric stiffness matrices. Furthermore, all of the terms necessary to form the equations of motion can be obtained from any finite element analysis code capable of nonlinear static and linear dynamic analysis. The development and implementation of this method is the subject of Chapter 4.

1.3 Summary of Contents

Equations of motion are derived in Chapter 2 for undamped rotating flexible structures that are free of applied forces and moments. The formulation is based upon the use of a floating reference frame which follows the overall rigid body motion. An assumed displacement approach is adopted whereby elastic deformations of the structure are expressed as functions of n generalized degrees of freedom. An important result is the development of a nonlinear transformation of variables which puts the equations of motion into a canonical form. In particular, it is shown that the equations of motion are equivalent to a Hamiltonian system with $n + 1$ degrees of freedom. This result serves as the basis for the development of Chapter 3.

A method is presented in Chapter 3 for determining the nonlinear stability of flexible structures spinning about a principal axis of inertia. The method has its foundation on

the equivalence of the equations of motion to a Hamiltonian system. Transformation of the equivalent system Hamiltonian to its so-called normal form permits application of the work of previous authors to the question of stability. A closed-form stability analysis of an example problem is provided to illustrate the method. Results of the analysis are confirmed by numerical integration of the equations of motion.

The development and implementation of a recently proposed method for modeling rotating flexible structures is the subject of Chapter 4. The method utilizes a floating reference frame in accordance with the development of Chapter 2. Within this reference frame, deformations are expressed in terms of a quadratically-coupled set of deformation modes. The method is applicable to general structures and its implementation is facilitated through the use of a nonlinear finite element analysis code. The application of the new method of modeling is illustrated by several examples. Comparison of results are made for problems found in the literature for the purpose of verification. The computational advantages of the method over a commercially available finite element analysis code are demonstrated for a specific example.

The principal results and conclusions of the report are presented in Chapter 5. Also included is a discussion of the significant contributions of the present work to the areas of the stability analysis and modeling of rotating flexible structures.

2. Equations of Motion

The subject of this chapter is the development of governing equations of motion for rotating flexible structures. Key to the development is the use of a reference frame which follows the overall rigid body motion of the structure. Within this frame, elastic deformations are assumed to be functions of n generalized degrees of freedom. It is shown using a nonlinear transformation of variables that the governing equations are equivalent to a Hamiltonian system of equations with $n+1$ degrees of freedom. This result serves as the basis for the method of stability analysis presented in Chapter 3.

Equations of motion are derived in the first section from fundamental principles of dynamics. Equivalent sets of equations better suited for numerical integration and stability analysis are also formulated. The second section is concerned with the development of a transformation of variables which puts the equations of motion into a canonical form. The chapter concludes with a simple application of this transformation.

2.1 Derivation of Equations

2.1.1 Introduction

A system of interconnected particles each of mass m^i $(i = 1, \ldots, N_p)$ is depicted in Figure 2.1. Also shown in the figure are a floating reference frame, B, and an inertial frame, N. Orthogonal, dextral sets of unit vectors $\mathbf{b}_1, \mathbf{b}_2, \mathbf{b}_3$ and $\mathbf{n}_1, \mathbf{n}_2, \mathbf{n}_3$ are fixed in B and N, respectively.

The origin, O, of B is chosen to coincide with either the mass center or a fixed point of the system. The orientation of B in N depends upon the particular choice for the floating frame. Regardless of this choice, the intention is for B to follow the nominal rigid body motion of the system. The central principal axes of the system are assumed to be parallel to $\mathbf{b}_1, \mathbf{b}_2, \mathbf{b}_3$ for motions of simple spin about a principal axis.

The angular velocity vector of B in N is expressed in terms of the unit vectors fixed in B as

$$\boldsymbol{\omega} = \omega_1 \mathbf{b}_1 + \omega_2 \mathbf{b}_2 + \omega_3 \mathbf{b}_3 \tag{2.1}$$

The position vector from O to the i'th particle when the system is undeformed is denoted by $\mathbf{r}^i$ (see Fig. 2.1). Similarly, the displacement vector of the i'th particle from its undeformed position is denoted by $\mathbf{u}^i$. Expressions for $\mathbf{r}^i$ and $\mathbf{u}^i$ are given by

$$\mathbf{r}^i = r_1^i \mathbf{b}_1 + r_2^i \mathbf{b}_2 + r_3^i \mathbf{b}_3 \tag{2.2}$$

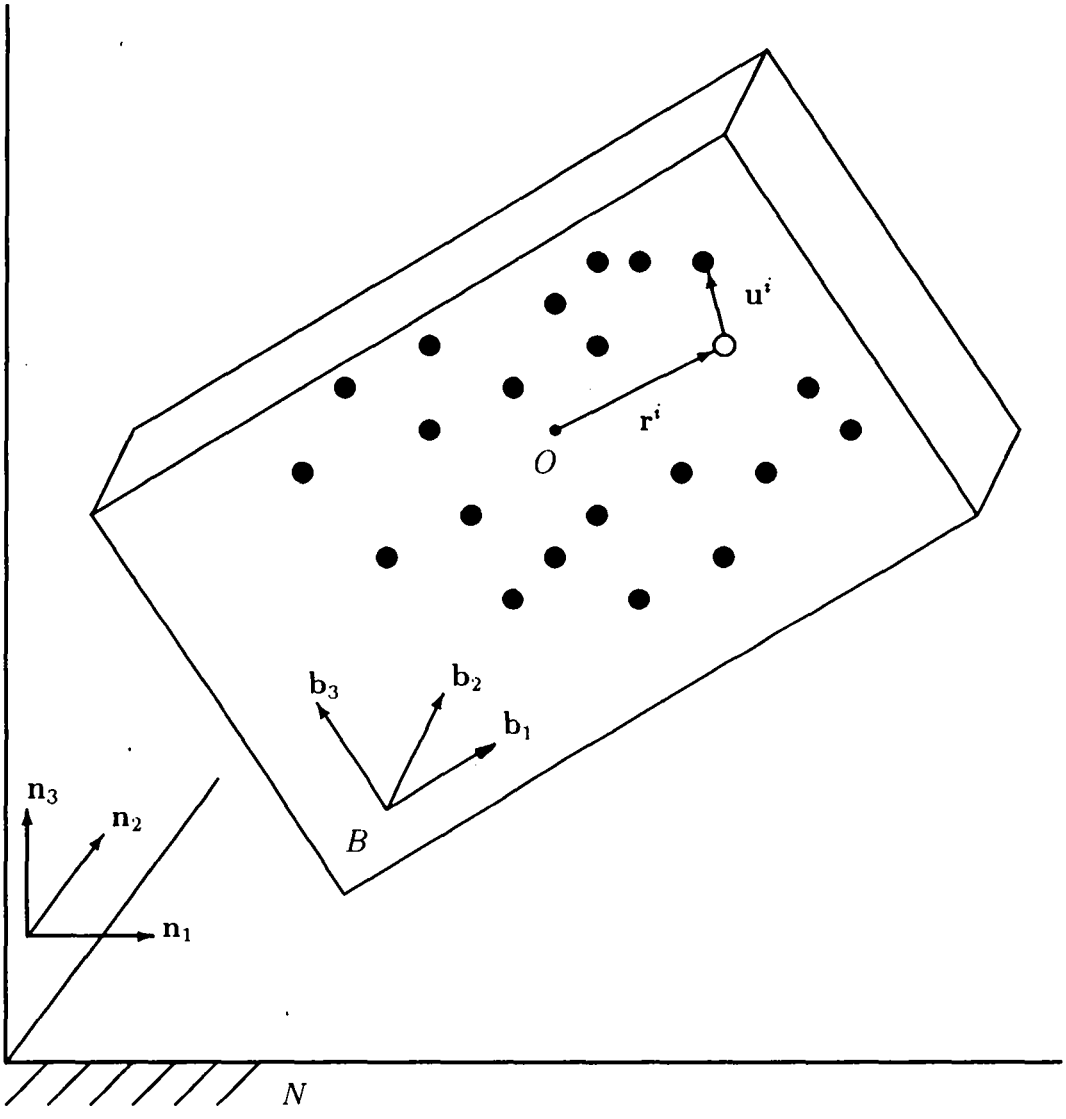

Figure 2.1. Sketch of the system of particles and reference frames.

and

$$\mathbf{u}^i = u_1^i \mathbf{b}_1 + u_2^i \mathbf{b}_2 + u_3^i \mathbf{b}_3 \tag{2.3}$$

The scalars r_1^i, r_2^i, r_3^i in Eq. (2.2) are all constant, whereas u_1^i, u_2^i, u_3^i in Eq. (2.3) are functions of dimensionless generalized degrees of freedom $q_1, \ldots, q_n$.

Two notational conventions from [37] are adopted here. The first is the practice of denoting the time derivative of the vector $\mathbf{p}$ in the reference frame A by $\frac{^A d}{dt}\mathbf{p}$. The second is the placement of numbers along with the equality sign in an equation. For example, the appearance of $(1,2)$ in the equation $y \overset{(1,2)}{=} mx + b$ indicates that the result is obtained with reference to Eqs. (1) and (2).

Einstein's summation convention is employed as a notational convenience. With this convention, the repeated appearance of an index implies summation over all possible values of the index. For example, Eq. (2.3) is written more compactly as $\mathbf{u}^i = u_k^i \mathbf{b}_k$.

2.1.2 Derivation

The basic approach of this section is to apply fundamental principles of classical mechanics to derive the governing equations of motion. Equations associated with the motion of the floating reference frame are obtained from conservation of linear momentum and the angular momentum principle. The remaining equations of motion are given by Lagrange's equations.

It is assumed that there are no energy losses in the system caused by internal damping. The assumption is also made that the system is free of any external forces and moments, unless O is a fixed point. In this case, reaction forces acting at O are permitted.

The velocity of O can always be set equal to zero regardless of whether or not O is a fixed point. If O is not fixed, then it is the center of mass of a system free of external forces. Conservation of linear momentum implies that the velocity of O is constant. No loss of generality results by setting the constant velocity equal to zero.

Let $\mathbf{v}^i$ denote the velocity of the i'th particle in N. Using a basic kinematical relationship one obtains

$$\begin{aligned} \mathbf{v}^i &= \frac{^B d}{dt}(\mathbf{r}^i + \mathbf{u}^i) + \boldsymbol{\omega} \times (\mathbf{r}^i + \mathbf{u}^i) \\ &\overset{(2.2-2.3)}{=} \left[\frac{\partial u_k^i}{\partial q_j}\dot{q}_j + \epsilon_{klm}\omega_l(r_m^i + u_m^i)\right]\mathbf{b}_k \qquad (2.4) \\ &= v_k^i \mathbf{b}_k \qquad (2.5) \end{aligned}$$

where $(\dot{})$ denotes time differentiation and ϵ_{klm} is the permutation symbol defined as

$$\epsilon_{klm} = \begin{cases} 1 & \text{for even permutations of } (k,l,m) \\ -1 & \text{for odd permutations of } (k,l,m) \\ 0 & \text{otherwise} \end{cases} \tag{2.6}$$

The angular momentum vector, $\mathbf{H}$, of the system about O is defined as

$$\mathbf{H} = \sum_{i=1}^{N_p} m^i(\mathbf{r}^i + \mathbf{u}^i) \times \mathbf{v}^i \tag{2.7}$$

$$= h_1\mathbf{b}_1 + h_2\mathbf{b}_2 + h_3\mathbf{b}_3 \tag{2.8}$$

Application of the angular momentum principle yields

$$\frac{{}^B d}{dt}\mathbf{H} + \boldsymbol{\omega} \times \mathbf{H} = \mathbf{0} \tag{2.9}$$

or, equivalently,

$$\frac{d}{dt}h_1 = \omega_3 h_2 - \omega_2 h_3 \tag{2.10}$$

$$\frac{d}{dt}h_2 = \omega_1 h_3 - \omega_3 h_1 \tag{2.11}$$

$$\frac{d}{dt}h_3 = \omega_2 h_1 - \omega_1 h_2 \tag{2.12}$$

It follows from Eqs. (2.10-2.12) that the magnitude of the angular momentum vector, defined as

$$h = \sqrt{h_1^2 + h_2^2 + h_3^2}, \tag{2.13}$$

is constant. Equation (2.13) is used later to reduce the number of equations of motion by one.

It is useful to obtain expressions for the momenta variables h_1, h_2, h_3 in terms of the system kinetic energy, T, defined as

$$T = \frac{1}{2}\sum_{i=1}^{N_p} m^i \mathbf{v}^i \cdot \mathbf{v}^i$$

$$\overset{(2.4)}{=} \frac{1}{2}\sum_{i=1}^{N_p} m^i \left[\frac{\partial u_k^i}{\partial q_j}\dot{q}_j + \epsilon_{klm}\omega_l(r_m^i + u_m^i)\right]\left[\frac{\partial u_k^i}{\partial q_p}\dot{q}_p + \epsilon_{kqr}\omega_q(r_r^i + u_r^i)\right] \tag{2.14}$$

Upon differentiation of Eq. (2.14) with respect to ω_s one obtains

$$\frac{\partial T}{\partial \omega_s} = \sum_{i=1}^{N_p} m^i \epsilon_{ksm}(r_m^i + u_m^i)v_k^i \qquad (s = 1,2,3) \tag{2.15}$$

from which follows

$$\frac{\partial T}{\partial \omega_1}\mathbf{b}_1 + \frac{\partial T}{\partial \omega_2}\mathbf{b}_2 + \frac{\partial T}{\partial \omega_3}\mathbf{b}_3 = \sum_{i=1}^{N_p} m^i \epsilon_{ksm}(r_m^i + u_m^i)v_k^i \mathbf{b}_s$$
$$= \sum_{i=1}^{N_p} m^i(\mathbf{r}^i + \mathbf{u}^i) \times \mathbf{v}^i \qquad (2.16)$$

Comparison of Eqs. (2.7), (2.8) and (2.16) shows that

$$h_k = \frac{\partial T}{\partial \omega_k} \qquad (k = 1, 2, 3) \qquad (2.17)$$

which, upon substitution into Eqs. (2.10-2.12), yields

$$\frac{d}{dt}\left(\frac{\partial T}{\partial \omega_1}\right) = \omega_3 \frac{\partial T}{\partial \omega_2} - \omega_2 \frac{\partial T}{\partial \omega_3} \qquad (2.18)$$

$$\frac{d}{dt}\left(\frac{\partial T}{\partial \omega_2}\right) = \omega_1 \frac{\partial T}{\partial \omega_3} - \omega_3 \frac{\partial T}{\partial \omega_1} \qquad (2.19)$$

$$\frac{d}{dt}\left(\frac{\partial T}{\partial \omega_3}\right) = \omega_2 \frac{\partial T}{\partial \omega_1} - \omega_1 \frac{\partial T}{\partial \omega_2} \qquad (2.20)$$

Equations (2.18-2.20) are analogous to Euler's equations for a rigid body and govern the rotational motion of the floating frame. Notice that the introduction of generalized coordinates associated with the orientation of B in N is avoided. An alternative derivation of Eqs. (2.18-2.20) based upon the use of quasi-coordinates with Lagrange's equations is also possible (see [52]).

The remaining equations of motion are given by the Lagrangian equations

$$\frac{d}{dt}\left(\frac{\partial T}{\partial \dot{q}_j}\right) = \frac{\partial T}{\partial q_j} - \frac{\partial U}{\partial q_j} \qquad (j = 1, \ldots, n) \qquad (2.21)$$

where U denotes the strain energy of the system.

Additional kinematic variables must be introduced if the orientation of B in N is required. Several possibilities exist including Euler angles, direction cosines, Euler parameters and Rodrigues parameters (see, e.g., [53]). It is noted that Eqs. (2.18-2.21) are in no way affected by the kinematic variables associated with the orientation of B in N.

2.1.3 Alternative Equations I

An alternative form of the equations of motion better suited for numerical integration is presented in this section. The basic approach is to obtain a set of $2n$ first order

differential equations equivalent to the n second order equations in Eq. (2.21). This set of equations along with Eqs. (2.10-2.12) are then put into a dimensionless form suitable for explicit time integration.

To begin, Eq. (2.14) is expressed in matrix notation as

$$T = \frac{1}{2}[\omega_1\ \omega_2\ \omega_3\ \dot{q}_1\ \ldots\ \dot{q}_n]M[\omega_1\ \omega_2\ \omega_3\ \dot{q}_1\ \ldots\ \dot{q}_n]^T \tag{2.22}$$

where the mass matrix, M, is symmetric, positive definite, and a function of $q_1, \ldots, q_n$.

Upon differentiation of Eq. (2.22) with respect to $\omega_1, \omega_2, \omega_3$ and $\dot{q}_1, \ldots, \dot{q}_n$ one obtains

$$[h_1\ h_2\ h_3\ p_1\ \ldots\ p_n]^T \overset{(2.17)}{=} M[\omega_1\ \omega_2\ \omega_3\ \dot{q}_1\ \ldots\ \dot{q}_n]^T \tag{2.23}$$

where the momenta variables $p_1, \ldots, p_n$ are defined as

$$p_i = \frac{\partial T}{\partial \dot{q}_i} \qquad (i = 1, \ldots, n) \tag{2.24}$$

Premultiplication of Eq. (2.23) by M^{-1} yields

$$[\omega_1\ \omega_2\ \omega_3\ \dot{q}_1\ \ldots\ \dot{q}_n]^T = M^{-1}[h_1\ h_2\ h_3\ p_1\ \ldots\ p_n]^T \tag{2.25}$$

or, equivalently,

$$\omega_k = \sum_{l=1}^{3} m^{-1}_{kl} h_l + \sum_{s=1}^{n} m^{-1}_{k,s+3} p_s \qquad (k = 1, 2, 3) \tag{2.26}$$

$$\frac{d}{dt}q_j = \sum_{l=1}^{3} m^{-1}_{j+3,l} h_l + \sum_{s=1}^{n} m^{-1}_{j+3,s+3} p_s \qquad (j = 1, \ldots, n) \tag{2.27}$$

Substitution of Eqs. (2.22) and (2.24-2.25) into Eq. (2.21) yields

$$\frac{d}{dt}p_j = \frac{1}{2}[h_1\ h_2\ h_3\ p_1\ \ldots\ p_n]M^{-1}\frac{\partial M}{\partial q_j}M^{-1}[h_1\ h_2\ h_3\ p_1\ \ldots\ p_n]^T - \frac{\partial U}{\partial q_j} \qquad (j = 1, \ldots, n) \tag{2.28}$$

Equations (2.10-2.12) and (2.27-2.28) constitute a set of $2n + 3$ first order ordinary differential equations. The primary variables are $h_1, h_2, h_3, q_1, \ldots, q_n$ and $p_1, \ldots, p_n$. The secondary variables $\omega_1, \omega_2, \omega_3$ appearing in Eqs. (2.10-2.12) are given in terms of the primary variables by Eq. (2.26).

It is useful to put the governing equations into a dimensionless form. To this end, it is assumed that the spinning motion is nominally about an axis passing through O and parallel to $\mathbf{b}_1$ (see Fig. 2.1). The nominal spin rate, Ω, is defined as

$$\Omega = h/J \tag{2.29}$$

where J denotes the (1,1) element of the mass matrix for $q_1, \ldots, q_n$ all equal to zero. In physical terms, J is simply the moment of inertia about the first principal axis of the undeformed system.

Defining,

$$\tau = \Omega t \tag{2.30}$$
$$x_{j+1} = q_j \qquad (j = 1, \ldots, n) \tag{2.31}$$
$$y_{j+1} = p_j/h \qquad (j = 1, \ldots, n) \tag{2.32}$$
$$m_k = h_k/h \qquad (k = 1, 2, 3) \tag{2.33}$$
$$\tilde{M} = M/J \tag{2.34}$$

the governing equations assume the dimensionless form

$$\frac{d}{d\tau} m_1 \overset{(2.10)}{=} \tilde{\omega}_3 m_2 - \tilde{\omega}_2 m_3 \tag{2.35}$$
$$\frac{d}{d\tau} m_2 \overset{(2.11)}{=} \tilde{\omega}_1 m_3 - \tilde{\omega}_3 m_1 \tag{2.36}$$
$$\frac{d}{d\tau} m_3 \overset{(2.12)}{=} \tilde{\omega}_2 m_1 - \tilde{\omega}_1 m_2 \tag{2.37}$$
$$\frac{d}{d\tau} x_{j+1} \overset{(2.27)}{=} \sum_{l=1}^{3} \tilde{m}^{-1}_{j+3,l} m_l + \sum_{s=1}^{n} \tilde{m}^{-1}_{j+3,s+3} y_{s+1} \qquad (j = 1, \ldots, n) \tag{2.38}$$
$$\frac{d}{dt} y_{j+1} \overset{(2.28)}{=} \frac{1}{2} [m_1 \; m_2 \; m_3 \; y_2 \; \ldots \; y_{n+1}] \tilde{M}^{-1} \frac{\partial \tilde{M}}{\partial x_{j+1}} \tilde{M}^{-1} [m_1 \; m_2 \; m_3 \; y_2 \; \ldots \; y_{n+1}]^T$$
$$- \frac{1}{J\Omega^2} \frac{\partial U}{\partial q_j} \qquad (j = 1, \ldots, n) \tag{2.39}$$

where

$$\tilde{\omega}_k = \sum_{l=1}^{3} \tilde{m}^{-1}_{kl} m_l + \sum_{s=1}^{n} \tilde{m}^{-1}_{k,s+3} y_{s+1} \qquad (k = 1, 2, 3) \tag{2.40}$$

It is clear from Eqs. (2.35-2.40) that the equations of motion can be formed entirely in terms of the mass matrix, M, and the strain energy, U. A method of modeling which provides expressions for M and U in terms of $q_1, \ldots, q_n$ is given in Chapter 4.

2.1.4 Alternative Equations II

The equations of motion presented in 2.1.3 involve a combination of both primary and secondary variables. Although such a formulation is useful for numerical integration, it offers little advantage for stability analysis.

In this section, the equations of motion are formulated entirely in terms of $q_1, \ldots, q_n$ and the momenta variables. The total number of equations is reduced by one through

the use of a constant of motion. The set of equations obtained has a structure quite similar to a Hamiltonian system and serves as the starting point for the development in the following section.

Let $\hat{T}$ denote the kinetic energy of the system expressed entirely in terms of $q_1, \ldots, q_n$ and the momenta variables. Substitution of Eq. (2.25) into Eq. (2.22) leads to

$$\hat{T} = \frac{1}{2}[h_1 \; h_2 \; h_3 \; p_1 \; \ldots \; p_n] M^{-1} [h_1 \; h_2 \; h_3 \; p_1 \; \ldots \; p_n]^T \tag{2.41}$$

which, upon differentiation with respect to p_j and q_j, yields

$$\begin{aligned} \frac{\partial \hat{T}}{\partial p_j} &= \sum_{l=1}^{3} m^{-1}_{j+3,l} h_l + \sum_{s=1}^{n} m^{-1}_{j+3,s+3} p_s \\ &\overset{(2.27)}{=} \frac{d}{dt} q_j \qquad (j = 1, \ldots, n) \end{aligned} \tag{2.42}$$

and

$$\begin{aligned} \frac{\partial \hat{T}}{\partial q_j} &= \frac{1}{2}[h_1 \; h_2 \; h_3 \; p_1 \; \ldots \; p_n] \frac{\partial M^{-1}}{\partial q_j} [h_1 \; h_2 \; h_3 \; p_1 \; \ldots \; p_n]^T \\ &= \frac{1}{2}[h_1 \; h_2 \; h_3 \; p_1 \; \ldots \; p_n] M^{-1} \left[M \frac{\partial M^{-1}}{\partial q_j} - \frac{\partial}{\partial q_j} \left(M M^{-1} \right) \right] [h_1 \; h_2 \; h_3 \; p_1 \; \ldots \; p_n]^T \\ &= -\frac{1}{2}[h_1 \; h_2 \; h_3 \; p_1 \; \ldots \; p_n] M^{-1} \frac{\partial M}{\partial q_j} M^{-1} [h_1 \; h_2 \; h_3 \; p_1 \; \ldots \; p_n]^T \\ &\overset{(2.28)}{=} -\frac{d}{dt} p_j - \frac{\partial U}{\partial q_j} \qquad (j = 1, \ldots, n) \end{aligned} \tag{2.43}$$

Equations (2.42-2.43) are expressed more compactly as

$$\frac{d}{dt} q_j = \frac{\partial E}{\partial p_j} \qquad (j = 1, \ldots, n) \tag{2.44}$$

$$\frac{d}{dt} p_j = -\frac{\partial E}{\partial q_j} \qquad (j = 1, \ldots, n) \tag{2.45}$$

where

$$E = \hat{T} + U \tag{2.46}$$

It is useful now to solve Eq. (2.13) for h_1 giving

$$h_1 = \sqrt{h^2 - h_2^2 - h_3^2} \tag{2.47}$$

Substitution of Eqs. (2.47) and (2.41) into Eq. (2.46), and subsequent differentiation with respect to h_2 yields

$$\frac{\partial E}{\partial h_2} = \frac{1}{h_1}[-h_2 \; h_1 \; 0 \; 0 \; \ldots \; 0] M^{-1} [h_1 \; h_2 \; h_3 \; p_1 \; \ldots \; p_n]^T$$

$$
\begin{aligned}
&= \frac{1}{h_1}\left[-h_2\left(\sum_{l=1}^{3} M_{1l}^{-1}h_l + \sum_{m=1}^{n} M_{1,m+3}^{-1}p_m\right) + \right. \\
&\quad \left. h_1\left(\sum_{l=1}^{3} M_{2l}^{-1}h_l + \sum_{m=1}^{n} M_{2,m+3}^{-1}p_m\right)\right] \\
&\overset{(2.26)}{=} (\omega_2 h_1 - \omega_1 h_2)/h_1 \\
&\overset{(2.12)}{=} \frac{1}{h_1}\frac{d}{dt}h_3
\end{aligned} \tag{2.48}
$$

or, equivalently,

$$
\frac{d}{dt}h_3 \overset{(2.47)}{=} \sqrt{h^2 - h_2^2 - h_3^2}\frac{\partial E}{\partial h_2} \tag{2.49}
$$

Similarly,

$$
\frac{d}{dt}h_2 = -\sqrt{h^2 - h_2^2 - h_3^2}\frac{\partial E}{\partial h_3} \tag{2.50}
$$

Defining the dimensionless system energy, G, as

$$
G = E/(h\Omega) \tag{2.51}
$$

it is deduced that

$$
\begin{aligned}
G &\overset{(2.41,2.46,2.51)}{=} \frac{1}{h\Omega}\left[\frac{1}{2}[h_1\ h_2\ h_3\ p_1\ \ldots\ p_n]M^{-1}[h_1\ h_2\ h_3\ p_1\ \ldots\ p_n]^T + U\right] \\
&\overset{(2.33)}{=} \frac{h}{\Omega}\left[\frac{1}{2}[m_1\ m_2\ m_3\ y_2\ \ldots\ y_{n+1}]M^{-1}[m_1\ m_2\ m_3\ y_2\ \ldots\ y_{n+1}]^T\right] + \frac{1}{h\Omega}U \\
&\overset{(2.29,2.34)}{=} \frac{1}{2}[m_1\ m_2\ m_3\ y_2\ \ldots\ y_{n+1}]\tilde{M}^{-1}[m_1\ m_2\ m_3\ y_2\ \ldots\ y_{n+1}]^T + U/(J\Omega^2) \\
&\overset{(2.47,2.33)}{=} \frac{1}{2}[\sqrt{1 - m_2^2 - m_3^2}\ m_2\ m_3\ y_2\ \ldots\ y_{n+1}]\tilde{M}^{-1} \\
&\quad [\sqrt{1 - m_2^2 - m_3^2}\ m_2\ m_3\ y_2\ \ldots\ y_{n+1}]^T + U/(J\Omega^2)
\end{aligned} \tag{2.52}
$$

Expression of Eqs. (2.44-2.45) and (2.49-2.50) in terms of the dimensionless quantities defined in Eqs. (2.30-2.33) and (2.51) yields

$$
\frac{d}{d\tau}m_3 = \sqrt{1 - m_2^2 - m_3^2}\frac{\partial G}{\partial m_2} \tag{2.53}
$$

$$
\frac{d}{d\tau}m_2 = -\sqrt{1 - m_2^2 - m_3^2}\frac{\partial G}{\partial m_3} \tag{2.54}
$$

$$
\frac{d}{d\tau}x_j = \frac{\partial G}{\partial y_j} \qquad (j = 2, \ldots, n+1) \tag{2.55}
$$

$$
\frac{d}{d\tau}y_j = -\frac{\partial G}{\partial x_j} \qquad (j = 2, \ldots, n+1) \tag{2.56}
$$

Notice that Eqs. (2.53-2.56) would form a Hamiltonian system were it not for the presence of $\sqrt{1-m_2^2-m_3^2}$ in Eqs. (2.53-2.54). Transformation of these equations to an equivalent Hamiltonian system is the topic of the following section.

2.2 Transformation to Canonical Form

A transformation of variables involving m_2 and m_3 is developed which permits the expression of Eqs. (2.53-2.56) as a Hamiltonian system of equations. Closed-form expressions are obtained for the transformation and its inverse.

New variables x_1 and y_1 are introduced as functions of m_2 and m_3. Letting H denote the function G expressed in terms of $x_1, \ldots, x_{n+1}$ and $y_1, \ldots, y_{n+1}$, one has

$$H(x_1, \ldots, x_{n+1}, y_1, \ldots, y_{n+1}) = G(m_2, m_3, x_2, \ldots, x_{n+1}, y_2, \ldots, y_{n+1}) \tag{2.57}$$

Application of the chain rule for differentiation to Eq. (2.57) yields

$$\frac{\partial G}{\partial m_2} = \frac{\partial H}{\partial x_1}\frac{\partial x_1}{\partial m_2} + \frac{\partial H}{\partial y_1}\frac{\partial y_1}{\partial m_2} \tag{2.58}$$

$$\frac{\partial G}{\partial m_3} = \frac{\partial H}{\partial x_1}\frac{\partial x_1}{\partial m_3} + \frac{\partial H}{\partial y_1}\frac{\partial y_1}{\partial m_3} \tag{2.59}$$

$$\frac{\partial G}{\partial x_j} = \frac{\partial H}{\partial x_j} \qquad (j = 2, \ldots, n+1) \tag{2.60}$$

$$\frac{\partial G}{\partial y_j} = \frac{\partial H}{\partial y_j} \qquad (j = 2, \ldots, n+1) \tag{2.61}$$

from which follows

$$\begin{aligned} \frac{d}{d\tau}x_1 &= \frac{\partial x_1}{\partial m_2}\frac{d}{d\tau}m_2 + \frac{\partial x_1}{\partial m_3}\frac{d}{d\tau}m_3 \\ &\overset{(2.53-2.54)}{=} \sqrt{1-m_2^2-m_3^2}\left[\frac{\partial x_1}{\partial m_3}\frac{\partial G}{\partial m_2} - \frac{\partial x_1}{\partial m_2}\frac{\partial G}{\partial m_3}\right] \\ &\overset{(2.58-2.59)}{=} \sqrt{1-m_2^2-m_3^2}\left[\frac{\partial x_1}{\partial m_3}\frac{\partial y_1}{\partial m_2} - \frac{\partial x_1}{\partial m_2}\frac{\partial y_1}{\partial m_3}\right]\frac{\partial H}{\partial y_1} \end{aligned} \tag{2.62}$$

Similarly,

$$\frac{d}{d\tau}y_1 = -\sqrt{1-m_2^2-m_3^2}\left[\frac{\partial x_1}{\partial m_3}\frac{\partial y_1}{\partial m_2} - \frac{\partial x_1}{\partial m_2}\frac{\partial y_1}{\partial m_3}\right]\frac{\partial H}{\partial x_1} \tag{2.63}$$

$$\frac{d}{d\tau}x_j \overset{(2.55,2.61)}{=} \frac{\partial H}{\partial y_j} \qquad (j = 2, \ldots, n+1) \tag{2.64}$$

$$\frac{d}{d\tau}y_j \overset{(2.56,2.60)}{=} -\frac{\partial H}{\partial x_j} \qquad (j = 2, \ldots, n+1) \tag{2.65}$$

Equations (2.62-2.65) are equivalent to the Hamiltonian system

$$\frac{d}{d\tau}x_j = \frac{\partial H}{\partial y_j} \qquad (j = 1, \ldots, n+1) \tag{2.66}$$

$$\frac{d}{d\tau}y_j = -\frac{\partial H}{\partial x_j} \qquad (j = 1, \ldots, n+1) \tag{2.67}$$

provided that

$$\frac{\partial x_1}{\partial m_3}\frac{\partial y_1}{\partial m_2} - \frac{\partial x_1}{\partial m_2}\frac{\partial y_1}{\partial m_3} = \frac{1}{\sqrt{1 - m_2^2 - m_3^2}} \tag{2.68}$$

The goal is to obtain a solution to the partial differential equation given by Eq. (2.68). To this end, consider the transformation of variables

$$x_1 = m_3 c(m_2^2 + m_3^2) \tag{2.69}$$

$$y_1 = m_2 c(m_2^2 + m_3^2) \tag{2.70}$$

and its inverse

$$m_2 = y_1 d(x_1^2 + y_1^2) \tag{2.71}$$

$$m_3 = x_1 d(x_1^2 + y_1^2) \tag{2.72}$$

where c and d are functions of the specified arguments. Substitution of Eqs. (2.69-2.70) into Eq. (2.68) yields

$$2sc(s)c'(s) + [c(s)]^2 = \frac{1}{\sqrt{1-s}} \tag{2.73}$$

where

$$s = m_2^2 + m_3^2 \tag{2.74}$$

A simple solution to the nonlinear ordinary differential equation in Eq. (2.73) is not apparent. The first approach taken to obtain a solution was to express c as a power series in the variable s. Coefficients of the series were then determined by equating like powers of s in Eq. (2.73). A similar series expansion was also developed for the function d.

An interesting observation was made concerning the function d during the course of an analysis presented later in this chapter. Letting d_m denote the series expansion of d truncated after the m'th term, it was observed that

$$\left[d_m(x_1^2 + y_1^2)\right]^2 = 1 - \frac{x_1^2 + y_1^2}{4} + \mathcal{O}\left[(x_1^2 + y_1^2)^m\right] \tag{2.75}$$

This observation motivated the proposition that

$$d(x_1^2 + y_1^2) = \sqrt{1 - \frac{x_1^2 + y_1^2}{4}} \tag{2.76}$$

The objective is to verify the validity of Eq. (2.76). In so doing, a closed-form solution for the function c is also obtained. Squaring Eqs. (2.69-2.72) and adding the results leads to

$$x_1^2 + y_1^2 = (m_2^2 + m_3^2)\left[c(m_2^2 + m_3^2)\right]^2 \tag{2.77}$$

$$m_2^2 + m_3^2 = (x_1^2 + y_1^2)\left[d(x_1^2 + y_1^2)\right]^2 \tag{2.78}$$

Substitution of Eq. (2.78) into Eq. (2.77) yields

$$\begin{aligned} 1 &= c\left(r[d(r)]^2\right) d(r) \\ &\overset{(2.76)}{=} c\left(r(1 - r/4)\right)\sqrt{1 - r/4} \end{aligned} \tag{2.79}$$

where

$$r = x_1^2 + y_1^2 \tag{2.80}$$

Equation (2.79) can also be written as

$$c(w)\sqrt{1 - r/4} = 1 \tag{2.81}$$

where

$$w = r(1 - r/4) \tag{2.82}$$

Solving Eq. (2.82) for r and substituting the result into Eq. (2.81) yields

$$c(s) = \sqrt{\frac{2(1 - \sqrt{1 - s})}{s}} \tag{2.83}$$

or, equivalently,

$$c(m_2^2 + m_3^2) = \sqrt{\frac{2(1 - \sqrt{1 - m_2^2 + m_3^2})}{m_2^2 + m_3^2}} \tag{2.84}$$

It can be verified that Eq. (2.83) is the solution to Eq. (2.73) for the initial condition $c(0) = 1$. Thus, in the linear approximation, $x_1 = m_3$ and $y_1 = m_2$.

Obtaining closed-form solutions for the functions c and d was a serendipitous result. Only after development of the associated power series did the simple form of d, and later c, become apparent. Plots of the functions c and d are provided in Figure 2.2. The domains of physical significance for c and d are from 0 to 1 and 0 to 2, respectively.

The procedure for transforming the original equations of motion to an equivalent Hamiltonian system is summarized below.

1. Obtain expressions for the mass matrix, M, and strain energy, U, in terms of the generalized degrees of freedom $q_1, \ldots, q_n$ (see Eqs. (2.14) and (2.22)).

2. Obtain an expression for the dimensionless system energy, G, in terms of the variables $m_2, m_3, x_2, \ldots, x_{n+1}$ and $y_2, \ldots, y_{n+1}$ (see Eqs. (2.34) and (2.52)).

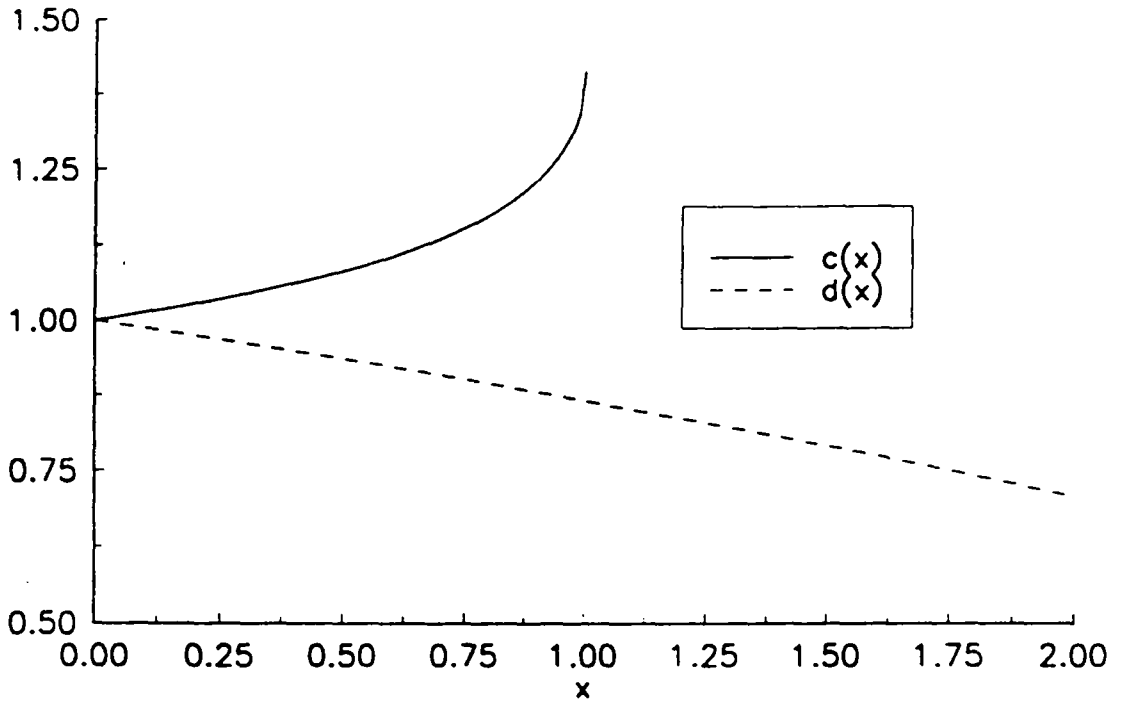

Figure 2.2. The functions c and d as given by Eqs. (2.84) and (2.76).

3. Obtain the Hamiltonian, H, by substitution of Eqs. (2.71-2.72) and (2.76) into the expression for G.

The governing equations in the new variables x_j, y_j $(j = 1, \ldots, n+1)$ are given by Eqs. (2.66-2.67).

The net result of the transformation is to permit the expression of the original equations of motion as a Hamiltonian system with $n+1$ degrees of freedom. Such a result for a rigid body ($n = 0$) has been attributed to Andoyer (see [54]). The present tranformation differs fundamentally from Andoyer's by never requiring the introduction of Euler angles.

2.3 Example Application

A simple example is presented which illustrates the procedure developed in the previous section. Euler's equations for the torque-free motion of a rigid body are transformed to an equivalent Hamiltonian system. Periodic solutions of the Hamiltonian system are then analyzed. A similar analysis is made using an established method. Results of the two analyses are then compared.

2.3.1 Problem Statement

The problem under consideration deals with the torque-free motion of a rigid body. For this problem, the floating reference frame and the rigid body move together and the strain energy is identically zero. It is assumed that the central principal moments of inertia satisfy the inequalities

$$I_1 > I_2 > I_3 \tag{2.85}$$

The assumption for the ordering of I_1, I_2, I_3 is made simply to facilitate comparison of results from the two different analyses.

The rotational kinetic energy of the rigid body is expressed as

$$T = \frac{1}{2}(I_1\omega_1^2 + I_2\omega_2^2 + I_3\omega_3^2) \tag{2.86}$$

which, upon substitution into Eqs. (2.18-2.20), leads to the Euler equations

$$I_1\frac{d}{dt}\omega_1 = (I_2 - I_3)\omega_2\omega_3 \tag{2.87}$$

$$I_2\frac{d}{dt}\omega_2 = (I_3 - I_1)\omega_3\omega_1 \tag{2.88}$$

$$I_3\frac{d}{dt}\omega_3 = (I_1 - I_2)\omega_1\omega_2 \tag{2.89}$$

Of present interest are the solutions to Eqs. (2.87-2.89) for the initial conditions

$$\omega_1(0) = \hat{\omega}_1 \tag{2.90}$$

$$\omega_2(0) = \hat{\omega}_2 \tag{2.91}$$

$$\omega_3(0) = 0 \tag{2.92}$$

It turns out that the solutions to Eqs. (2.87-2.89) are periodic functions of time. The period of the solutions generally depends on both the initial conditions and the values of the inertia ratios I_2/I_1 and I_3/I_1.

Two different approaches are used to determine the period of the solutions. In the first, Euler's equations are transformed to an equivalent Hamiltonian system. The period is then determined from the normal form of the Hamiltonian. Exact solutions to Euler's equations are used to determine the period in a second approach.

2.3.2 Approach I

The three steps outlined near the end of 2.2 are applied to the present problem.

Step 1: The mass matrix is readily identified from Eq. (2.86) as

$$M = diag(I_1, I_2, I_3) \tag{2.93}$$

Step 2:

$$\tilde{M}^{-1} \overset{(2.34)}{=} diag(1, I_1/I_2, I_1/I_3) \tag{2.94}$$

$$G \overset{(2.52)}{=} \frac{1}{2}\left[1 + (I_1/I_2 - 1)m_2^2 + (I_1/I_3 - 1)m_3^2\right] \tag{2.95}$$

Step 3:

$$H \overset{(2.57)}{=} \frac{1}{2}\left[(I_1/I_3 - 1)x_1^2 + (I_1/I_2 - 1)y_1^2\right] + \frac{1}{8}\left[(1 - I_1/I_3)x_1^4 + (2 - I_1/I_2 - I_1/I_3)x_1^2y_1^2 + (1 - I_1/I_2)y_1^4\right] \tag{2.96}$$

Throughout this development, the initial value of a variable is designated by placing a hat "^" above the variable. Using the initial conditions in Eqs. (2.90-2.92) one obtains

$$\hat{m}_2 \overset{(2.33)}{=} I_2\hat{\omega}_2/\sqrt{(I_1\hat{\omega}_1)^2 + (I_2\hat{\omega}_2)^2} \tag{2.97}$$

$$\hat{m}_3 \overset{(2.33)}{=} 0 \tag{2.98}$$

which, upon substitution into Eqs. (2.69-2.70), yields

$$\hat{x}_1 = 0 \tag{2.99}$$

$$\hat{y}_1 = \hat{m}_2\sqrt{\frac{2(1 - \sqrt{1 - \hat{m}_2^2})}{\hat{m}_2^2}} \tag{2.100}$$

In order to use computer-based normalization procedures, it is necessary to have numerical values for the coefficients in the expansion of the Hamiltonian. As a specific example, the case of $I_2/I_1 = 0.8$ and $I_3/I_1 = 0.5$ is considered. For these values of the inertia ratios, Eq. (2.96) becomes

$$H = \frac{1}{2}x_1^2 + \frac{1}{8}y_1^2 - \frac{1}{8}x_1^4 - \frac{5}{32}x_1^2y_1^2 - \frac{1}{32}y_1^4 \tag{2.101}$$

The normalized Hamiltonian, $\tilde{H}$, is expressed in terms of the action-angle variables ρ and θ as

$$\tilde{H}(\rho, \theta) = \sum_{l=1}^{n_d} a_l\rho^l \tag{2.102}$$

where $2n_d$ is the degree to which the normalization is carried out.

Hamilton's equations in the action-angle variables are given by

$$\frac{d}{d\tau}\theta = \frac{\partial\tilde{H}}{\partial\rho} \tag{2.103}$$

$$\frac{d}{d\tau}\rho = -\frac{\partial\tilde{H}}{\partial\theta} \tag{2.104}$$

It is apparent from Eqs. (2.102-2.104) that ρ is constant and

$$\theta = \left(\sum_{l=1}^{n_d} l a_l \rho^{l-1} \right) \tau + \hat{\theta} \tag{2.105}$$

Setting θ equal to $2\pi + \hat{\theta}$ in Eq. (2.105) and solving for τ yields

$$T = \frac{2\pi}{\sum_{l=1}^{n_d} l a_l \rho^{l-1}} \tag{2.106}$$

where T denotes the period in dimensionless units. The action is expressed in terms of $\hat{y}_1$ by

$$\rho = \sum_{l=1}^{n_d} b_l \hat{y}_1^{2l} \tag{2.107}$$

The coefficients a_l and b_l ($l = 1, \ldots, 5$) appearing in Eqs. (2.106-2.107) and reported in Table 2.1 were determined using a normalization procedure similar to the one described in [55].

The procedure to determine the period given $\hat{\omega}_1$ and $\hat{\omega}_2$ is summarized below.

$$\hat{\omega}_1, \hat{\omega}_2 \overset{(2.97)}{\Longrightarrow} \hat{m}_2 \overset{(2.100)}{\Longrightarrow} \hat{y}_1 \overset{(2.107)}{\Longrightarrow} \rho \overset{(2.106)}{\Longrightarrow} T \tag{2.108}$$

2.3.3 Approach II

An alternative procedure to determine the period is presented below. The analysis works directly with the solutions to Euler's equations and is based upon a development given in [53].

The solutions to Eqs.(2.87-2.89) for $\hat{\omega}_1$ and $\hat{\omega}_2$ greater than zero are given by

$$\omega_1 = \frac{h^2 - eI_3}{I_1(I_1 - I_3)} dn[p(t - t_0)|m] \tag{2.109}$$

$$\omega_2 = \frac{h^2 - eI_1}{I_2(I_2 - I_1)} sn[p(t - t_0)|m] \tag{2.110}$$

$$\omega_3 = -\frac{h^2 - eI_1}{I_3(I_3 - I_1)} cn[p(t - t_0)|m] \tag{2.111}$$

where sn, cn and dn are Jacobi elliptic functions, and

$$h^2 = (I_1\hat{\omega}_1)^2 + (I_2\hat{\omega}_2)^2 \tag{2.112}$$

$$e = I_1\hat{\omega}_1^2 + I_2\hat{\omega}_2^2 \tag{2.113}$$

$$z_1 = \frac{h^2 - e(I_2 + I_3)}{I_2 I_3} \tag{2.114}$$

$$z_2 = \frac{h^2 - e(I_3 + I_1)}{I_3 I_1} \tag{2.115}$$

$$z_3 = \frac{h^2 - e(I_1 + I_2)}{I_1 I_2} \tag{2.116}$$

$$p = \sqrt{z_1 - z_2} \tag{2.117}$$

$$m = (z_3 - z_2)/(z_1 - z_2) \tag{2.118}$$

$$cn[-pt_0|m] = 0 \tag{2.119}$$

The Jacobi elliptic functions are periodic and satisfy the identities

$$sn[pt + 4K(m)|m] = sn[pt|m] \tag{2.120}$$

$$cn[pt + 4K(m)|m] = cn[pt|m] \tag{2.121}$$

where $K(m)$ is the complete elliptic integral of the first kind.

Following a significant amount of algebraic manipulation, it can be deduced that

$$m = \hat{m}_2^2 \left[\frac{I_2 - I_3}{I_1} \frac{I_1/I_2 - 1}{(1 - I_2/I_1)[1 - (I_3/I_1)[1 + \hat{m}_2^2(I_1/I_2 - 1)]]} \right] \tag{2.122}$$

and

$$T = 4K(m) \left[\frac{(I_2/I_1)(I_3/I_1)}{(1 - I_2/I_1)[1 - (I_3/I_1)[1 + \hat{m}_2^2(I_1/I_2 - 1)]]} \right]^{1/2} \tag{2.123}$$

2.3.4 Comparison of Results

Plots of the period as a function of $\hat{m}_2$ are shown in Figure 2.3 for the inertia ratios $I_2/I_1 = 0.8$ and $I_3/I_1 = 0.5$. Results are presented for both the exact analysis (Approach II) and the approximate one (Approach I) based upon normalization of the Hamiltonian.

Physically meaningful values for $\hat{m}_2$ range from negative one to one. Results are only shown for positive values of $\hat{m}_2$ in the figure since the plot is symmetric about the vertical axis. Values of $\hat{m}_2$ near to zero are associated with nominal spinning motions about the first (maximum) principal axis. Motions about the second (intermediate) principal axis correspond to values of $\hat{m}_2$ near unity.

It is interesting to observe that the period increases monotonically with $\hat{m}_2$. This behavior is predicted by both the exact analysis and the approximate one for $n_d > 1$. In the limit as $\hat{m}_2 \to 1$, $m \to 1$ and the period approaches infinity.

It is clear from Figure 2.3 that the approximate solutions improve as the degree of normalization is increased. Normalization of the Hamiltonian through quadratic terms

Table 2.1. Coefficients a_l and b_l appearing in Eqs. (2.106-2.107).

l	a_l	b_l
1	5.00000×10^{-1}	2.50000×10^{-1}
2	-3.12500×10^{-1}	-2.34375×10^{-2}
3	-7.03125×10^{-2}	-5.12695×10^{-3}
4	-1.09863×10^{-1}	-1.01852×10^{-3}
5	-1.87042×10^{-1}	-2.01881×10^{-4}

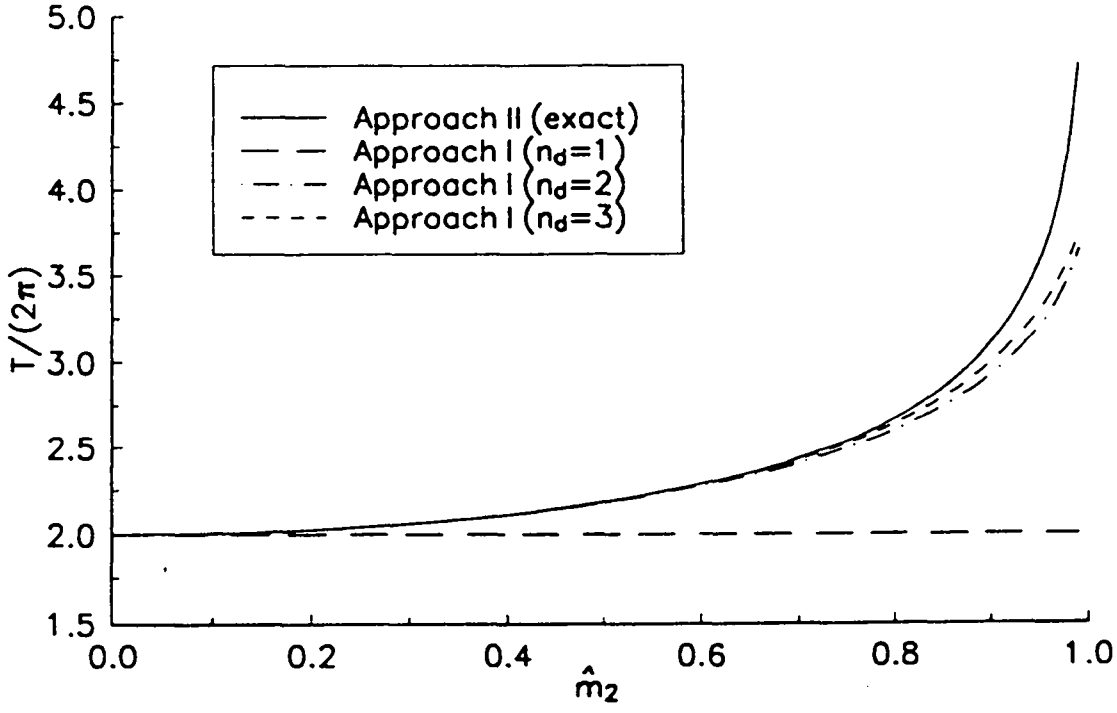

Figure 2.3. The period, T, as a function of $\hat{m}_2$ for $\frac{I_2}{I_1} = 0.8$ and $\frac{I_3}{I_1} = 0.5$.

($n_d = 1$) predicts a constant period. This result is consistent with a linear analysis of Euler's equations.

The favorable agreement between the two analyses provides a positive check of the transformations developed in 2.2. For this example, transformation of the equations of motion to an equivalent Hamiltonian system is an unnecessary complication. The utility of the transformation is primarily in the context of stability analysis, as is shown in Chapter 3.

2.4 Summary

Equations of motion are developed in this chapter for rotating flexible structures. Central to the development is the use of a floating reference frame which follows the overall rigid body motion of the structure. Elastic deformations within this frame are assumed to be functions of n generalized degrees of freedom.

Fundamental principles of dynamics are used to derive the equations of motion. Equations associated with the motion of the floating reference frame are obtained from conservation of linear and angular momentum. The remaining equations associated with elastic deformations are given by Lagrange's equations. Equivalent sets of equations better suited for numerical integration and stability analysis are also formulated.

A nonlinear transformation of variables is developed which permits the expression of the equations of motion as a Hamiltonian system with $n + 1$ degrees of freedom. This result is of fundamental importance to Chapter 3 because of its relevance to the stability analysis of rotating structures. Application of the transformation is illustrated for a problem involving the torque-free motion of a rigid body.

3. Stability Analysis

The subject of this chapter is the stability analysis of unrestrained, flexible structures rotating about a principal axis of inertia. This area of study has important applications in the design of rotating space structures such as spin-stabilized satellites. A unique feature of the present work is its focus on the stability of spin about the axis of minimum moment of inertia. Previous work in the literature has dealt almost exclusively with the analysis of spin about the axis of maximum moment of inertia.

The results developed herein are based upon the equivalence of the governing equations of motion to a Hamiltonian system. Recall from Chapter 2 that this equivalence was established through the introduction of a transformation of variables. Thus, the wealth of knowledge existing for Hamiltonian systems can be applied to the stability analysis of rotating structures.

Following a brief presentation of background material, a discussion is provided on stability and its meaning in the context of rotating structures. An introduction to the theory of Hamiltonian systems is then given, followed by development of a method to assess stability. The chapter concludes with a stability analysis of an example problem. Results of the stability analysis are confirmed by simulations based upon numerical integration of the equations of motion.

3.1 Background

A classical result of dynamics states that the spinning motion of a rigid body is stable about the axis of either maximum (major) or minimum (minor) moment of inertia when external moments are absent. Spin about the axis of intermediate moment of inertia is unstable. Generalization of this result to flexible bodies is only possible for the case of spin about the intermediate axis.

Stability criteria for spin about the major axis are often established using Liapunov's direct (second) method. Useful results can be obtained either in the presence or absence of internal energy dissipation. In contrast, spin about the minor axis is usually unstable for damped systems. This result can be shown for specific problems either from a linear analysis of the equations of motion or by application of Chetayev's instability theorem.

The stability analysis of undamped, flexible structures spinning about the minor axis has received very little attention in the literature. The limited amount of work in this area is understandable since all structures are damped to some extent. The work presented here was originally motivated by a need to predict the short-term behavior of lightweight, flexible structures in an exoatmospheric experiment.

Use of Liapunov's direct method for proving the stability of spin about the major axis typically involves construction of a Liapunov function from the angular momentum integrals (constants of motion) and the total energy. Such an approach can not be used to show stability for spin about the minor axis, even for undamped structures. At least one more integral of motion is required in order to construct a Liapunov function. It turns out, however, that integrals in addition to those of energy and momentum are the exception.

The nonlinear stability of rotating flexible structures has been studied in great detail for cases of spin about the major axis. The contribution of the present work is towards the development of a means to assess the nonlinear stability of undamped flexible structures spinning about the minor axis. Results are applicable to discrete models of elastic bodies that are free of applied forces and moments. Dual spin satellites and multi-body configurations are not considered.

3.2 Stability Concepts

The purpose of this section is to provide a brief review of stability and to introduce Liapunov's direct method. The meaning of stability in the context of spin about a principal axis is also discussed.

Consider an autonomous system of first order differential equations given by

$$\frac{d}{dt}z_i(t) = Z_i(z_1(t), \ldots, z_m(t)) \qquad i = 1, \ldots, m \tag{3.1}$$

It is assumed that the null solution, defined as

$$n_i(t) = 0 \qquad 0 \leq t < \infty, \qquad i = 1, \ldots, m \tag{3.2}$$

satisfies (3.1). That is, $Z_i(0, \ldots, 0) = 0$ for $i = 1, \ldots, m$. A general solution to Eq. (3.1) is denoted by $\mathbf{z}(t)$ and its norm defined as

$$||\mathbf{z}(t)|| = \sqrt{\sum_{i=1}^{m} [z_i(t)]^2} \tag{3.3}$$

Depending upon the particular application, there are several possible definitions of stability. In the present context, attention is restricted to the concept of Liapunov stability. The following definitions and theorem are taken from Meirovitch [56].

Definition 3.1 *The null solution is stable in the sense of Liapunov if for any positive ϵ there exists a $\delta = \delta(\epsilon) > 0$ such that if the inequality*

$$||\mathbf{z}(0)|| < \delta$$

is satisfied, then the inequality

$$||\mathbf{z}(t)|| < \epsilon, \qquad 0 \leq t < \infty,$$

is implied.

Definition 3.2 *The null solution is said to be unstable if for any arbitrarily small δ such that*

$$||\mathbf{z}(0)|| < \delta,$$

we have at some other finite time t_1 the situation

$$||\mathbf{z}(t_1)|| = \epsilon, \qquad t_1 > 0.$$

Definition 3.3 *The function $V(\mathbf{z})$ is called positive (negative) definite in a certain domain D_h if $V(\mathbf{z}) > 0$ (< 0) for all $\mathbf{z} \neq \mathbf{0}$ in D_h.*

Definition 3.4 *The function $V(\mathbf{z})$ is said to be positive (negative) semidefinite in a certain domain D_h if $V(\mathbf{z}) \geq 0$ (≤ 0), and it can vanish also for some $\mathbf{z} \neq \mathbf{0}$ in D_h.*

Theorem 3.1 *If there exists for the system (3.1) a positive (negative) definite function $V(\mathbf{z})$ whose total time derivative $\dot{V}(\mathbf{z})$ is negative (positive) semidefinite along every trajectory of (3.1), then the null solution is Liapunov stable.*

The classic example of a ball rolling on a curved surface is presented to help illustrate the first two definitions. Four different cases are shown in Figure 3.1. In each case, the ball is shown in an equilibrium position and gravity acts downward.

The issue of stability is concerned with the qualitative motion of the ball subsequent to a disturbance (nudge). Generally speaking, a stable equilibrium implies that "small" disturbances do not cause the ball to move a "large" distance from its original position.

Cases (a) and (d) in Figure 3.1 are classified as Liapunov stable, but (d) is practically stable only for small disturbances. Cases (b) and (c) are Liapunov unstable, although (c) might be considered stable depending upon the application.

It is clear from Cases (c) and (d) that determining just the Liapunov stability of an equilibrium might not be adequate for all situations. Sometimes it may be necessary to provide additional information such as the magnitude of disturbances for which the motion is guaranteed to remain near to the equilibrium. Example problems analogous to Cases (c) and (d) are presented later in the chapter.

Theorem 3.1 and its attending definitions provide a concise statement of Liapunov's direct method. A major advantage of Liapunov's direct method is that actual solutions

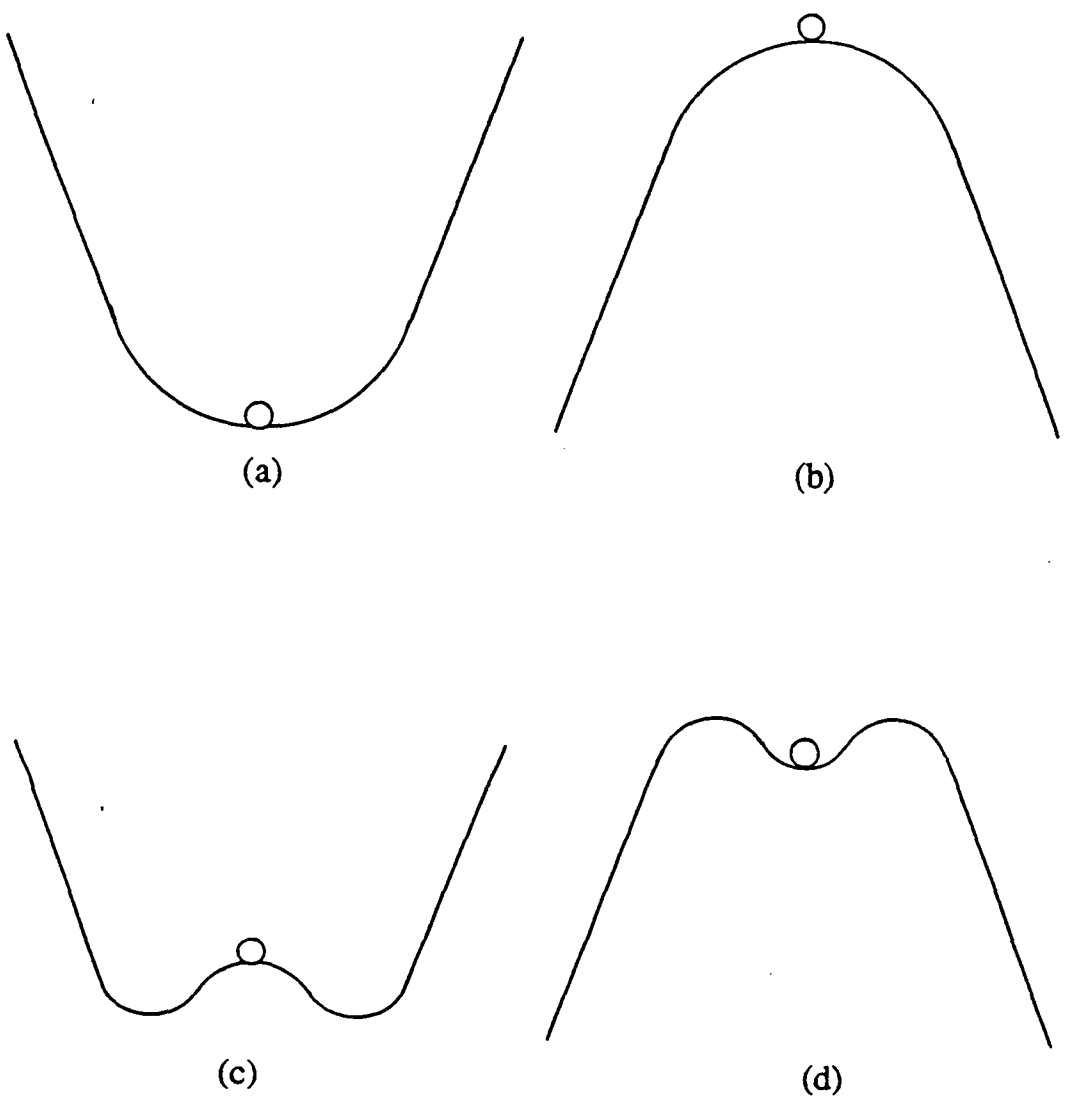

Figure 3.1. Simple illustration of stability concepts. (a) Liapunov stable. (b) Liapunov unstable. (c) Liapunov unstable (may be stable for practical purposes). (d) Liapunov stable (may be unstable for practical purposes).

to the governing equations are not required to prove stability. The primary difficulty with applying this method is in finding a Liapunov function, $V(\mathbf{z})$.

There are three possible equilibria for a rotating flexible structure. Each equilibrium corresponds to a motion of simple spin about a principal axis whereby the elastic deformations remain constant. Stability of a simple spin implies that small disturbances do not lead to large changes in the structure's attitude or elastic deformations.

Recall from Chapter 2 that the nominal spin is assumed to be about an axis parallel to the unit vector $\mathbf{b}_1$. One possible measure of the departure from simple spin is the angle, ϕ, between $\mathbf{b}_1$ and the angular momentum vector. For an axisymmetric rigid body, ϕ is the half cone angle.

Using a property of the vector cross product, one obtains

$$\begin{aligned} |\sin\phi| &= ||(\mathbf{b}_1 \times \mathbf{H})||/||\mathbf{H}|| \\ &\overset{(2.8,2.13)}{=} ||(h_2\mathbf{b}_3 - h_3\mathbf{b}_2)||/h \\ &\overset{(2.33)}{=} \sqrt{m_2^2 + m_3^2} \\ &\overset{(2.71,2.72)}{=} \sqrt{x_1^2 + y_1^2}\, d(x_1^2 + y_1^2) \end{aligned} \tag{3.4}$$

It is evident from Eq. (3.4) that small magnitudes of x_1 and y_1 imply small departures from simple spin as measured by the angle ϕ. Likewise, small magnitudes of $x_2, \ldots, x_{n+1}$ imply small elastic deformations. Thus, it is reasonable to state that a simple spin is stable if the null solution[2]

$$x_j(\tau) = 0 \qquad 0 \le \tau < \infty, \qquad j = 1, \ldots, n+1 \tag{3.5}$$

$$y_j(\tau) = 0 \qquad 0 \le \tau < \infty, \qquad j = 1, \ldots, n+1 \tag{3.6}$$

to Eqs. (2.66-2.67) is stable in the sense of Liapunov.

A simple spin may be accompanied by constant elastic deformations caused by centrifugal loading. Nevertheless, the variables $x_2, \ldots, x_{n+1}$ can be defined in such a manner that Eq. (3.5) is satisfied.

3.3 Hamiltonian Systems

3.3.1 Background

Certain aspects of Hamiltonian systems pertinent to later discussions are presented here. To begin, consider a Hamiltonian system of differential equations given by

$$\frac{d}{dt}x_i = \frac{\partial H}{\partial y_i} \qquad i = 1, \ldots, m \tag{3.7}$$

[2]The terms null solution, equilibrium, and equilibrium point are often used interchangeably when referring to stability.

$$\frac{d}{dt}y_i = -\frac{\partial H}{\partial x_i} \qquad i = 1, \ldots, m \tag{3.8}$$

The Hamiltonian, H, is a function of the variables $(x, y) = (x_1, \ldots, x_m, y_1, \ldots, y_m)$ and is assumed not to explicitly depend upon time. It follows from this assumption that H is constant along trajectories of Eqs. (3.7-3.8).

Assuming that $(x, y) = (0, 0)$ is an equilibrium point and H can be expanded as a Taylor series, one has

$$H(x, y) = H_0 + H_2(x, y) + H_3(x, y) + \cdots \tag{3.9}$$

where $H_s(x, y)$ is a homogeneous polynomial of degree s in the variables (x, y). Often the constant, H_0, is neglected in Eq. (3.9) since it does not affect Eqs. (3.7-3.8).

Key to the analysis of Hamiltonian systems is the use of canonical transformations. A canonical transformation of variables $(x, y) \to (\tilde{x}, \tilde{y})$ preserves Hamilton's equations. That is, if

$$\tilde{H}(\tilde{x}, \tilde{y}) = H(x, y) \tag{3.10}$$

then

$$\frac{d}{dt}\tilde{x}_i = \frac{\partial \tilde{H}}{\partial \tilde{y}_i} \qquad i = 1, \ldots, m \tag{3.11}$$

$$\frac{d}{dt}\tilde{y}_i = -\frac{\partial \tilde{H}}{\partial \tilde{x}_i} \qquad i = 1, \ldots, m \tag{3.12}$$

It is possible through the use of canonical transformations to put a Hamiltonian into its so-called normal form (see, e.g., [57, 54]). Assuming stability in the linear approximation, a Hamiltonian normalized to degree k satisfies the properties

$$H_2(x, y) = \sum_{i=1}^{m} \frac{\Omega_i}{2}\left(x_i^2 + y_i^2\right) \tag{3.13}$$

and

$$[H_j, H_2]_{(x,y)} = 0 \qquad j = 3, 4, \ldots, k \tag{3.14}$$

The left hand side of Eq. (3.14) denotes the Poisson bracket of the indicated functions and is defined as

$$[H_j, H_2]_{(x,y)} = \sum_{i=1}^{m}\left[\frac{\partial H_j}{\partial x_i}\frac{\partial H_2}{\partial y_i} - \frac{\partial H_j}{\partial y_i}\frac{\partial H_2}{\partial x_i}\right] \tag{3.15}$$

The characteristic frequencies, $\Omega_1, \ldots, \Omega_m$, appearing in Eq. (3.13) are said to satisfy a resonance relation of order $l > 0$ if there exist integers $k_1, \ldots, k_m$ such that

$$k_1\Omega_1 + \cdots + k_m\Omega_m = 0 \tag{3.16}$$

and

$$|k_1| + \cdots + |k_m| = l \tag{3.17}$$

Notice from Eqs. (3.9) and (3.13) that if cubic and higher degree terms in the Hamiltonian are neglected, then Eqs. (3.7-3.8) simplify to those for a set of uncoupled harmonic oscillators with frequencies $|\Omega_1|, \ldots, |\Omega_m|$. It is shown in 2.3.2 that the normal form can also be used to predict the dependence of frequency on amplitude. Thus, the theory of the normal form provides a generalization of linear modal analysis.

3.3.2 Stability

The governing equations for a rotating flexible structure given by Eqs. (2.66-2.67) are inherently nonlinear. Nonlinearities arise because of the presence of cubic and higher degree terms in the expansion of the Hamiltonian. Such is the case even for the simple problem of rigid body motion.

Determination of stability for nonlinear Hamiltonian systems may or may not be a simple matter. In many instances, the instability of an equilibrium can be determined from a linear analysis of the nonlinear differential equations. If the general solution to the linear equations involves a term with exponential growth, then the equilibrium is unstable. This result holds for the nonlinear differential equations as well.

If the general solution to the linear equations does not contain any terms with exponential growth, then no conclusion can be made regarding stability for the nonlinear system. That is, an equilibrium stable in the linear approximation may not be stable when nonlinear terms in Hamilton's equations are included.

For the remainder of this discussion, it is assumed that the null solution to Eqs. (2.66-2.67) is stable in the linear approximation and that the Hamiltonian is normalized to at least degree four. Accordingly, one has

$$H(x,y) = \sum_{i=1}^{n+1} \frac{\Omega_i}{2} \left(x_i^2 + y_i^2\right) + H_3(x,y) + H_4(x,y) + \cdots \tag{3.18}$$

The Hamiltonian itself is a Liapunov function when all of the characteristic frequencies in Eq. (3.18) have the same sign. This result follows from the sign definiteness of $H_2(x,y)$ and the constancy of $H(x,y)$ along trajectories of Hamilton's equations.

Although there are exceptions, the characteristic frequencies are often all positive for spin about the major axis. Consequently, $H(x,y)$ is a Liapunov function and stability follows from Theorem 3.1. Apparently, cubic and higher degree terms in the Hamiltonian have no effect on Liapunov stability in these cases. An equivalent statement is that stability is determined solely from consideration of the linearized equations.

The situation is considerably different for spin about the minor axis. In such cases, the characteristic frequencies can never all be of the same sign. Consequently, the Hamiltonian is no longer a Liapunov function and can not be used to prove stability. It still may be possible to prove stability using Liapunov's direct method if an integral of motion in addition to the Hamiltonian exists. The existence of additional integrals, however, is the exception.

The quest for a general method of proving the stability of Hamiltonian systems remains open. Indeed, even relatively simple systems such as the three body problem have defied complete analysis. Elements of two theories having application to the stability analysis of spin about the minor axis are described below.

KAM Theory

A significant advancement in the understanding of Hamiltonian systems was provided by the development of KAM theory. Named in recognition of the collective work of Kolmogorov, Arnold and Moser, KAM theory has important applications to the study of stability. Detailed descriptions of the theory and its applications are available in [58, 54].

Most Hamiltonian systems are nonintegrable. That is, the number of degrees of freedom exceeds the number of integrals (constants). Notable exceptions include linear systems and systems with only a single degree of freedom.

Under certain conditions, KAM theory can be used to show that the trajectories of nonintegrable systems often behave as if the systems were integrable. Near a stable equilibrium (in the linear approximation), a large fraction of the phase space is filled by so-called KAM surfaces (see [58]). Trajectories lying on these surfaces are associated with the regular motion of an integrable system. Such trajectories are stable, remaining within a given neighborhood of the equilibrium for all times.

The fact that the phase space is not entirely filled by KAM surfaces precludes the possibility of inferring Liapunov stability from KAM theory. An exception is for isoenergetically nondegenerate two degree of freedom systems. Here, trajectories not lying on a KAM surface are constrained forever between adjacent surfaces. For systems with more than two degrees of freedom, a slow drift from the equilibrium known as Arnold diffusion is possible. Nevertheless, from the viewpoint of measure theory, stability can be shown for most initial conditions near the equilibrium since the number of points in the phase space not on a KAM surface is of measure zero.

If there are no resonance relations of order four or less, then Eq. (3.18) can be expressed as

$$H(\rho,\theta) = \sum_{i=1}^{n+1} \Omega_i \rho_i + \frac{1}{2} \sum_{i=1}^{n+1} \sum_{j=1}^{n+1} \beta_{ij} \rho_i \rho_j + \mathcal{O}(|\rho|^{5/2}) \tag{3.19}$$

where $\beta_{ij} = \beta_{ji}$, $|\rho| = \rho_1 + \cdots + \rho_{n+1}$, and the action-angle variables (ρ, θ) are related to the original variables (x, y) by the canonical transformation

$$x_i = \sqrt{2\rho_i}\sin\theta_i \qquad i = 1, \ldots, n+1 \tag{3.20}$$

$$y_i = \sqrt{2\rho_i}\cos\theta_i \qquad i = 1, \ldots, n+1 \tag{3.21}$$

A system is said to be nondegenerate if

$$\det \begin{pmatrix} \beta_{11} & \beta_{12} & \cdots & \beta_{1,n+1} \\ \beta_{12} & \beta_{22} & \cdots & \beta_{2,n+1} \\ \vdots & \vdots & \ddots & \vdots \\ \beta_{1,n+1} & \beta_{2,n+1} & \cdots & \beta_{n+1,n+1} \end{pmatrix} \neq 0 \tag{3.22}$$

and isoenergetically nondegenerate if

$$\det \begin{pmatrix} \beta_{11} & \beta_{12} & \cdots & \beta_{1,n+1} & \Omega_1 \\ \beta_{12} & \beta_{22} & \cdots & \beta_{2,n+1} & \Omega_2 \\ \vdots & \vdots & \ddots & \vdots & \vdots \\ \beta_{1,n+1} & \beta_{2,n+1} & \cdots & \beta_{n+1,n+1} & \Omega_{n+1} \\ \Omega_1 & \Omega_2 & \cdots & \Omega_{n+1} & 0 \end{pmatrix} \neq 0 \tag{3.23}$$

KAM theory can be applied if a system is either nondegenerate or isoenergetically nondegenerate.

An example is provided to help illustrate some aspects of nonintegrable systems and KAM theory. The example deals with the motion of the rotating flexible system described in the Appendix. Elastic deformations are described in terms of a single generalized coordinate ($n = 1$). Therefore, the system has a total of two degrees of freedom.

A commonly used method for illustrating the behavior of two degree of freedom systems is the Poincaré surface of section (see, e.g. [59, 58]). The method, as applied to the example problem, is summarized below.

1. Choose initial conditions for x_2 and y_2.
2. Set m_3 equal to zero.
3. Pick m_2 so that G (see Eq. (A.9)) is equal to zero.
4. Set m_1 equal to $\sqrt{1 - m_2^2}$.
5. Numerically integrate Eqs. (2.35-2.39) over some specified period of time, plotting x_2 and y_2 each time that m_3 becomes equal to zero.
6. Return to Step 1 to begin a new trajectory.

The conditions imposed in Steps 3 and 4 ensure that all of the trajectories have the same energy and angular momentum as a simple spin.

Poincaré surfaces of section are shown in Figures 3.2-3.4 for the values of the physical parameters given in Table 3.1. The parameters used for Figure 3.2 were specifically chosen to result in an integrable system ($I_2 = I_3$). Parameters associated with nonintegrable systems were used for Figures 3.3 and 3.4. In all three figures, the point (0,0) is associated with a simple spin about the axis of minimum moment of inertia.

A trajectory lying on a KAM surface is indicated by a set of points forming a smooth closed curve. Not surprisingly, all of the points in Figure 3.2 appear to lie on smooth curves. This result follows from the fact that KAM surfaces fill the entire phase space for integrable systems. The trajectories associated with Figure 3.3 also appear to lie on KAM surfaces, even though the system is nonintegrable.

Notice in Figures 3.2 and 3.3 that all of the points are enclosed within a region of the $x_2 - y_2$ plane bounded by a solid line. Initial conditions outside of this region are not physically possible because of the constraints imposed in Steps 2-4. As the spring stiffness in the model is increased, the region of the x_2-y_2 plane which is accessible becomes smaller.

The observations of the previous paragraph have relevance to the stability analysis of relatively stiff structures. If a structure is sufficiently stiff, then the region of phase space which is physically accessible may preclude the possibility of large changes in attitude or elastic deformations. This point is illustrated later in the chapter by an example problem.

Comparison of Figures 3.3 and 3.4 shows that a significant change in the system behavior results by reducing the value of the spring constant. Although KAM surfaces are also evident in Figure 3.4, not all of the trajectories appear to lie on such surfaces. The unstructured distribution of some points in Figure 3.4 is associated with a single chaotic trajectory. The positions in the figure located at (0,0) and near (1.45,0) are associated with stable periodic trajectories in which the system moves as a rigid body. The position located near (-1.25,0) is associated with an unstable periodic solution.

As a final note, stability of spin about the minor axis can be proved for the integrable system using Liapunov's direct method. The procedure simply involves construction of a Liapunov function from two independent integrals. The stability of the nonintegrable system follows from KAM theory and the isoenergetic nondegeneracy of the system (see [60]).

Formal and Approximate Integrals

Another approach to the analysis of stability involves the use of formal integrals. As an introduction, let r denote the total number of independent resonance relations among the characteristic frequencies for the Hamiltonian in Eq. (3.18). The resonance relations

Table 3.1. Physical parameters used for Figures 3.2-3.4.

Figure	$\frac{I_2}{I_1}$	$\frac{I_3}{I_1}$	$\frac{\tilde{m}l^2}{I_1}$	$\frac{kl^2}{I_1\Omega^2}$	a_5	β
3.2	2.0	2.0	0.15	1.00	0	1
3.3	2.0	1.5	0.15	1.00	0	1
3.4	2.0	1.5	0.15	0.10	0	1

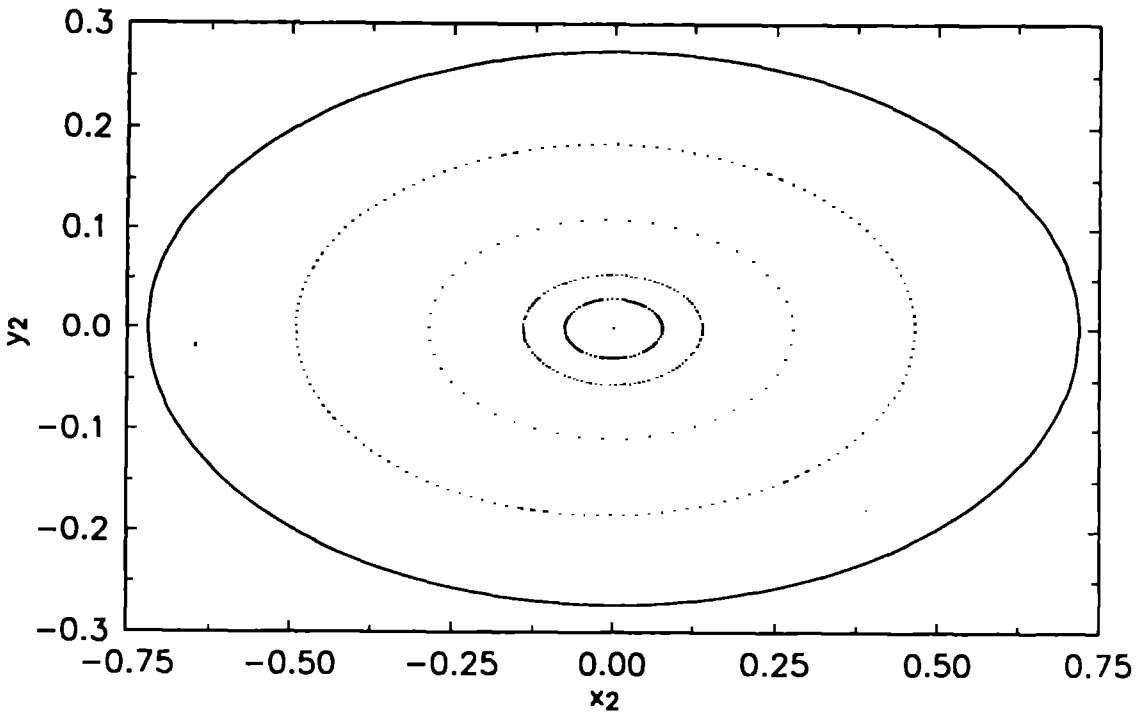

Figure 3.2. Poincaré surface of section for an integrable system ($\frac{kl^2}{I_1\Omega^2} = 1.0$).

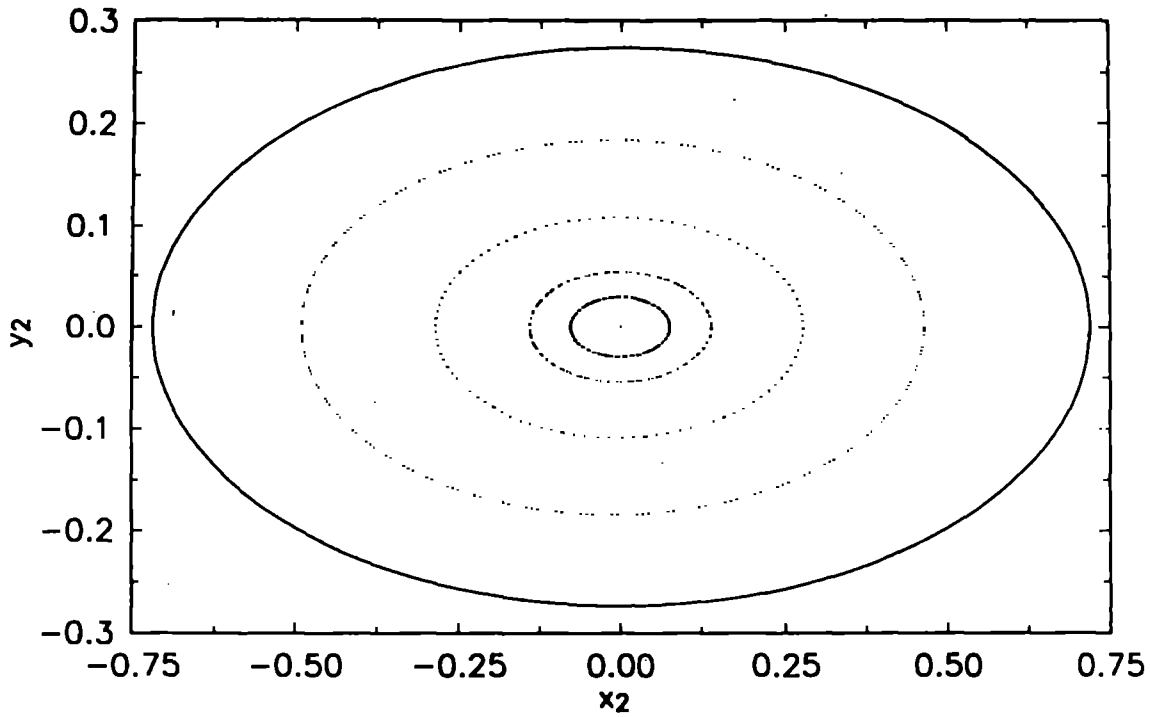

Figure 3.3. Poincaré surface of section for a nonintegrable system ($\frac{kl^2}{I_1\Omega^2} = 1.0$).

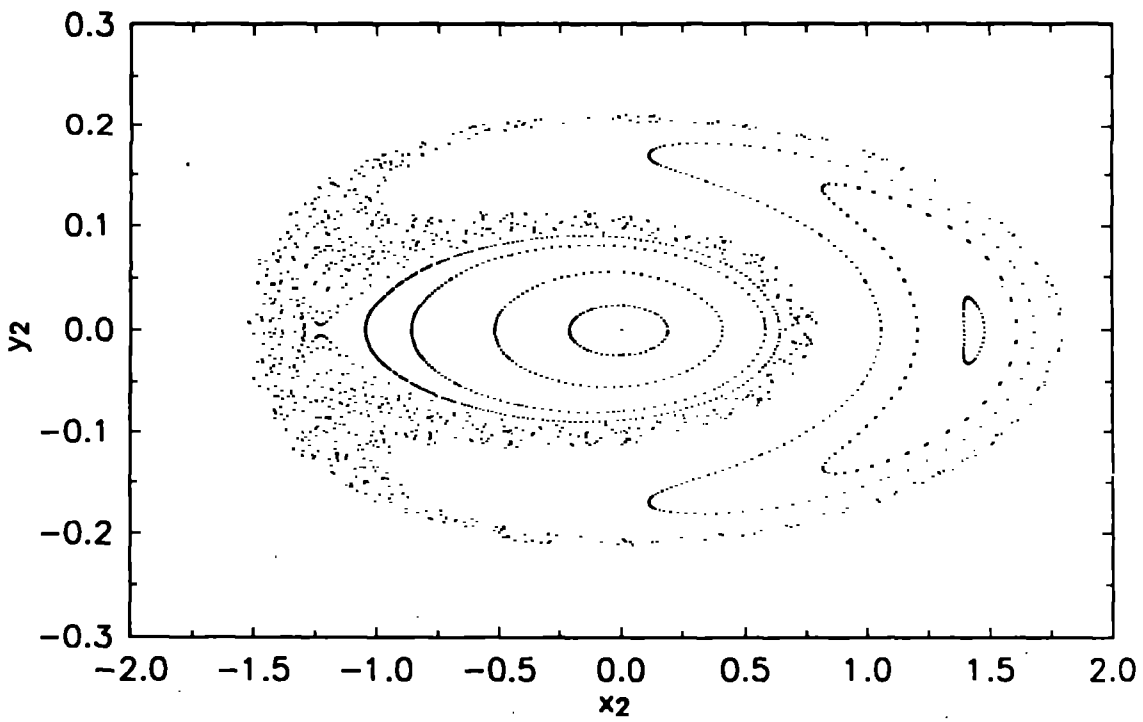

Figure 3.4. Poincaré surface of section for a nonintegrable system ($\frac{kl^2}{I_1\Omega^2} = 0.1$).

can be expressed in matrix notation as

$$K\Omega = 0 \tag{3.24}$$

where

$$K = \begin{bmatrix} k_{11} & k_{12} & \cdots & k_{1,n+1} \\ \vdots & \vdots & \ddots & \vdots \\ k_{r1} & k_{r2} & \cdots & k_{r,n+1} \end{bmatrix} \tag{3.25}$$

and

$$\Omega = \begin{bmatrix} \Omega_1 & \Omega_2 & \cdots & \Omega_{n+1} \end{bmatrix}^T \tag{3.26}$$

The columns of a matrix C are assumed to span the null space of K. That is,

$$KC = 0 \tag{3.27}$$

According to the theory of the normal form, formal integrals of the Hamiltonian system are given by

$$I_l(x,y) = \frac{1}{2}\sum_{i=1}^{n+1} c_{il}\left(x_i^2 + y_i^2\right) \qquad l = 1,\ldots,n+1-r \tag{3.28}$$

If the formal integrals can be combined with the Hamiltonian to form a positive definite function, then the equilibrium $(x,y) = (0,0)$ is said to be formally stable. According to Bruno [61], no example of Liapunov instability has been found for formally stable systems.

One obstacle to showing formal stability for actual problems is that the characteristic frequencies are known only to limited precision. Uncertainty in the values for the characteristic frequencies is an inevitable consequence of ever-present modeling errors. As a result of this uncertainty, the number of independent resonance relations to all orders can not be known.

An alternative to formal integrals is realized by consideration of only lower order resonances. Let $\hat{r}$ denote the number of independent resonance relations of order k or less. Matrices $\hat{K}$ and $\hat{C}$ associated with these resonance relations are defined analogously to K and C.

Approximate integrals for the Hamiltonian system are given by

$$\hat{I}_l(x,y) = \frac{1}{2}\sum_{i=1}^{n+1} \hat{c}_{il}\left(x_i^2 + y_i^2\right) \qquad l = 1,\ldots,n+1-\hat{r} \tag{3.29}$$

The above integrals are approximate in the sense that their time derivatives are zero if terms following $H_k(x,y)$ in Eq. (3.18) are neglected. Stated differently, the approximate

integrals are exact integrals for an alternate system with the Hamiltonian

$$\hat{H}(x,y) = \sum_{i=1}^{n+1} \frac{\Omega_i}{2}\left(x_i^2 + y_i^2\right) + H_3(x,y) + H_4(x,y) + \cdots + H_k(x,y) \tag{3.30}$$

Liapunov stability holds for the alternate system if the approximate integrals and $\hat{H}$ can be combined to form a positive definite function.

In some situations, there may exist a greater number of approximate integrals than is given by Eq. (3.29). For example, integrable systems always possess $n+1$ independent integrals regardless of the number of resonance relations. Determination of all the approximate integrals can be made during the calculation of the normal form.

Approximate integrals also have application in establishing lower bounds on the time interval during which a trajectory remains within a certain neighborhood of the equilibrium. In this regard, mention is made of the work of Celletti and Giorgilli [62] on the restricted three body problem.

A brief explanation of a simple approach to obtain the aforementioned bounds is presented below. Let the Hamiltonian for a system be normalized to degree k and assume that the associated approximate integrals are combined to form a positive definite function given by

$$L(x,y) = \sum_{i=1}^{n+1} a_i\left(x_i^2 + y_i^2\right) \tag{3.31}$$

The function, $\epsilon(x,y)$, defined as

$$\epsilon = \sqrt{L(x,y)} \tag{3.32}$$

can be thought of as a measure of the distance between the point (x,y) and the origin of the phase space.

Within a specified neighborhood of the equilibrium, it can be shown that

$$\frac{d}{d\tau}L(x,y) < A[L(x,y)]^{(k+1)/2} \tag{3.33}$$

where A is a positive constant. The inequality above follows from $L(x,y)$ being an approximate integral and normalization of the Hamiltonian to order k.

Integration of Eq. (3.33) between the limits $0 < \tau < T$ yields

$$[(k+1)/2 - 1]AT > [L(x_0,y_0)]^{1-(k+1)/2} - [L(x_T,y_T)]^{1-(k+1)/2} \tag{3.34}$$

which, followed by substitution of Eq. (3.32), yields

$$T > \frac{1-(1/a)^{k-1}}{A[(k+1)/2-1]}[1/\epsilon(x_0,y_0)]^{k-1} \tag{3.35}$$

where

$$a = \epsilon(x_T, y_T)/\epsilon(x_0, y_0) \qquad (a > 1) \tag{3.36}$$

Equation (3.35) provides a lower bound on the time required for $\epsilon(x, y)$ to increase from its initial value, $\epsilon(x_0, y_0)$, to some arbitrary value, $\epsilon(x_T, y_T)$. Such a bound may be useful if stability must be shown only during a finite time interval.

3.4 Stability Criteria

In the light of the KAM theory, it is reasonable to focus attention on systems possessing at least one resonance relation of order four or less. In the following section, it is assumed that only a single resonance relation exists among the characteristic frequencies and that $\Omega_j \neq 0$ for $j = 0, \ldots, n$. Guidelines for the stability analysis of systems with multiple low-order resonance relations are discussed separately.

3.4.1 Single Resonance Relation

Stability criteria are presented below for systems with a single resonance relation of order four or less. All systems satisfying these criteria are formally stable. Two degree of freedom systems ($n = 1$) satisfying the criteria are also Liapunov stable.

One can assume, without loss of generality, that the integer k_1 in Eq. (3.16) is positive. Furthermore, it is necessary only to consider cases for which $k_2, \ldots, k_{n+1}$ are all greater than or equal to zero. Otherwise, it follows that the system is formally stable.

The development below for a resonance relation of order two is a simple extension of Sokolskii [63]. In this case, one can consider k_1 and k_2 equal to unity and $k_3, \ldots, k_{n+1}$ equal to zero. The normal form of the Hamiltonian is given by

$$\begin{aligned} H(\rho, \theta) \;=\; & \sum_{j=1}^{n+1} \Omega_j \rho_j + \sum_{i=1}^{n+1} \sum_{j=1}^{n+1} a_{ij} \rho_i \rho_j + A \rho_1 \rho_2 \sin 2(\theta_1 + \theta_2 + \psi_1) + \\ & B \rho_1 \sqrt{\rho_1 \rho_2} \sin(\theta_1 + \theta_2 + \psi_2) + C \rho_2 \sqrt{\rho_1 \rho_2} \sin(\theta_1 + \theta_2 + \psi_3) + \\ & \mathcal{O}(|\rho|^{5/2}) \end{aligned} \tag{3.37}$$

Let

$$F(\phi) = a + b \sin 2\phi + c \sin \phi + d \cos \phi \tag{3.38}$$

where

$$a = a_{00} + a_{01} + a_{10} + a_{11} \tag{3.39}$$

$$b = A \tag{3.40}$$

$$c = B \cos(\psi_2 - \psi_1) + C \cos(\psi_3 - \psi_1) \tag{3.41}$$

$$d = B \sin(\psi_2 - \psi_1) + C \sin(\psi_3 - \psi_1) \tag{3.42}$$

If $F(\phi)$ is not equal to zero for all $0 \leq \phi < 2\pi$, then the equilibrium is stable. If $F(\phi^*) = 0$ for some ϕ^* and $F'(\phi^*) \neq 0$, then the equilibrium is unstable.

The following results for resonance relations of third and fourth orders are adopted from Khazin [64]. The normal form of the Hamiltonian is given by

$$H(\rho,\theta) = \sum_{j=1}^{n+1} \Omega_j \rho_j + \sum_{i=1}^{n+1}\sum_{j=1}^{n+1} a_{ij}\rho_i\rho_j + A\sqrt{\rho_1^{k_1}\cdots\rho_{n+1}^{k_{n+1}}}\cos(k_1\theta_1 + \cdots + k_{n+1}\theta_{n+1}) + \mathcal{O}(|\rho|^{5/2}) \tag{3.43}$$

The stability criteria for a third order resonance relation are

$$A = 0 \quad \text{and} \quad \sum_{i=1}^{n+1}\sum_{j=1}^{n+1} a_{ij}k_ik_j \neq 0 \quad \Longrightarrow \quad \text{stability}$$

$$A \neq 0 \quad \Longrightarrow \quad \text{instability}$$

The stability criteria for a fourth order resonance relation are

$$|A| < |\sum_{i=1}^{n+1}\sum_{j=1}^{n+1} a_{ij}k_ik_j| / \sqrt{k_1^{k_1}\cdots k_{n+1}^{k_{n+1}}} \quad \Longrightarrow \quad \text{stability}$$

$$|A| > |\sum_{i=1}^{n+1}\sum_{j=1}^{n+1} a_{ij}k_ik_j| / \sqrt{k_1^{k_1}\cdots k_{n+1}^{k_{n+1}}} \quad \Longrightarrow \quad \text{instability}$$

The stability of a system on the borderline of any of the above criteria is determined by fifth or higher degree terms in the expansion of its Hamiltonian.

3.4.2 Multiple Resonance Relations

The stability analysis of systems with multiple resonance relations may prove difficult in certain situations. One potential complication to the analysis of such systems is that the normal forms may not be as simple as those for the single resonances. Consequently, the techniques used to establish stability criteria in the previous section may not be applicable. The present author is unaware of a general procedure to establish necessary and sufficient conditions for stability in the presence of multiple resonance relations of order four or less.

Regardless of the potential difficulties, it is often possible to prove stability to a certain level of approximation simply by construction of a Liapunov function from the available integrals. As an illustration, consider a hypothetical system with $\Omega_1 = -1$, $\Omega_2 = 50$, $\Omega_3 = 100$, $\Omega_4 = 101$, and $\Omega_5 = 102$. Neglecting all resonance relations of order five and greater, one has

$$K \overset{(3.25)}{=} \begin{bmatrix} 1 & 0 & -1 & 1 & 0 \\ 1 & 0 & 0 & -1 & 1 \\ 1 & -2 & 0 & 1 & 0 \end{bmatrix} \tag{3.44}$$

The columns of the matrix

$$C \overset{(3.27)}{=} \begin{bmatrix} 1 & 1 & 2 & 1 & 0 \\ -1 & 0 & 0 & 1 & 2 \end{bmatrix}^T \tag{3.45}$$

span the null space of K, therefore, the integrals

$$I_1(x,y) = (x_1^2 + y_1^2) + (x_2^2 + y_2^2) + 2(x_3^2 + y_3^2) + (x_4^2 + y_4^2) \tag{3.46}$$

$$I_2(x,y) = -(x_1^2 + y_1^2) + (x_4^2 + y_4^2) + 2(x_5^2 + y_5^2) \tag{3.47}$$

exist. Multiplication of Eq. (3.46) by a factor of 2 and addition with Eq. (3.47) leads to the Liapunov function

$$L(x,y) = (x_1^2 + y_1^2) + 2(x_2^2 + y_2^2) + 4(x_3^2 + y_3^2) + 3(x_4^2 + y_4^2) + 2(x_5^2 + y_5^2) \tag{3.48}$$

Stability is thus proved for the hypothetical system if degree five and higher terms in the expansion of the Hamiltonian are ignored.

Observe that stability of the hypothetical system is inferred solely from consideration of the characteristic frequencies. Once the matrix C is formed, it is apparent that a Liapunov function can be formed from the integrals given by Eq. (3.28). As a result, normalization of the Hamiltonian beyond degree two is not required.

It is noteworthy to mention again that there may exist integrals in addition to those given by Eq. (3.28). Consideration of all possible integrals is important if the integrals given by Eq. (3.28) can not be combined with the Hamiltonian to form a Liapunov function. Such considerations require the calculation of the normal form beyond degree two.

3.5 Example Problem

A stability analysis and numerical simulations are presented in this section for an example problem. The intended purpose of the analysis is to demonstrate the use of the stability criteria developed in the previous section. Simulations are included to also facilitate the discussion of certain aspects of stability which were heretofore only alluded to.

The problem under consideration deals with the two degree of freedom system described in the Appendix. Quadratic, cubic and quartic terms in the expansion of the Hamiltonian (see (A.10)) are given by

$$H_2(x,y) = \frac{1}{2}\left[(I_1/\bar{I}_3 - 1)x_1^2 + (I_1/\bar{I}_2 - 1)y_1^2 + \frac{kl^2}{I_1\Omega^2}x_2^2 + \frac{I_1}{\hat{m}l^2}y_2^2\right] \tag{3.49}$$

$$H_3(x,y) = \beta\frac{\hat{m}l^2}{I_1}\left[(I_1/\bar{I}_3)^2 x_1^2 x_2 + (I_1/\bar{I}_2)^2 y_1^2 x_2\right] \tag{3.50}$$

$$H_4(x,y) = \frac{1}{8}(1-I_1/\bar{I}_3)x_1^4 + \frac{1}{8}(1-I_1/\bar{I}_2)y_1^4 + \frac{1}{8}(2-I_1/\bar{I}_2-I_1/\bar{I}_3)x_1^2y_1^2 + \frac{1}{2}\frac{\hat{m}l^2}{I_1}(I_1/\bar{I}_3)^2[4\beta^2\frac{\hat{m}l^2}{I_1}(I_1/\bar{I}_3)-1]x_1^2x_2^2 + \frac{1}{2}\frac{\hat{m}l^2}{I_1}(I_1/\bar{I}_2)^2[4\beta^2\frac{\hat{m}l^2}{I_1}(I_1/\bar{I}_2)-1]y_1^2x_2^2 + a_5x_2^4 \quad (3.51)$$

Definitions of the various terms appearing in Eqs. (3.49-3.51) are provided in the Appendix.

The dimensionless quantities $I_1/\bar{I}_2$ and $I_1/\bar{I}_3$ are both less than unity for spin about the minor axis. Accordingly, the characteristic frequencies determined from normalization of $H_2(x,y)$ are given by

$$\Omega_1 \overset{(3.49)}{=} -\sqrt{(1-I_1/\bar{I}_2)(1-I_1/\bar{I}_3)} \quad (3.52)$$

$$\Omega_2 \overset{(3.49)}{=} \sqrt{\frac{kl^2}{I_1\Omega^2}\frac{I_1}{\hat{m}l^2}} \quad (3.53)$$

It follows from the application of the stability criteria developed in 3.4.1 that of all possible second, third, and fourth order resonance relations, the only two that can lead to instability in this example are

$$2\Omega_1 + \Omega_2 = 0 \quad (3.54)$$

$$\Omega_1 + \Omega_2 = 0 \quad (3.55)$$

3.5.1 Resonance Relation $2\Omega_1 + \Omega_2 = 0$

Normalization of the Hamiltonian through degree three (see [65]) shows that the constant A appearing in Eq. (3.43) is given by

$$A = \frac{\beta[\frac{\hat{m}l^2}{I_1}\frac{kl^2}{I_1\Omega^2}]^{1/4}}{2\sqrt{2}}\left[\frac{(I_1/\bar{I}_3)^2}{1-I_1/\bar{I}_3} - \frac{(I_1/\bar{I}_2)^2}{1-I_1/\bar{I}_2}\right] \quad (3.56)$$

According to the stability criteria established earlier, the simple spin is stable only if $A = 0$. This condition corresponds physically to either an axisymmetric body ($I_2 = I_3$) or the rest position of the particle coinciding with the carrier body mass center ($\beta = 0$). Satisfaction of either of these two conditions guarantees spin stability.

A series of simulations is presented in Figures 3.5-3.12 to help illustrate the behavior of the system when the resonance relation $2\Omega_1 + \Omega_2 = 0$ is satisfied or nearly satisfied. Shown in the figures are plots of the momentum scalar, m_2, and generalized coordinate, x_2, as functions of the dimensionless time variable, τ. Results were obtained from numerical integration of Eqs. (2.35-2.39) using the parameter values and initial conditions

Table 3.2. Physical parameters and initial conditions used in Figures 3.5-3.12 and 16-17. Initial conditions for m_1 are given by $m_1(0) = [1 - m_2^2(0) - m_3^2(0)]^{1/2}$.

Figure(s)	$\frac{I_2}{I_1}$	$\frac{I_3}{I_1}$	$\frac{\hat{m}l^2}{I_1}$	$\frac{kl^2}{I_1\Omega^2}$	a_5	β	$m_2(0)$	$m_3(0)$	$x_2(0)$	$y_2(0)$
3.5-3.6	2.0	1.3	0.15	0.0996	0.00	1	0.035	0	0	0.010
3.7-3.8	2.0	1.3	0.15	0.1046	0.00	1	0.035	0	0	0.010
3.9-3.10	2.0	1.3	0.15	0.1046	0.00	1	0.071	0	0	0.020
3.11-3.12	2.0	1.3	0.15	0.0996	0.10	1	0.035	0	0	0.010
3.16	2.0	1.5	0.20	0.0449	0.00	1	0.045	0	0	0.015
3.17	2.0	1.1	0.20	0.0252	0.00	1	0.045	0	0	0.015

reported in Table 3.2. Initial conditions were chosen so that the energy and momentum correspond to those for a simple spin.

It is evident from Figures 3.5 and 3.6 that satisfaction of the resonance relation $2\Omega_1 + \Omega_2$ leads to instability. Notice that although the motion is unstable, the magnitudes of m_2 and x_2 are bounded. This result follows from the fact that the total energy of the system must remain constant.

As was noted earlier (see Eq. (3.4)), the angle ϕ provides a measure of the departure from simple spin. For the simulation associated with Figures 3.5 and 3.6, the value of ϕ varies from about 2 degrees at $\tau = 0$ up to approximately 60 degrees around $\tau = 355$. Such variations in ϕ indicate large changes in the attitude of the structure.

Similar plots are shown in Figures 3.7-3.10 when the system satisfies the near resonance condition $2.05\Omega_1 + \Omega_2 = 0$. The simulations associated with Figures 3.7-3.8 and 3.9-3.10 are identical in every respect except for the choice of the initial conditions (see Table 3.2).

Liapunov stability is expected since neither of the resonance relations in Eqs. (3.54) and (3.55) is satisfied. The stable behavior displayed in Figures 3.7 and 3.8 is consistent with this expectation. In constrast, the unstable growth exhibited in Figures 3.9 and 3.10 is somewhat unexpected. The simple spin is indeed Liapunov stable, but for practical purposes the motion may be considered unstable. The situation is analogous to the one depicted in Figure 3.1(d).

The observations in the previous paragraph show that a resonance relation need not be satisfied exactly for unstable motion to occur. Such considerations are important in practical applications, especially when the values of the characteristic frequencies are only known approximately.

A fourth illustration of the system behavior for $2\Omega_1 + \Omega_2 = 0$ is provided in Figures 3.11 and 3.12. Here, the parameters and initial conditions are identical to those

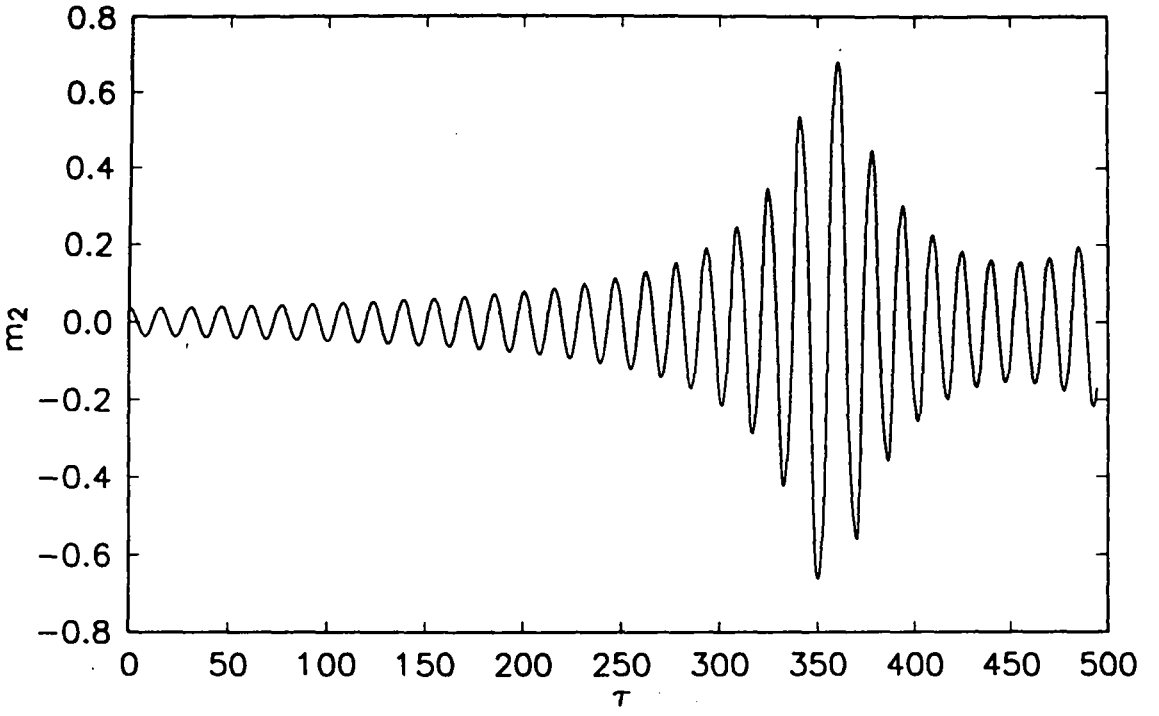

Figure 3.5. Variation of m_2 with time for the resonance relation $2\Omega_1 + \Omega_2 = 0$.

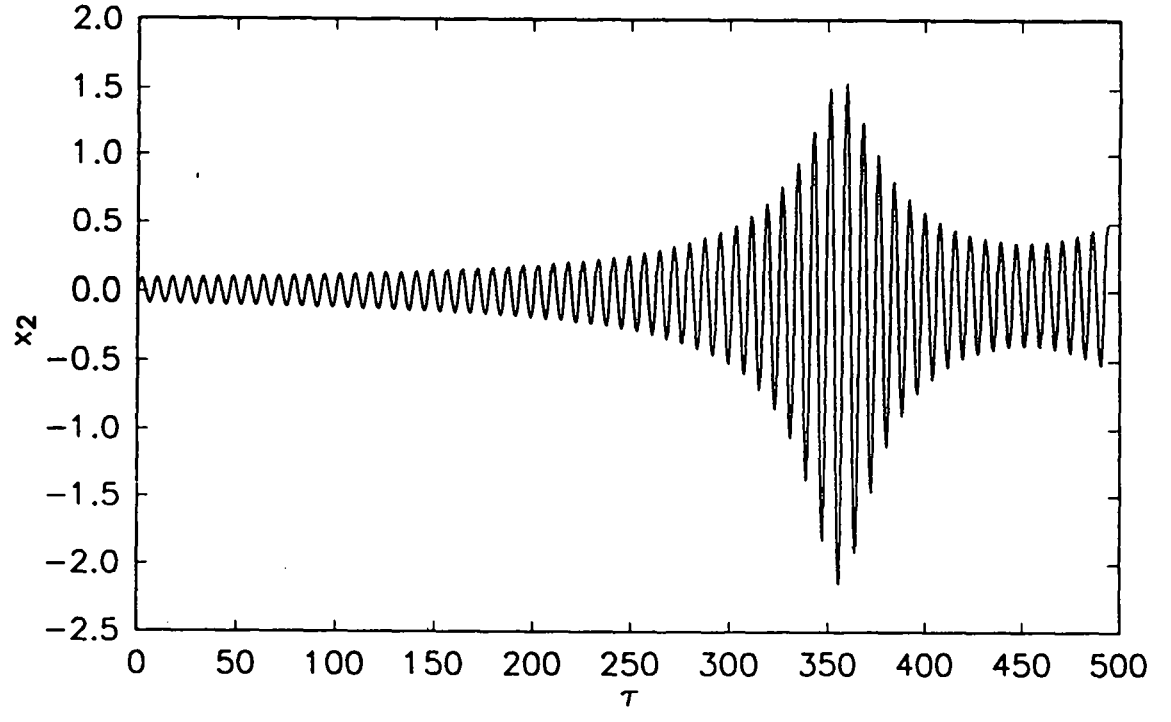

Figure 3.6. Variation of x_2 with time for the resonance relation $2\Omega_1 + \Omega_2 = 0$.

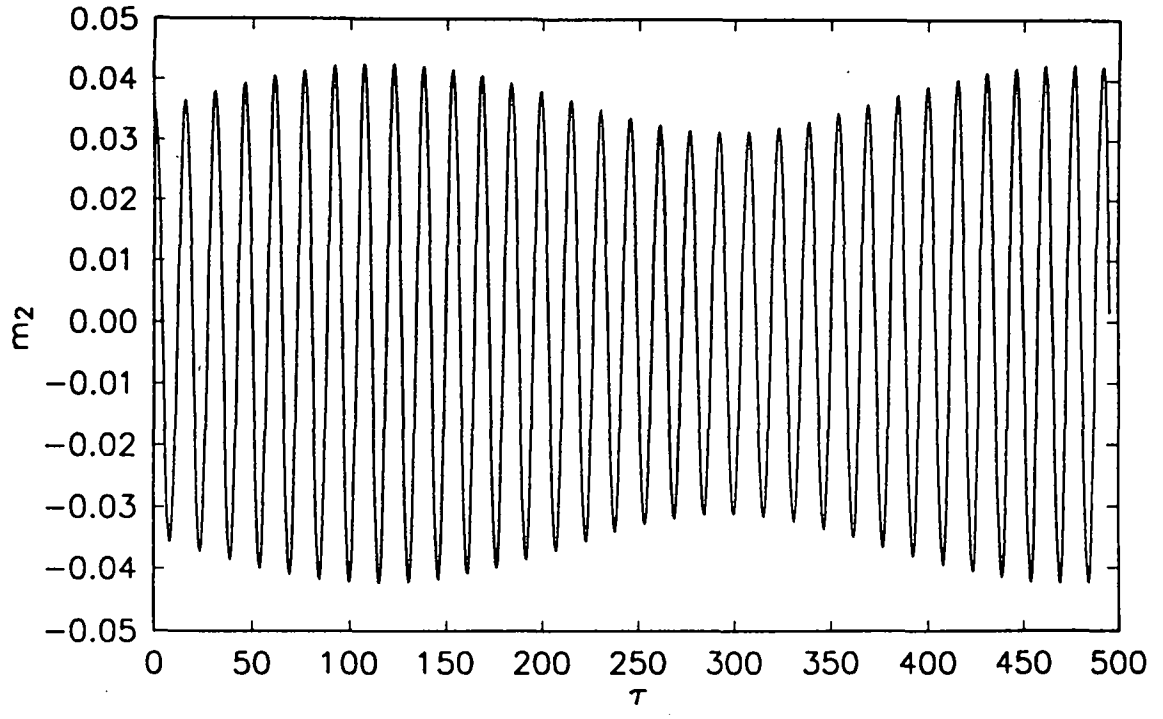

Figure 3.7. Variation of m_2 with time for the resonance relation $2.05\Omega_1 + \Omega_2 = 0$ (small initial conditions).

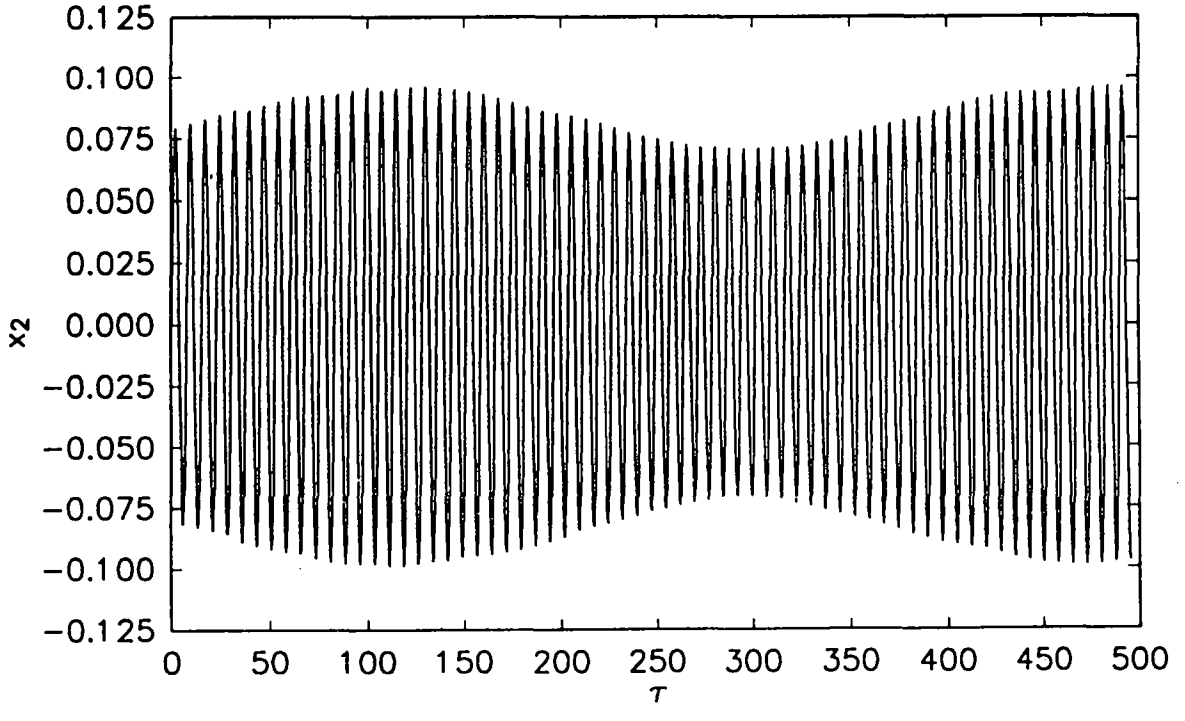

Figure 3.8. Variation of x_2 with time for the resonance relation $2.05\Omega_1 + \Omega_2 = 0$ (small initial conditions).

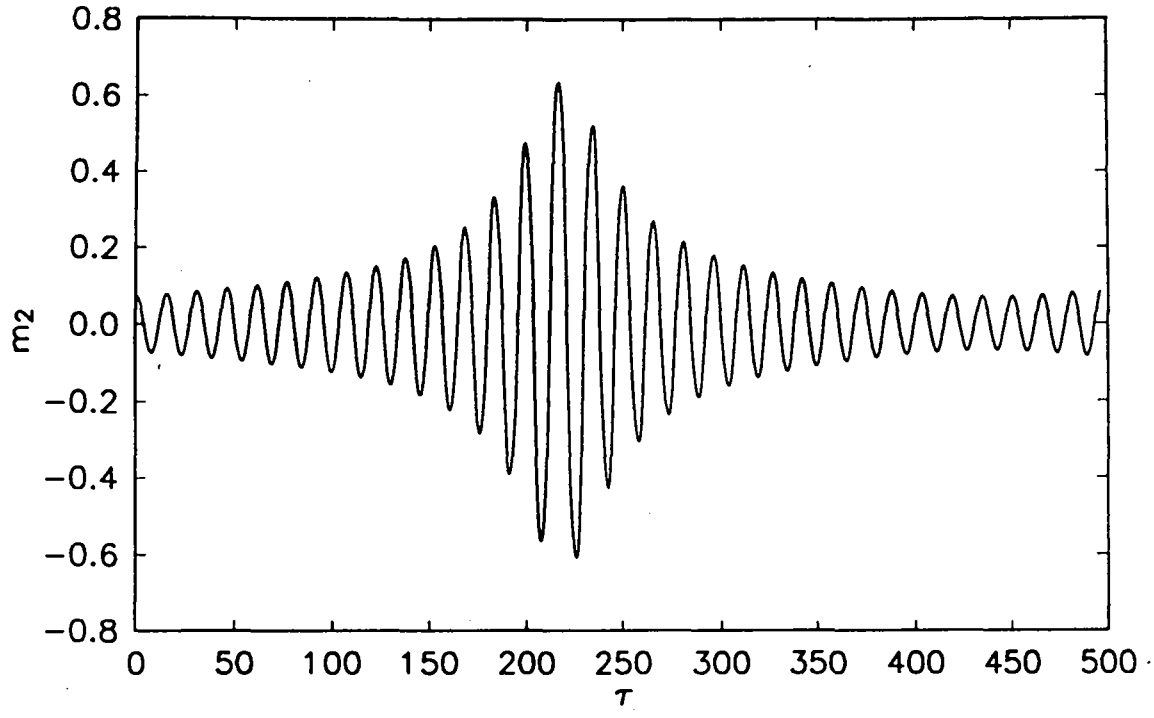

Figure 3.9. Variation of m_2 with time for the resonance relation $2.05\Omega_1 + \Omega_2 = 0$ (moderate initial conditions).

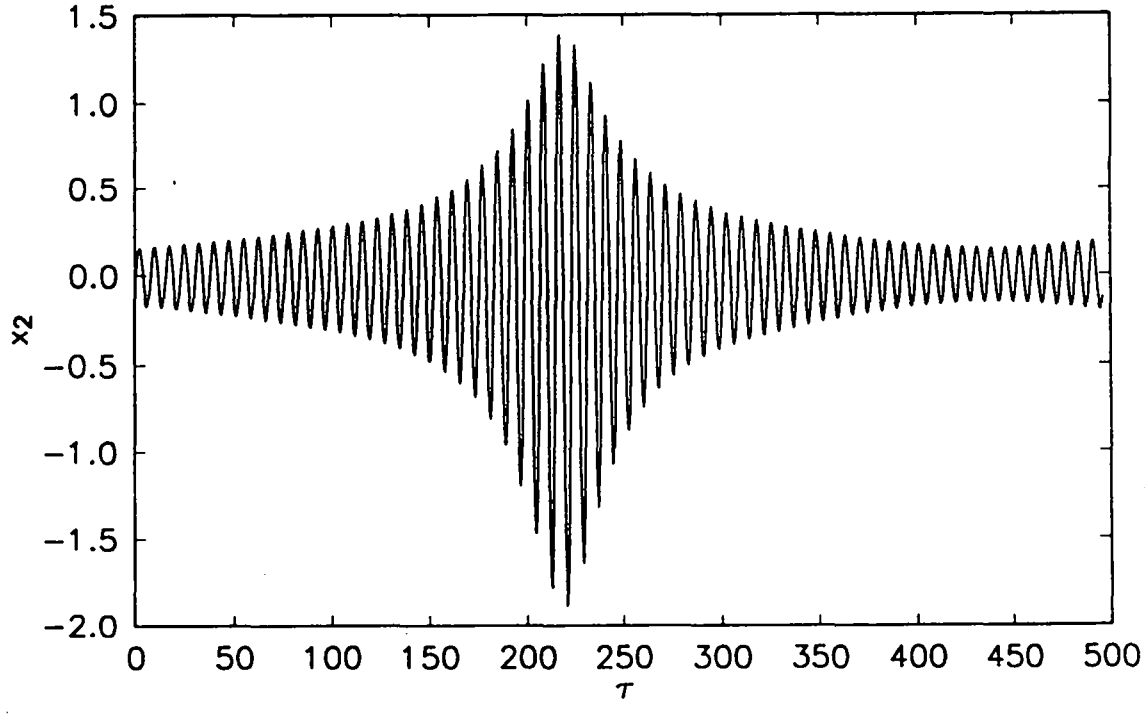

Figure 3.10. Variation of x_2 with time for the resonance relation $2.05\Omega_1 + \Omega_2 = 0$ (moderate initial conditions).

used for Figures 3.5 and 3.6, with the exception that the parameter a_5 is nonzero. A nonzero value of this parameter is associated with a cubic nonlinearity in the spring force-deflection relation, leading to a quartic term in the Hamiltonian (see Eq. (3.51)).

The initial growth of the solutions displayed in Figures 3.11 and 3.12 indicates that the simple spin may be unstable. Such a result is expected since the parameter a_5 does not appear in Eq. (3.56). Although the motion is Liapunov unstable, it appears to be stable for practical purposes. The situation is analogous to the one depicted in Figure 3.1(c).

The relatively small growth of x_2 in Figure 3.12 can be explained using an argument based upon energy considerations. Regardless of the manner in which the motion evolves, the strain energy in a system can never exceed the total energy initially imparted to the system. Because of the significant hardening of the spring, moderately-sized elastic deformations are associated with values of strain energy in excess of the total energy. Consequently, the magnitude of x_2 is constrained to relatively small values.

3.5.2 Resonance Relation $\Omega_1 + \Omega_2 = 0$

Normalization of the Hamiltonian through degree four (see [63]) results in the following expressions for the nonzero constants appearing in Eq. (3.43).

$$a_{11} = (2 - I_1/\bar{I}_2 - I_1/\bar{I}_3)/4 - \beta^2 \frac{\hat{m}l^2}{I_1} \left[5(b_2^2 + b_3^2)/12 + 7b_2b_3/6\right] \tag{3.57}$$

$$a_{12} + a_{21} = -(b_2 + b_3)/2 + \beta^2 \frac{\hat{m}l^2}{I_1} \left[b_2(2I_1/\bar{I}_2 + 2b_2/3) + b_3(2I_1/\bar{I}_3 + 2b_3/3) - 4b_2b_3/3\right] \tag{3.58}$$

$$a_{22} = \frac{3a_5}{2(1 - I_1/\bar{I}_2)(1 - I_1/\bar{I}_3)\left(\frac{\hat{m}l^2}{I_1}\right)^2} \tag{3.59}$$

$$A = (b_2 - b_3)/4 + \beta^2 \frac{\hat{m}l^2}{I_1} \left[b_3(I_1/\bar{I}_3 + b_3) - b_2(I_1/\bar{I}_2 + b_2)\right] \tag{3.60}$$

where

$$b_k = (I_1/\bar{I}_k)^2/(1 - I_1/\bar{I}_k) \qquad (k = 2, 3) \tag{3.61}$$

According to the stability criteria for the $\Omega_1 + \Omega_2 = 0$ resonance relation, spin about the minor axis is stable if

$$|a_{11} + a_{12} + a_{21} + a_{22}| > |A| \tag{3.62}$$

Stability diagrams in the $I_1/\bar{I}_2$-$I_1/\bar{I}_3$ parameter space are given in Figures 3.13-3.15. Boundaries of stability are obtained by finding the locus of points that satisfies the equation

$$|a_{11} + a_{12} + a_{21} + a_{22}| = |A| \tag{3.63}$$

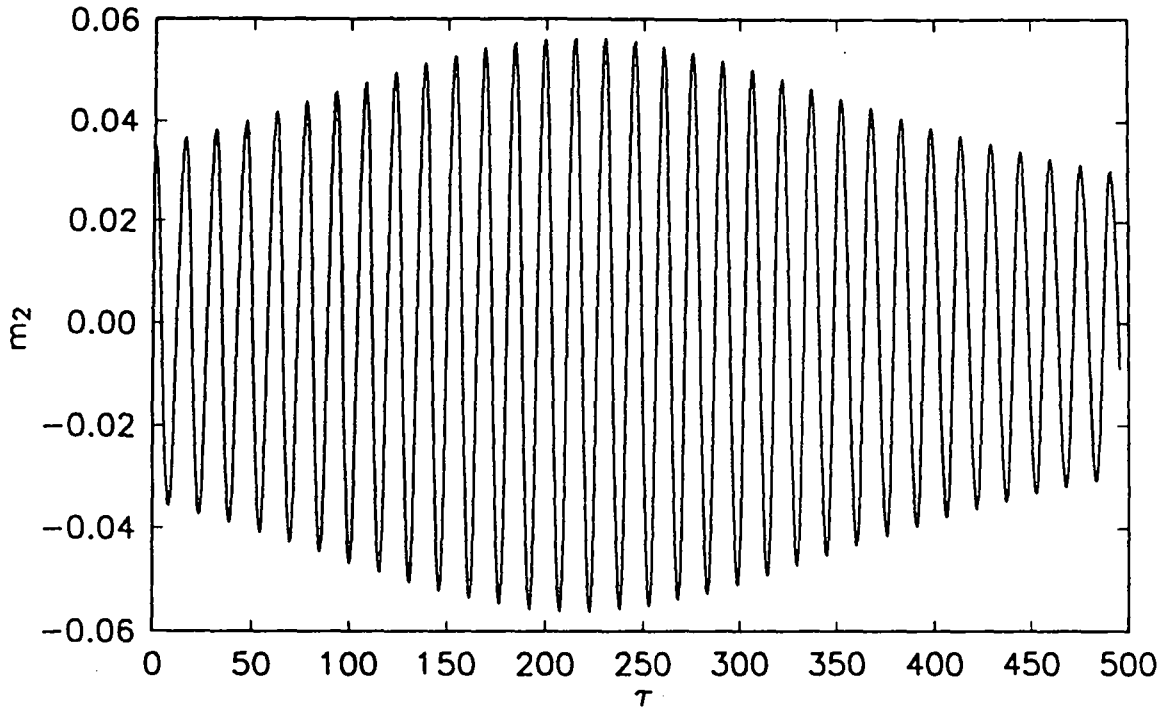

Figure 3.11. Variation of m_2 with time for the resonance relation $2\Omega_1 + \Omega_2 = 0$ ($a_5 = 0.10$).

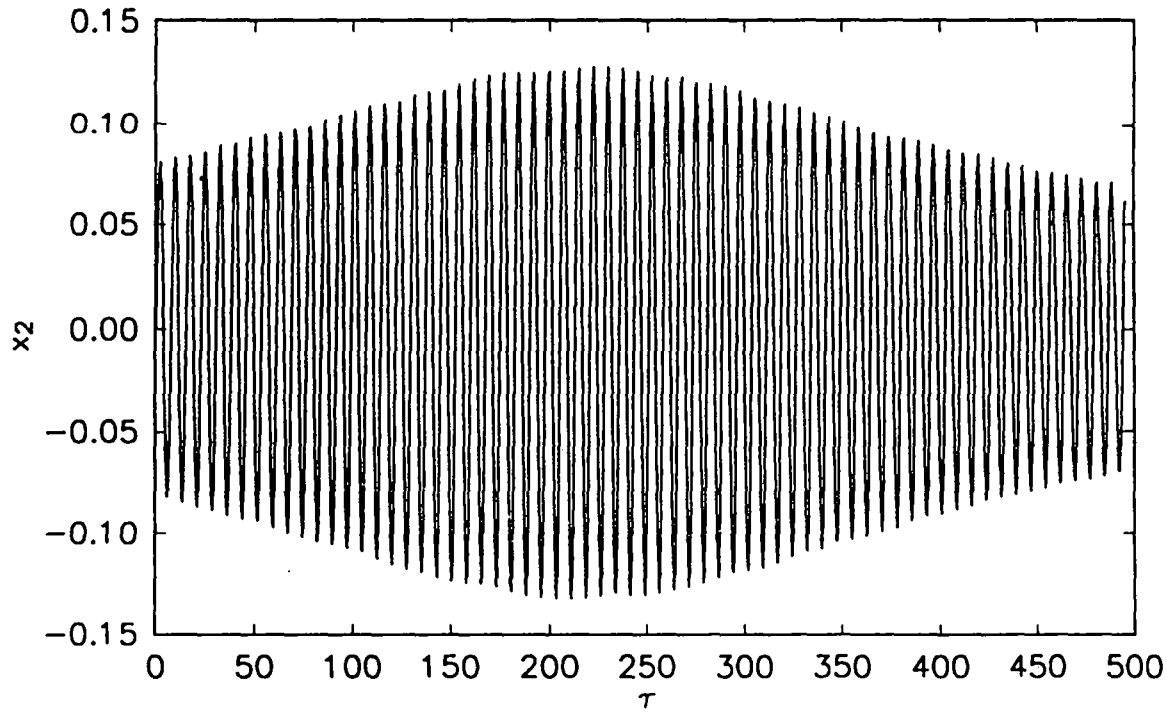

Figure 3.12. Variation of x_2 with time for the resonance relation $2\Omega_1 + \Omega_2 = 0$ ($a_5 = 0.10$).

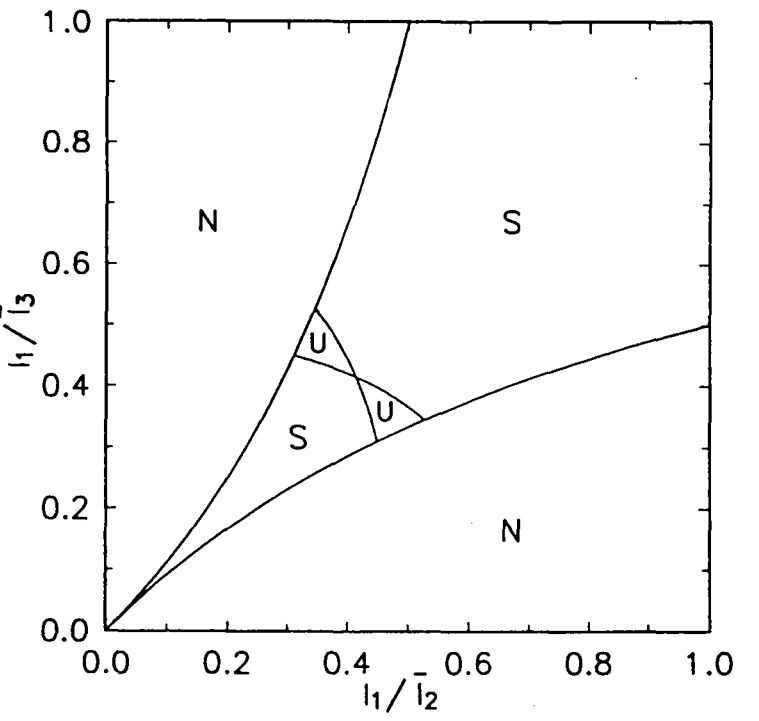

Figure 3.13. Stability diagram in the $I_1/\bar{I}_2$-$I_1/\bar{I}_3$ parameter space for $\beta^2\frac{\hat{m}l^2}{I_1} = 0$.

Regions labeled as (S) and (U) are stable and unstable, respectively. Points within regions labeled as (N) are not physically realizable; the sum of two principal moments of inertia in these regions does not exceed the third.

Notice from Eqs. (3.57-3.62) that the parameters affecting stability are $I_1/\bar{I}_2$, $I_1/\bar{I}_3$, $\beta^2\frac{\hat{m}l^2}{I_1}$ and a_5. The value of $\beta^2\frac{\hat{m}l^2}{I_1}$ is increased uniformly from zero in Figure 3.13 to 0.20 in Figure 3.15. In each of the three figures a_5 is equal to zero.

It is evident from Figures 3.13-3.15 that increasing the value of $\beta^2\frac{\hat{m}l^2}{I_1}$ increases the total area of the unstable regions. Increasing $\beta^2\frac{\hat{m}l^2}{I_1}$ corresponds physically to moving the rest position of the particle away from the carrier body mass center.

Results of two different simulations are presented in Figures 3.16 and 3.17 as a check of the stability diagram given in Figure 3.15. Specific values of the parameters $I_1/\bar{I}_2$ and $I_1/\bar{I}_3$ used in the simulations correspond to the two marked points in Figure 3.15. Values of all the other parameters and initial conditions are reported in Table 3.2. The stable and unstable behavior exhibited in Figures 3.16 and 3.17, respectively, is consistent with the stability diagram in Figure 3.15.

3.6 Summary

An investigation is made in this chapter of the stability of flexible structures spinning about a principal axis of inertia. Particular attention is paid to the stability anal-

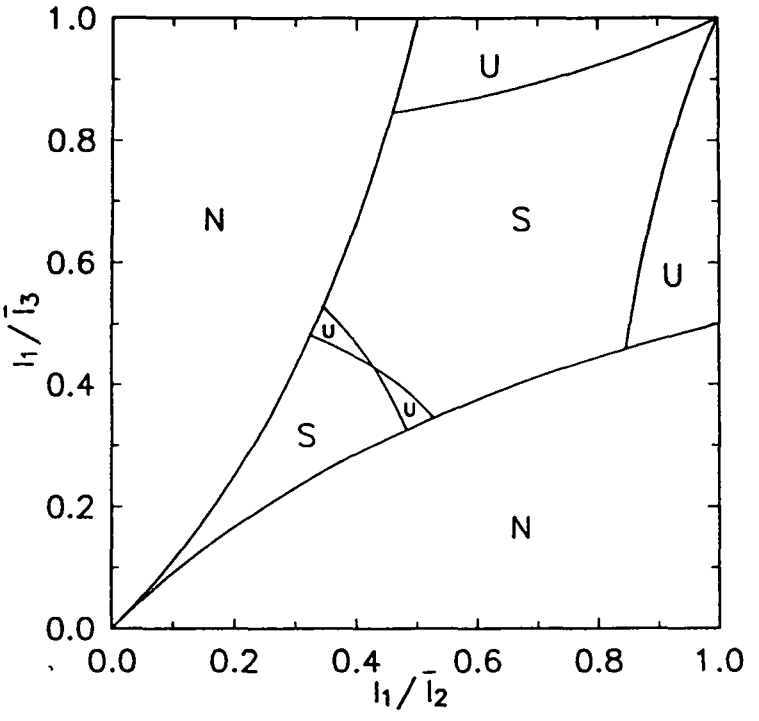

Figure 3.14. Stability diagram in the $I_1/\bar{I}_2$-$I_1/\bar{I}_3$ parameter space for $\beta^2\frac{\hat{m}l^2}{I_1} = 0.1$.

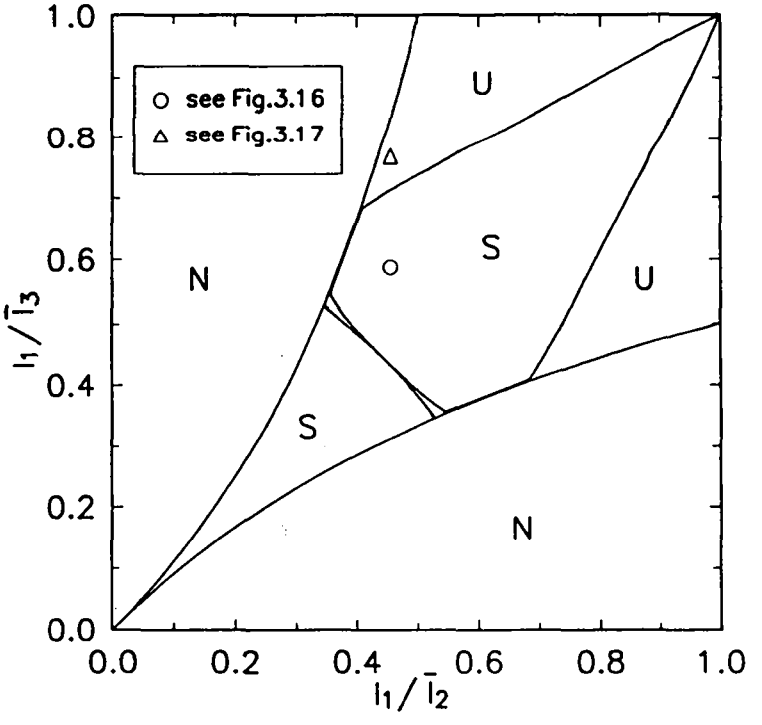

Figure 3.15. Stability diagram in the $I_1/\bar{I}_2$-$I_1/\bar{I}_3$ parameter space for $\beta^2\frac{\hat{m}l^2}{I_1} = 0.2$.

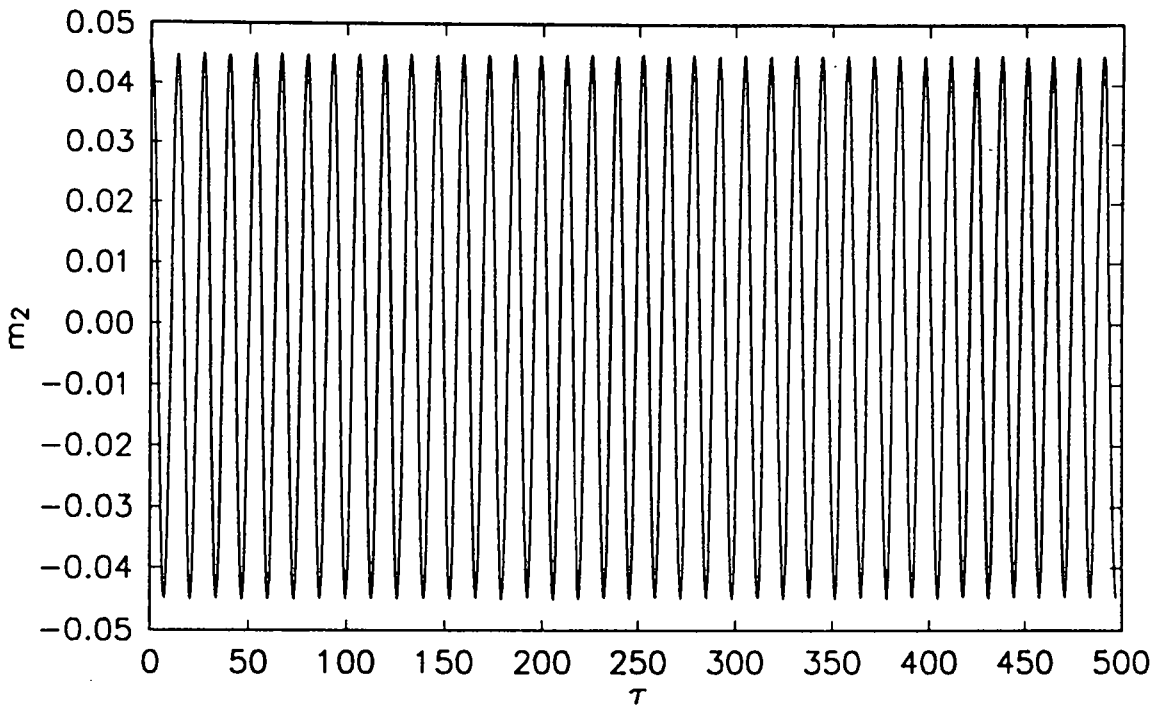

Figure 3.16. Variation of m_2 with time for the resonance relation $\Omega_1 + \Omega_2 = 0$ (stable response).

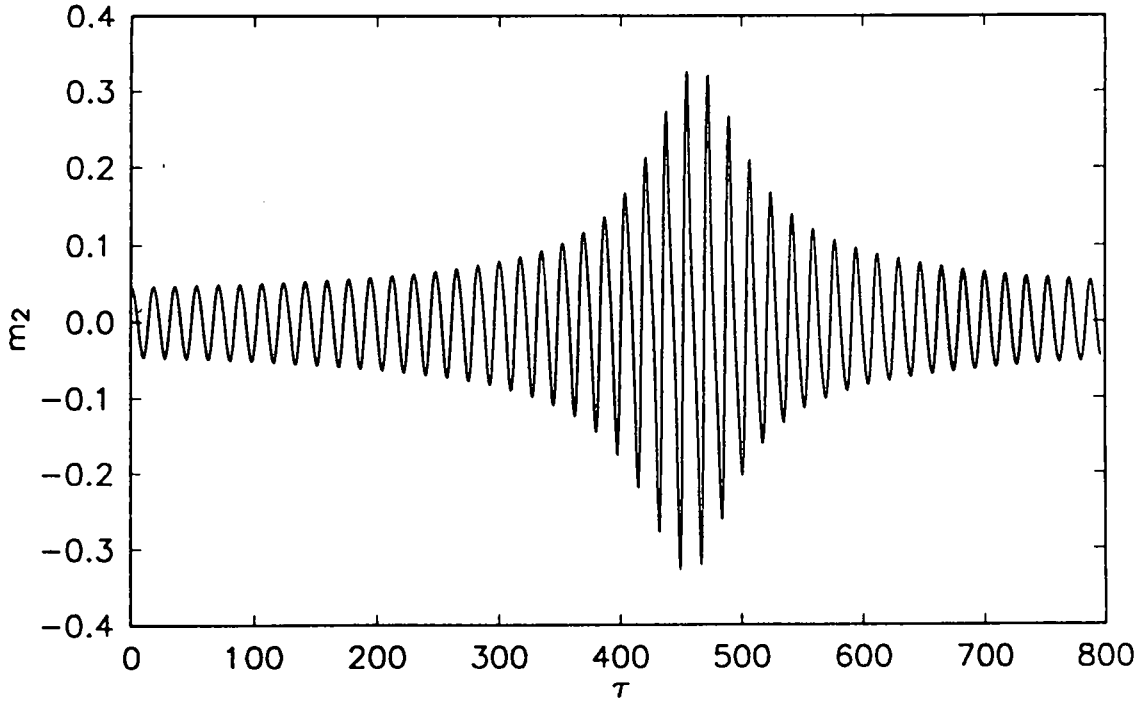

Figure 3.17. Variation of m_2 with time for the resonance relation $\Omega_1 + \Omega_2 = 0$ (unstable response).

ysis of spin about the minor axis. The structures under consideration are assumed to be completely unrestrained, undamped, and free of applied moments. Central to the development is the equivalence of the governing equations of motion to a Hamiltonian system (see Chapter 2). Using this equivalence, existing theory for Hamiltonian systems is applied to the stability analysis of rotating structures.

It is shown that a motion which is spin stable in the linear approximation may be unstable when nonlinear terms are included. For linearly stable systems, the existence of at least one low-order resonance relation among the characteristic frequencies is typically required for instability. Stability criteria are developed for systems satisfying a single resonance relation of order four or less. Guidelines are also provided for determining the stability of systems possesssing multiple resonance relations. An example is provided to demonstrate the application of the stability criteria. Results based upon numerical integration of the equations of motion are shown to be consistent with the results of the stability analysis.

4. Modeling

This chapter is concerned with the investigation and development of a recently formulated method for modeling rotating flexible structures. Originally proposed by Segalman and Dohrmann [51], the method employs a quadratically coupled set of deformation modes to account for geometric stiffening effects. These stiffening effects are not accounted for when conventional linear approaches are adopted.

An exposition is presented of the key features of the new method. Expressions are derived for the strain energy and kinetic energy of a structure in terms of a set of generalized degrees of freedom. These expressions can be used together with results from Chapter 2 to form the equations of motion. Reciprocal relations are established between the deformation modes using an argument based upon conservation of energy.

Computational techniques are developed which facilitate the application of the method. It is shown how all of the terms appearing in the equations of motion can be determined using a finite element analysis code. Motion studies of specific problems found in the literature are provided for purposes of verification. The computational advantages of the new method over a commercially available finite element analysis code are also shown.

4.1 Background

As was noted in Chapter 1, the literature on rotating flexible structures is quite extensive. It is apparent that a great deal of attention has been focused on the analysis of beam-type structures. A lesser, yet significant, effort has been directed towards rotating plates and shells. In both cases, the approaches vary in complexity from the use of fully nonlinear, geometrically exact theories to linearization of the governing equations about an equilibrium.

Unfortunately, a large segment of the literature may not be of much practical use to the analyst. Many papers offer fundamental insight into the behavior of rotating structures, but their usefulness for quantitative prediction is limited to the specific problem analyzed. Such limitations provided much of the impetus for the present work.

Introduction of the finite element method significantly broadened the size and types of problems that can be analyzed. The dynamic response of nonrotating structures can be determined in a straightforward, efficient manner using any one of a number of commercially available programs. Commercial codes can also be used to study the dynamics of structures undergoing large angle motions, but the computational requirements may become excessive even for relatively simple structures.

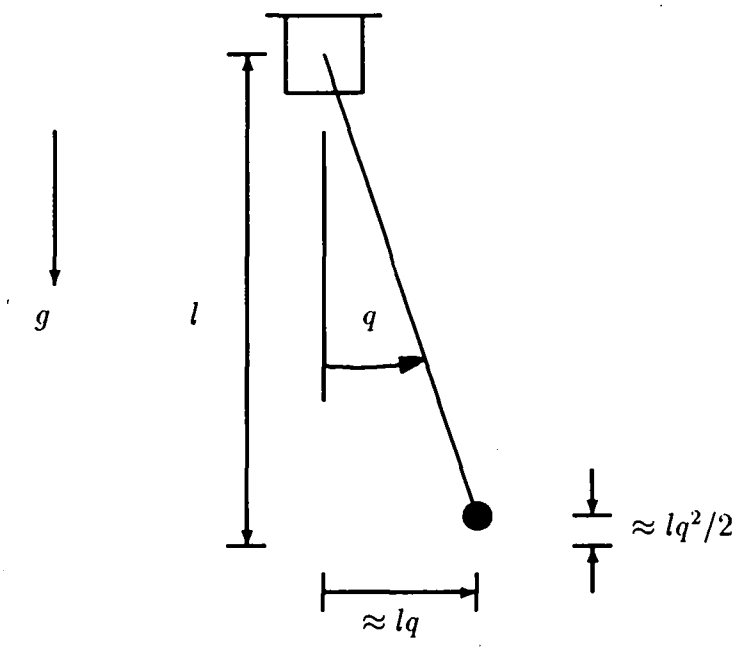

Figure 4.1. Simple illustration of linear and quadratic modes for a pendulum.

Several authors have presented theories for efficiently incorporating finite element methods into the analysis of rotating flexible structures. Most closely related to the present method is the work of Zeiler [49] and Banerjee and Dickens [50]. In both of these approaches, geometric stiffness matrices are calculated for different combinations of steady inertial loads. These matrices are then used during a dynamic simulation to provide the geometric (centrifugal) stiffening. Not unlike the present method, these approaches reduce the computational requirements for a problem by using a relatively small number of generalized degrees of freedom.

4.2 Introduction

The present method is similar to a conventional assumed mode approach with the addition that nonlinear terms are retained in the kinematics of deformation. As an illustration, consider the small amplitude motion of the vertical pendulum shown in Figure 4.1. The linear mode is associated with the horizontal motion and the quadratic mode is associated with the smaller vertical motion. The terminology "quadratic" mode derives from the observation that for horizontal displacements of amplitude q, the vertical displacements have amplitudes proportional to q^2.

Linear and quadratic modes can be calculated analytically for simple problems like the pendulum, or, as is shown later, with a finite element analysis code for more complicated structures. Once obtained, the mode shapes are used in forming the equations of

motion.

The contribution of the quadratic modes to the equations of motion becomes important when existing loads have a significant geometric stiffening effect. For the pendulum shown in Figure 4.1, the restoring effect of gravity is predicted only if the second order motion in the vertical direction is included. An analogous situation is observed in beams where the effect of an axial load on the transverse stiffness is accounted for only when a nonlinear theory is used.

The present method provides an efficient means for modeling the dynamics of rotating flexible structures. The method accounts for nonlinear effects such as geometric stiffening and is applicable to a broad range of structures. Practical application of the method is facilitated through the use of a nonlinear finite element analysis code.

4.3 Theoretical Development

The basic idea underlying the present approach is to express elastic deformations in terms of the nonlinear response of a structure to a set of static loads. To illustrate, consider the system of particles shown in Figure 2.1. Fixing the reference frame B, the system is subjected to a static loading in which the force acting on the l'th particle is given by

$$\mathbf{f}^l(q_1,\ldots,q_n) = \sum_{i=1}^{n} q_i \mathbf{f}_i^l \qquad (l = 1,\ldots,N_p) \tag{4.1}$$

where $q_1,\ldots,q_n$ denote generalized degrees of freedom. The set of vectors $\mathbf{f}_i^l$ for $l = 1,\ldots,N_p$ is collectively referred to as the i'th basis force.

The complete, nonlinear, static response to the loading given by Eq. (4.1) can be expressed as a Taylor series expansion. Retaining only the linear and quadratic terms of this expansion, one obtains

$$\mathbf{u}^l(q_1,\ldots,q_n) = \sum_{i=1}^{n} q_i \boldsymbol{\phi}_i^l + \sum_{i=1}^{n}\sum_{j=1}^{n} q_i q_j \boldsymbol{\psi}_{ij}^l \qquad (l = 1,\ldots,N_p) \tag{4.2}$$

where $\boldsymbol{\phi}_i^l$ and $\boldsymbol{\psi}_{ij}^l$ denote elements of the linear and quadratic modes, respectively. It is assumed, without loss of generality, that $\boldsymbol{\psi}_{ij}^l = \boldsymbol{\psi}_{ji}^l$ for all i and j.

Notice that Eq. (4.2) simplifies to a conventional assumed mode approach if the quadratic terms in the q_i's are neglected. It is shown later that the quadratic terms in Eq. (4.2) must be retained in order to account for geometric stiffening.

It is evident from Eqs. (4.1) and (4.2) that the linear and quadratic modes are determined by the choice of the basis forces. Often it is appropriate to associate the basis forces with the natural modes of vibration, however, there is no restriction on their choice.

4.3.1 Reference Frames

Recall from Chapter 2 that the reference frame B is intended to follow the nominal rigid body motion of the system. A discussion of several options for accomplishing this is given by Canavin and Likins [32]. Two such options, the locally attached and Buckens frames, are discussed below.

For a locally attached frame, B is rigidly fixed to a specific part of the system. A simple illustration is provided by a turbine in which blades are attached to a rigid, rotating hub. Here, the reference frame B could be chosen as the hub itself. Example problems are presented later which make use of locally attached frames.

A second option which is useful for unrestrained systems is the Buckens frame. It was shown by de Veubeke [31] that such a frame has the appealing feature that the mean square of relative displacement is minimized. In addition, a condition of zero relative linear momentum and a linearized condition of zero relative angular momentum are satisfied.

It is assumed in the previous section that B remains fixed during the static loading. In the context of the illustration for the locally attached frame, this condition simply means that the hub is made stationary. For the Buckens frame, this condition implies that

$$\sum_{i=1}^{N_p} m_i(\mathbf{r}^i + \mathbf{u}^i) = 0 \tag{4.3}$$

and

$$\sum_{i=1}^{N_p} m_i(\mathbf{r}^i \times \mathbf{u}^i) = 0 \tag{4.4}$$

Implicit in Eq. (4.3) is the assumption that the origin of B coincides with the mass center of the system.

Equations (4.3) and (4.4) represent linear constraints which are imposed during the static loading. Such constraints are easily accomodated by the finite element method.

4.3.2 Strain Energy

An expression for the strain energy in terms of the q_i's is derived in this section. To begin, consider a quasi-static application of the basis forces to the system. Fixing the q_i's, the loads on the system are assumed to be given by

$$\mathbf{f}^l(s) = \sum_{i=1}^{n} sq_i\mathbf{f}_i^l \qquad (l = 1, \ldots, N_p) \tag{4.5}$$

where s varies from zero to unity.

It follows from conservation of energy that the work done by the applied loads equals the change in the strain energy, U, of the system. Thus,

$$\begin{aligned} U &= \sum_{l=1}^{N_p} \int \mathbf{f}^l(s) \cdot d\mathbf{u}^l \\ &\overset{(4.2,4.5)}{=} \sum_{l=1}^{N_p} \left(\frac{1}{2} \sum_{i=1}^{n} \sum_{j=1}^{n} q_i q_j \mathbf{f}_i^l \cdot \boldsymbol{\phi}_j^l + \frac{2}{3} \sum_{i=1}^{n} \sum_{j=1}^{n} \sum_{k=1}^{n} q_i q_j q_k \mathbf{f}_i^l \cdot \boldsymbol{\psi}_{jk}^l \right) \end{aligned} \tag{4.6}$$

It is assumed in the derivation of Eq. (4.6) that all of the loads are applied simultaneously. Consider an alternative scenario in which:

1. The loads associated with the basis force i are applied.
2. While holding the loads from Step 1 constant, the loads associated with the basis force j are applied.

The changes in strain energy resulting from Steps 1 and 2 are given, respectively, by

$$U_i = \sum_{l=1}^{N_p} \frac{1}{2} q_i^2 \mathbf{f}_i^l \cdot \boldsymbol{\phi}_i^l + \frac{2}{3} q_i^3 \mathbf{f}_i^l \cdot \boldsymbol{\psi}_{ii}^l \tag{4.7}$$

and

$$\begin{aligned} U_j &= \sum_{l=1}^{N_p} \frac{1}{2} q_j^2 \mathbf{f}_j^l \cdot \boldsymbol{\phi}_j^l + \frac{2}{3} q_j^3 \mathbf{f}_j^l \cdot \boldsymbol{\psi}_{jj}^l + q_i q_j \mathbf{f}_i^l \cdot \boldsymbol{\phi}_j^l + \\ &\quad 2 q_i^2 q_j \mathbf{f}_i^l \cdot \boldsymbol{\psi}_{ij}^l + q_i q_j^2 (\mathbf{f}_j^l \cdot \boldsymbol{\psi}_{ij}^l + \mathbf{f}_i^l \cdot \boldsymbol{\psi}_{jj}^l) \end{aligned} \tag{4.8}$$

The total change in strain energy, U_{ij}, is the sum of U_i and U_j. Thus,

$$\begin{aligned} U_{ij} &\overset{(4.7,4.8)}{=} \sum_{l=1}^{N_p} \frac{1}{2} (q_i^2 \mathbf{f}_i^l \cdot \boldsymbol{\phi}_i^l + q_j^2 \mathbf{f}_j^l \cdot \boldsymbol{\phi}_j^l) + \frac{2}{3} (q_i^3 \mathbf{f}_i^l \cdot \boldsymbol{\psi}_{ii}^l + q_j^3 \mathbf{f}_j^l \cdot \boldsymbol{\psi}_{jj}^l) + \\ &\quad q_i q_j \mathbf{f}_i^l \cdot \boldsymbol{\phi}_j^l + 2 q_i^2 q_j \mathbf{f}_i^l \cdot \boldsymbol{\psi}_{ij}^l + q_i q_j^2 (\mathbf{f}_j^l \cdot \boldsymbol{\psi}_{ij}^l + \mathbf{f}_i^l \cdot \boldsymbol{\psi}_{jj}^l) \end{aligned} \tag{4.9}$$

The strain energy is independent of the order of the loading, hence,

$$U_{ij} = U_{ji} \tag{4.10}$$

Substitution of Eq. (4.9) into Eq. (4.10) and equating like powers in the q_i's yields the reciprocal relations

$$\sum_{l=1}^{N_p} \mathbf{f}_i^l \cdot \boldsymbol{\phi}_j^l = \sum_{l=1}^{N_p} \mathbf{f}_j^l \cdot \boldsymbol{\phi}_i^l \qquad (i, j = 1, \ldots, n) \tag{4.11}$$

and

$$\sum_{l=1}^{N_p} \mathbf{f}_i^l \cdot \boldsymbol{\psi}_{ij}^l = \sum_{l=1}^{N_p} \mathbf{f}_j^l \cdot \boldsymbol{\psi}_{ii}^l \qquad (i,j = 1,\ldots,n) \tag{4.12}$$

Equations (4.11) and (4.12) can be used as a check once the linear and quadratic modes are determined.

4.3.3 Kinetic Energy

Recall from Chapter 2 that the kinetic energy of the system can be expressed conveniently in terms of the mass matrix, M. Expressions are developed in this section for the elements of M in terms of the q_i's.

Equations (2.14) and (2.22) are repeated below for convenience.

$$T = \frac{1}{2}\sum_{l=1}^{N_p} m_l \left[\frac{\partial u_k^l}{\partial q_i}\dot{q}_i + \epsilon_{kmp}\omega_m(r_p^l + u_p^l)\right]\left[\frac{\partial u_k^l}{\partial q_j}\dot{q}_j + \epsilon_{kqr}\omega_q(r_r^l + u_r^l)\right] \tag{4.13}$$

$$T = \frac{1}{2}[\omega_1\ \omega_2\ \omega_3\ \dot{q}_1\ \ldots\ \dot{q}_n]M[\omega_1\ \omega_2\ \omega_3\ \dot{q}_1\ \ldots\ \dot{q}_n]^T \tag{4.14}$$

Expansion of Eqs. (4.13) and (4.14) and equating the coefficients of like terms yields

$$m_{11} = \sum_{l=1}^{N_p} m_l\left[(r_2^l + u_2^l)^2 + (r_3^l + u_3^l)^2\right] \tag{4.15}$$

$$m_{22} = \sum_{l=1}^{N_p} m_l\left[(r_3^l + u_3^l)^2 + (r_1^l + u_1^l)^2\right] \tag{4.16}$$

$$m_{33} = \sum_{l=1}^{N_p} m_l\left[(r_1^l + u_1^l)^2 + (r_2^l + u_2^l)^2\right] \tag{4.17}$$

$$m_{12} = -\sum_{l=1}^{N_p} m_l(r_1^l + u_1^l)(r_2^l + u_2^l) \tag{4.18}$$

$$m_{13} = -\sum_{l=1}^{N_p} m_l(r_1^l + u_1^l)(r_3^l + u_3^l) \tag{4.19}$$

$$m_{23} = -\sum_{l=1}^{N_p} m_l(r_2^l + u_2^l)(r_3^l + u_3^l) \tag{4.20}$$

$$m_{1,j+3} = \sum_{l=1}^{N_p} m_l\left[(r_2^l + u_2^l)\frac{\partial u_3^l}{\partial q_j} - (r_3^l + u_3^l)\frac{\partial u_2^l}{\partial q_j}\right] \qquad (j = 1,\ldots,n) \tag{4.21}$$

$$m_{2,j+3} = \sum_{l=1}^{N_p} m_l\left[(r_3^l + u_3^l)\frac{\partial u_1^l}{\partial q_j} - (r_1^l + u_1^l)\frac{\partial u_3^l}{\partial q_j}\right] \qquad (j = 1,\ldots,n) \tag{4.22}$$

$$m_{3,j+3} = \sum_{l=1}^{N_p} m_l \left[(r_1^l + u_1^l)\frac{\partial u_2^l}{\partial q_j} - (r_2^l + u_2^l)\frac{\partial u_1^l}{\partial q_j} \right] \qquad (j = 1, \ldots, n) \qquad (4.23)$$

$$m_{i+3,j+3} = \sum_{l=1}^{N_p} m_l \left[\frac{\partial u_1^l}{\partial q_i}\frac{\partial u_1^l}{\partial q_j} + \frac{\partial u_2^l}{\partial q_i}\frac{\partial u_2^l}{\partial q_j} + \frac{\partial u_3^l}{\partial q_i}\frac{\partial u_3^l}{\partial q_j} \right] \qquad (i, j = 1, \ldots, n) \qquad (4.24)$$

Equations with explicit dependence on the q_i's are obtained from substitution of

$$u_k^l \overset{(4.2)}{=} \sum_{r=1}^{n} q_r \boldsymbol{\phi}_r^l \cdot \mathbf{b}_k + \sum_{r=1}^{n}\sum_{s=1}^{n} q_r q_s \boldsymbol{\psi}_{rs}^l \cdot \mathbf{b}_k \qquad (k = 1, 2, 3) \qquad (4.25)$$

into Eqs. (4.15-4.24).

It is shown in Chapter 2 that the equations of motion can be expressed entirely in terms of the strain energy and the mass matrix. Thus, the governing equations can be formed once the right hand side of Eqs. (4.6) and (4.15-4.24) are known.

4.3.4 Effects of Moments and Rotational Inertia

Recall from 4.3 that the static loading used to determine the linear and quadratic modes only involves concentrated forces. Moreover, in the derivation of Eq. (4.13) the particles of the system are assumed to be point masses with zero rotational inertia. The development is extended in this section to account for the effects of concentrated moments and rotational inertia.

As before, the static forces acting on the system are assumed to be given by Eq. (4.1). Provision is now made for the loading to include concentrated moments as well. Letting $\mathbf{t}^l$ denote the moment acting on the l'th particle, one assumes that

$$\mathbf{t}^l(q_1, \ldots, q_n) = \sum_{i=1}^{n} q_i \mathbf{t}_i^l \qquad (l = 1, \ldots, N_p) \qquad (4.26)$$

where the vectors $\mathbf{t}_i^l$ $(l = 1, \ldots, N_p)$ comprise the i'th basis torque. Like the basis forces, the basis torques can be associated with the natural modes of vibration, however, there is no restriction on their choice.

The static response to the loading given by Eqs. (4.1) and (4.26) can be expanded as a Taylor series. The deflections of the particles are expressed as before by Eq. (4.2), whereas the rotations are given by

$$\boldsymbol{\theta}^l(q_1, \ldots, q_n) = \sum_{i=1}^{n} q_i \boldsymbol{\varphi}_i^l \qquad (l = 1, \ldots, N_p) \qquad (4.27)$$

Notice that only the linear terms of the Taylor series are retained in Eq. (4.27). This is in contrast to Eq. (4.2) where quadratic terms are retained in order to account for geometric stiffening.

The inclusion of applied moments and rotational inertia in the formulation necessitates slight modifications to the equations obtained earlier for the strain energy and the mass matrix. Once these modifications are made, the equations of motion are formed in the same manner as before. It is noted that in many problems the effects of rotational inertia can be neglected without affecting the results of simulations significantly.

Strain Energy

To determine the strain energy, it is necessary now to also include the work done by the concentrated moments. Therefore, one must add to the right hand side of Eq. (4.6) the term U^t, where

$$U^t = \sum_{l=1}^{N_p} \frac{1}{2} \sum_{i=1}^{n} \sum_{j=1}^{n} q_i q_j \mathbf{t}_i^l \cdot \boldsymbol{\varphi}_j^l \tag{4.28}$$

Mass Matrix

Let $\mathbf{c}_1^l$,$\mathbf{c}_2^l$,$\mathbf{c}_3^l$ denote unit vectors fixed in the l'th particle and parallel to $\mathbf{b}_1$,$\mathbf{b}_2$,$\mathbf{b}_3$ when the system is undeformed. It is assumed, for simplicity, that the inertia dyadic of the l'th particle is diagonal and given by

$$\mathbf{I}^l = I_1^l \mathbf{c}_1^l \mathbf{c}_1^l + I_2^l \mathbf{c}_2^l \mathbf{c}_2^l + I_3^l \mathbf{c}_3^l \mathbf{c}_3^l \tag{4.29}$$

Defining,

$$\varphi_{ik}^l \equiv \boldsymbol{\varphi}_i^l \cdot \mathbf{b}_k \qquad (k = 1,2,3) \tag{4.30}$$

and

$$\theta_k^l \equiv \sum_{i=1}^{n} q_i \varphi_{ik}^l \qquad (k = 1,2,3) \tag{4.31}$$

the rotational kinetic energy, T^{rl}, of the l'th particle is given by

$$T^{rl} = \frac{1}{2} \sum_{k=1}^{3} I_k^l (\omega_k^l)^2 \tag{4.32}$$

where

$$\omega_k^l = \omega_k + \epsilon_{kqr} \omega_q \theta_r^l + \sum_{i=1}^{n} \dot{q}_i \varphi_{ik}^l \qquad (k = 1,2,3) \tag{4.33}$$

It follows from Eqs. (4.32) and (4.33) that the required additions to the mass matrix are given by

$$m_{11}^r = \sum_{l=1}^{N_p} I_1^l + I_2^l (\theta_3^l)^2 + I_3^l (\theta_2^l)^2 \tag{4.34}$$

$$m_{22}^r = \sum_{l=1}^{N_p} I_2^l + I_3^l (\theta_1^l)^2 + I_1^l (\theta_3^l)^2 \tag{4.35}$$

$$m^r_{33} = \sum_{l=1}^{N_p} I^l_3 + I^l_1(\theta^l_2)^2 + I^l_2(\theta^l_1)^2 \tag{4.36}$$

$$m^r_{12} = \sum_{l=1}^{N_p} (I^l_1 - I^l_2)\theta^l_3 - I^l_3\theta^l_1\theta^l_2 \tag{4.37}$$

$$m^r_{13} = \sum_{l=1}^{N_p} (I^l_3 - I^l_1)\theta^l_2 - I^l_2\theta^l_3\theta^l_1 \tag{4.38}$$

$$m^r_{23} = \sum_{l=1}^{N_p} (I^l_2 - I^l_3)\theta^l_1 - I^l_1\theta^l_2\theta^l_3 \tag{4.39}$$

$$m^r_{1,j+3} = \sum_{l=1}^{N_p} I^l_1\varphi^l_{j1} + I^l_3\varphi^l_{j3}\theta^l_2 - I^l_2\varphi_{j2}\theta^l_3 \qquad (j = 1,\ldots,n) \tag{4.40}$$

$$m^r_{2,j+3} = \sum_{l=1}^{N_p} I^l_2\varphi^l_{j2} + I^l_1\varphi^l_{j1}\theta^l_3 - I^l_3\varphi_{j3}\theta^l_1 \qquad (j = 1,\ldots,n) \tag{4.41}$$

$$m^r_{3,j+3} = \sum_{l=1}^{N_p} I^l_3\varphi^l_{j3} + I^l_2\varphi^l_{j2}\theta^l_1 - I^l_1\varphi_{j1}\theta^l_2 \qquad (j = 1,\ldots,n) \tag{4.42}$$

$$m^r_{i+3,j+3} = \sum_{l=1}^{N_p} I^l_1\varphi^l_{i1}\varphi^l_{j1} + I^l_2\varphi^l_{i2}\varphi^l_{j2} + I^l_3\varphi^l_{i3}\varphi^l_{j3} \qquad (i,j = 1,\ldots,n) \tag{4.43}$$

4.4 Computational Techniques

The inertia properties and the linear and quadratic modes of a structure must be determined in order to apply the present approach. For simple problems, it may be possible to obtain closed-form expressions for these quantities. More complicated problems may require the use of numerical techniques.

A major advantage of the present approach is its applicability to a variety of problems. By utilizing a finite element analysis code capable of nonlinear static analysis, the linear and quadratic modes can be determined for a wide range of structures. Codes capable of linear dynamic analysis can be used to calculate the necessary mass and rotational inertia terms.

Computational techniques are presented in this section which make use of finite element analysis results to determine all of the required quantities. A discussion is also provided on how to determine the basis forces and torques associated with the natural modes of vibration.

4.4.1 Calculation of Linear and Quadratic Modes

Recall that the linear and quadratic modes are defined in terms of the static response of a system to the loading given by Eqs. (4.1) and (4.26).[3] Let $\mathbf{u}^l(s_i)$ denote the static deflection of the l'th particle for a loading in which $q_i = s_i$ and $q_j = 0$ for $j \neq i$. The Taylor series expansion of $\mathbf{u}^l(s_i)$ is given by

$$\mathbf{u}^l(s_i) = s_i\boldsymbol{\phi}_i^l + s_i^2\boldsymbol{\psi}_{ii}^l + {}^3P_i^l + {}^4P_i^l + {}^5P_i^l + \mathcal{O}(s_i^6) \tag{4.44}$$

where ${}^mP_i^l$ denotes a monomial of degree m in the variable s_i. Similarly,

$$\mathbf{u}^l(-s_i) = -s_i\boldsymbol{\phi}_i^l + s_i^2\boldsymbol{\psi}_{ii}^l - {}^3P_i^l + {}^4P_i^l - {}^5P_i^l + \mathcal{O}(s_i^6) \tag{4.45}$$

$$\mathbf{u}^l(2s_i) = 2s_i\boldsymbol{\phi}_i^l + 4s_i^2\boldsymbol{\psi}_{ii}^l + 8({}^3P_i^l) + 16({}^4P_i^l) + 32({}^5P_i^l) + \mathcal{O}(s_i^6) \tag{4.46}$$

$$\mathbf{u}^l(-2s_i) = -2s_i\boldsymbol{\phi}_i^l + 4s_i^2\boldsymbol{\psi}_{ii}^l - 8({}^3P_i^l) + 16({}^4P_i^l) - 32({}^5P_i^l) + \mathcal{O}(s_i^6) \tag{4.47}$$

It follows from Eqs. (4.44-4.47) that

$$\boldsymbol{\psi}_{ii}^l = \frac{\mathbf{u}^l(s_i) + \mathbf{u}^l(-s_i)}{2s_i^2} + \mathcal{O}(s_i^2) \qquad (i = 1, \ldots, n) \tag{4.48}$$

and

$$\boldsymbol{\psi}_{ii}^l = \frac{16[\mathbf{u}^l(s_i) + \mathbf{u}^l(-s_i)] - [\mathbf{u}^l(2s_i) + \mathbf{u}^l(-2s_i)]}{24s_i^2} + \mathcal{O}(s_i^4) \qquad (i = 1, \ldots, n) \tag{4.49}$$

The numerators in Eqs. (4.48) and (4.49) can be evaluated using nonlinear static finite element analysis results once a value of s_i is specified. Estimates for the quadratic modes are then obtained by neglecting the higher order terms in these equations.

The accuracy of the estimates for the quadratic modes depends to a large extent on the value chosen for s_i. If computers had unlimited precision, then one could simply assign a very small value to s_i and obtain excellent results. This is not advisable for practical purposes since s_i^2 appears in the denominators of Eqs. (4.48) and (4.49).

Experience indicates that for double precision arithmetic s_i should be chosen such that the maximum displacement is somewhere between 10^{-3} and 10^{-5} times the maximum dimension of the structure. The accuracy of the estimates can be measured by the agreement between the results from Eqs. (4.48) and (4.49). It may be necessary in some cases to modify the initial choice for s_i.

Equations for estimating the quadratic modes $\boldsymbol{\psi}_{ij}^l$ with $i \neq j$ are presented below. Let $\mathbf{u}^l(s_i, s_j)$ denote the static deflection of the l'th particle for a loading with $q_i = s_i$, $q_j = s_j$, and $q_k = 0$ for $k \neq i$ and $k \neq j$. Expanding $\mathbf{u}^l(s_i, s_j)$ as a Taylor series yields

$$\mathbf{u}^l(s_i, s_j) = s_i\boldsymbol{\phi}_i^l + s_j\boldsymbol{\phi}_j^l + s_i^2\boldsymbol{\psi}_{ii}^l + 2s_is_j\boldsymbol{\psi}_{ij}^l + s_j^2\boldsymbol{\psi}_{jj}^l + {}^3P_{ij}^l + {}^4P_{ij}^l + {}^5P_{ij}^l + \mathcal{O}(s_i^6 + s_j^6) \tag{4.50}$$

[3]Loads involving concentrated moments are permitted only for finite element models which have rotational degrees of freedom. Examples include structures modeled with beams, plates, or shells.

where ${}^m P_{ij}^l$ denotes a polynomial containing only degree m terms in the variables s_i and s_j.

Using Eqs. (4.44) and Eq. (4.50) one obtains

$$\hat{\mathbf{u}}^l(s_i, s_j) = 2s_i s_j \boldsymbol{\psi}_{ij}^l + {}^3\hat{P}_{ij}^l + {}^4\hat{P}_{ij}^l + {}^5\hat{P}_{ij}^l + \mathcal{O}(s_i^6 + s_j^6) \tag{4.51}$$

where

$$\hat{\mathbf{u}}^l(s_i, s_j) = \mathbf{u}^l(s_i, s_j) - \mathbf{u}^l(s_i) - \mathbf{u}^l(s_j) \tag{4.52}$$

and

$${}^m\hat{P}_{ij}^l = {}^m P_{ij}^l - {}^m P_i^l - {}^m P_j^l \tag{4.53}$$

Similarly,

$$\hat{\mathbf{u}}^l(-s_i, -s_j) = 2s_i s_j \boldsymbol{\psi}_{ij}^l - {}^3\hat{P}_{ij}^l + {}^4\hat{P}_{ij}^l - {}^5\hat{P}_{ij}^l + \mathcal{O}(s_i^6 + s_j^6) \tag{4.54}$$

$$\hat{\mathbf{u}}^l(2s_i, 2s_j) = 8s_i s_j \boldsymbol{\psi}_{ij}^l + 8({}^3\hat{P}_{ij}^l) + 16({}^4\hat{P}_{ij}^l) + 32({}^5\hat{P}_{ij}^l) + \mathcal{O}(s_i^6 + s_j^6) \tag{4.55}$$

$$\hat{\mathbf{u}}^l(-2s_i, -2s_j) = 8s_i s_j \boldsymbol{\psi}_{ij}^l - 8({}^3\hat{P}_{ij}^l) + 16({}^4\hat{P}_{ij}^l) - 32({}^5\hat{P}_{ij}^l) + \mathcal{O}(s_i^6 + s_j^6) \tag{4.56}$$

It follows from Eqs. (4.51) and (4.54-4.56) that

$$\boldsymbol{\psi}_{ij}^l = \frac{\hat{\mathbf{u}}^l(s_i, s_j) + \hat{\mathbf{u}}^l(-s_i, -s_j)}{4s_i s_j} + \mathcal{O}(s_i^2 + s_j^2) \qquad (i = 1, \ldots, n),\ (j = i+1, \ldots, n) \tag{4.57}$$

and

$$\boldsymbol{\psi}_{ij}^l = \frac{16[\hat{\mathbf{u}}^l(s_i, s_j) + \hat{\mathbf{u}}^l(-s_i, -s_j)] - [\hat{\mathbf{u}}^l(2s_i, 2s_j) + \hat{\mathbf{u}}^l(-2s_i, -2s_j)]}{48 s_i s_j} + \mathcal{O}(s_i^4 + s_j^4)$$
$$(i = 1, \ldots, n),\ (j = i+1, \ldots, n) \tag{4.58}$$

Estimates for the quadratic modes are obtained by neglecting the higher order terms in Eqs. (4.57) and (4.58). Here again, the accuracy of the estimates can be measured by the agreement between the results from these two equations.

The linear modes are determined by considering again the loading in which $q_i = s_i$ and $q_j = 0$ for $j \neq i$. The displacements and rotations calculated from a *linear* static finite element analysis are denoted by $\mathbf{u}_{lin}^l(s_i)$ and $\boldsymbol{\theta}_{lin}^l(s_i)$, respectively. The linear modes are given by

$$\boldsymbol{\phi}_i^l = \mathbf{u}_{lin}^l(s_i)/s_i \qquad (i = 1, \ldots, n) \tag{4.59}$$

and

$$\boldsymbol{\varphi}_i^l = \boldsymbol{\theta}_{lin}^l(s_i)/s_i \qquad (i = 1, \ldots, n) \tag{4.60}$$

Equations (4.48-4.49) and (4.57-4.58) show that the calculation of each quadratic mode requires four different analyses. Thus, the total number of nonlinear static analyses required is equal to $2n(n+1)$. A total of n linear static analyses are needed to calculate the linear modes.

4.4.2 Calculation of Masses and Rotational Inertias

A method is presented in this section for determining the particle masses and rotational inertias given a finite element model of the structure. The method is based upon the idea of identifying the particles with the nodes of a finite element model. Practical use of the method is facilitated by a finite element analysis code capable of linear dynamic analysis.

The linear equations of motion for a displacement-based finite element method are expressed in matrix notation as

$$M_{fe}\ddot{u} + K_{fe}u = f \tag{4.61}$$

where M_{fe} and K_{fe} are the mass and stiffness matrices, respectively. The column matrix u contains all of the translational and rotational nodal degrees of freedom; f contains the corresponding applied forces and moments.

If the elastic properties of each material in the model are reduced to zero, then all of the elements of the stiffness matrix become equal to zero. Accordingly, Eq. (4.61) simplifies to

$$M_{fe}\ddot{u} = f \tag{4.62}$$

Consider now imposing a constant value, a, of acceleration on all of the degrees of freedom associated with translation in the global 1-direction. The reaction forces necessary to accomplish this motion are contained in f, which can be determined from a single time step in a linear dynamic analysis. The mass of the l'th particle is then given by

$$m_l = (\mathbf{f}_r^l \cdot \mathbf{b}_1)/a \qquad (l = 1, \ldots, N_p) \tag{4.63}$$

where $\mathbf{f}_r^l$ is the reaction force acting on the l'th node.

Use of Eq. (4.63) amounts to lumping the mass of the structure at the nodes. Such an approximation is reasonable as long as there is a sufficient number of nodes in the model.

The rotational inertias of the particles are determined in a manner similar to that for the masses. Consider imposing a constant value, α_k, of angular acceleration on all of the degrees of freedom associated with rotation in the global k-direction. Assuming a diagonal inertia dyadic, the rotational inertia scalars are given by

$$I_k^l = (\mathbf{m}_{rk}^l \cdot \mathbf{b}_k)/\alpha_k \qquad (l = 1, \ldots, N_p),\ (k = 1, 2, 3) \tag{4.64}$$

where $\mathbf{m}_{rk}^l$ is the reaction moment acting on the l'th node.

4.4.3 Basis Forces and Torques for Natural Modes

The natural modes of vibration of a structure are often used in assumed mode approaches as a basis for the description of elastic deformations. A procedure for determining the basis forces and torques associated with these modes is described below.

In the context of the finite element method, the frequencies, ω_i, and the mode shapes, ϕ_i, for the natural modes of vibration are obtained by solving the generalized eigenvalue problem

$$(K_{fe} - \omega_i^2 M_{fe})\phi_i = 0 \tag{4.65}$$

The static loads, f_i, required to deform the structure into the mode shape ϕ_i are given by

$$f_i = K_{fe}\phi_i \tag{4.66}$$

Thus, one possible approach to determine the associated basis forces and torques is to impose the deformations given by ϕ_i in a linear static analysis and calculate the reaction forces and moments.

Solving Eq. (4.65) for $K_{fe}\phi_i$ and substituting the result into Eq. (4.66) yields

$$f_i = M_{fe}(\omega_i^2 \phi_i) \tag{4.67}$$

which, when compared with Eq. (4.62), motivates the following alternative approach for determining f_i which does not explicity require the mass matrix:

1. Reduce the elastic properties of each material in the model to zero.
2. Impose the accelerations given by $\omega_i^2\phi_i$ in one step of a linear dynamic analysis and calculate the reaction forces and moments.

The latter approach is preferred to the former because of the possible ill-conditioning of the stiffness matrix.

4.5 Example Problems

Example problems are presented in this section to demonstrate the use of the present approach. The first example involves a single degree of freedom system and is used to highlight the importance of quadratic kinematics in rotating structures. A rotating cantilevered beam is considered in the second example and comparisons made with results from the literature. The third example deals with the motion of a rotating cantilevered plate. Here, comparisons are made both with results from the literature and a commercial finite element analysis code capable of geometric nonlinear dynamic analysis. The final example examines the motion of an unrestrained, rotating flexible structure.

4.5.1 Example 1

The system for the first example is shown in Figure 4.2 and consists of a rigid link of length l pinned to a rigid hub of radius r. Relative angular motion between the link and the hub is restrained by a torsional spring with spring constant k. The mass, m, of

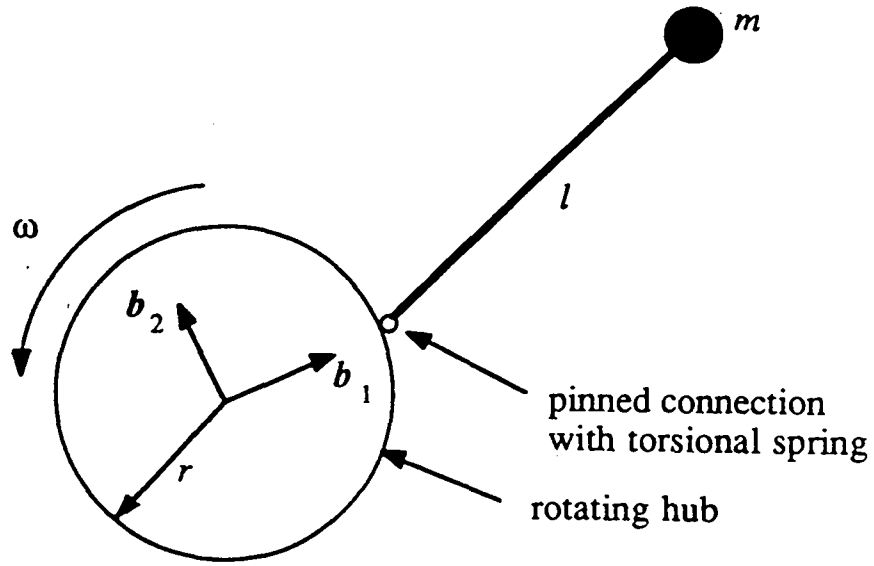

Figure 4.2. Sketch of the system for Example 1.

the link is concentrated at its tip, and unit vectors $\mathbf{b}_1$ and $\mathbf{b}_2$ are fixed within the hub. The rotation rate, ω, of the hub is assumed to be a specified function of time.

The primary purpose of this example is to provide a simple illustration of the importance of quadratic kinematics in rotating systems. This is accomplished by comparing the linearized equations of motion for the system obtained from two different approaches. In the first approach, both the linear and the quadratic modes are included in the derivation. In the second approach, only the linear mode is considered.

Quadratic Kinematics

A logical choice for the basis force associated with the tip mass is $(k/l)\mathbf{b}_2$. Thus,

$$\mathbf{f}(q) \overset{(4.1)}{=} (k/l)q\mathbf{b}_2 \tag{4.68}$$

The tip deflection (to second order in q) which results from fixing the hub and applying the force in Eq. (4.68) is given by

$$\mathbf{u}(q) \overset{(4.2)}{=} ql\mathbf{b}_2 + q^2\psi\mathbf{b}_1 \tag{4.69}$$

where

$$\psi = -l/2 \tag{4.70}$$

The velocity, $\mathbf{v}$, of the tip mass in an inertial frame, N, is given by

$$\mathbf{v} = {}^N\frac{d}{dt}[(r+l)\mathbf{b}_1 + \mathbf{u}(q)]$$

$$\overset{(4.69)}{=} (2q\dot{q}\psi - \omega q l)\mathbf{b}_1 + [\dot{q}l + \omega(r + l + q^2\psi)]\mathbf{b}_2 \tag{4.71}$$

and hence, the kinetic energy, T, is expressed as

$$T = \frac{1}{2}m\left[(2q\dot{q}\psi - \omega q l)^2 + [\dot{q}l + \omega(r + l + q^2\psi)]^2\right] \tag{4.72}$$

The strain energy, U, is given simply by

$$U = \frac{1}{2}kq^2 \tag{4.73}$$

Substitution of Eqs. (4.72) and (4.73) into Lagrange's equation and linearization of the result yields

$$\ddot{q} + [\omega_n^2 - \omega^2 - 2\omega^2(1 + r/l)(\psi/l)]q = -\dot{\omega}(1 + r/l) \tag{4.74}$$

where

$$\omega_n^2 = \frac{k}{ml^2} \tag{4.75}$$

Upon substitution of Eq. (4.70) into (4.74) one arrives at

$$\ddot{q} + [\omega_n^2 + \omega^2(r/l)]q = -\dot{\omega}(1 + r/l) \tag{4.76}$$

Linear Kinematics

Consideration of only linear kinematics amounts to setting ψ equal to zero in Eq. (4.69), and thus assuming

$$\mathbf{u}(q) = ql\mathbf{b}_2 \tag{4.77}$$

The linearized equation of motion derived under this assumption is obtained by setting ψ equal to zero in Eq. (4.74). The result is

$$\ddot{q} + [\omega_n^2 - \omega^2]q = -\dot{\omega}(1 + r/l) \tag{4.78}$$

Discussion

It is evident from comparison of Eqs. (4.76) and (4.78) that the two approaches result in different linearized equations of motion. The geometric (centrifugal) stiffening of the system is predicted correctly by Eq. (4.76) when the quadratic kinematics are included in the derivation. This is in contrast to Eq. (4.78) which indicates a softening of the system. The differences between the two equations become significant when the absolute value of the spin rate is of the same order of magnitude as ω_n.

This example illustrates that a conventional assumed mode approach based on linear kinematics may lead to spurious equations of motion unless some corrective measure is taken. The corrective measure in Refs. [49] and [50] is to include geometric stiffness matrices in the analysis. The present approach does not require the use of such matrices; geometric stiffening is accounted for implicitly by the quadratic modes.

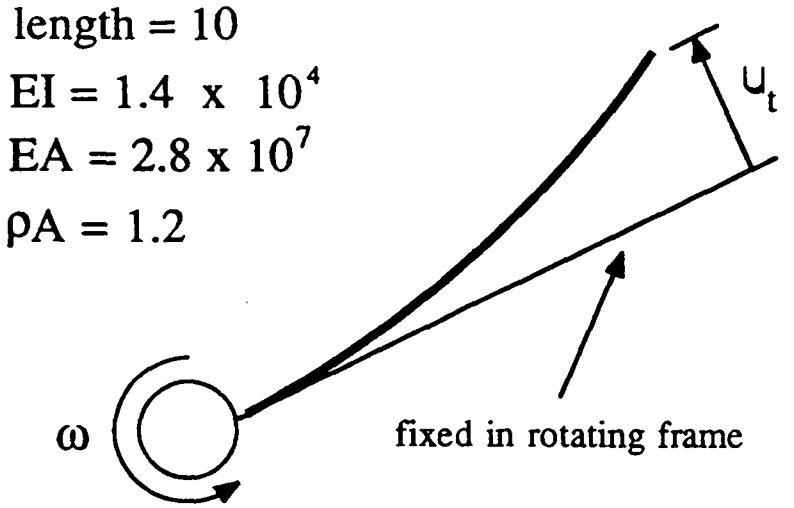

Figure 4.3. Sketch of the system for Example 2.

4.5.2 Example 2

This example deals with the motion of a cantilevered beam rotating about an axis perpendicular to its length. The beam properties are reported in Figure 4.3 and correspond to those for a problem considered previously in the literature. The spin rate, ω, of the cantilevered end of the beam is assumed to be a prescribed function of time given by

$$\omega(t) = \begin{cases} \Omega/T[t - (T/2\pi)\sin(2\pi t/T)] & 0 \le t \le T \\ \Omega & t > T \end{cases} \tag{4.79}$$

A finite element model consisting of eight linearly interpolated beam elements was constructed using the commercially available code, ABAQUS [66]. An eigenvalue analysis of the cantilevered beam was performed to determine the first two linear modes of vibration. The basis forces associated with these modes were then used to determine the quadratic modes. The effects of rotational inertia are small in this problem and therefore were neglected.

The linearized equations of motion are expressed in matrix notation as

$$M\ddot{q} + (K + \omega^2 K_{\omega^2})q = \dot{\omega} f \tag{4.80}$$

where, for $n = 2$,

$$M = \begin{bmatrix} 3.0342 & -0.0091 \\ -0.0091 & 3.2590 \end{bmatrix}, \quad K = \begin{bmatrix} 43.206 & -0.130 \\ -0.130 & 1776.7 \end{bmatrix} \tag{4.81}$$

$$K_{\omega^2} = \begin{bmatrix} 0.5658 & 2.1053 \\ 2.1053 & 16.445 \end{bmatrix}, \quad q = \begin{bmatrix} q_1 \\ q_2 \end{bmatrix}, \quad f = \begin{bmatrix} -34.444 \\ 5.8592 \end{bmatrix} \tag{4.82}$$

The equation of motion for a single generalized degree of freedom ($n = 1$) is obtained by setting $q_2 = 0$ in Eq. (4.80)

The transverse tip deflection, u_t, is given in terms of q_1 and q_2 by

$$u_t = (1.000)q_1 + (0.997)q_2 \tag{4.83}$$

The equations for a conventional assumed mode (CAM) approach based on linear kinematics are identical to Eqs. (4.80-4.83) with the exception that

$$K_{\omega^2} = \begin{bmatrix} -3.0341 & 0.0091 \\ 0.0091 & -3.2590 \end{bmatrix} \tag{4.84}$$

Plots of the transverse tip deflection are shown in Figure 4.4 for a spin-up maneuver defined by Eq. (4.79) with $\Omega = 6$ and $T = 15$. Very similar results are obtained with the present approach for the one mode ($n = 1$) and two mode ($n = 2$) approximations. In both cases, the results indicate a stable response of the beam. The results based upon the CAM approach exhibit unstable behavior.

The unstable growth of the CAM solution is explained by observing that at least one of the eigenvalues of the matrix $K + \omega^2 K_{\omega^2}$ is negative for $|\omega| > 3.77$ rad/sec. Thus, under these conditions, the homogeneous solution to Eq. (4.80) contains terms with exponential growth. In contrast, both eigenvalues of $K + \omega^2 K_{\omega^2}$ are always positive for the present approach since K_{ω^2} is positive definite.

Simo and Vu-Quoc [42] previously studied the motion of this same problem using beam elements which employ a finite strain theory capable of accounting for large rotations. A plot of the transverse tip deflection obtained using their approach is shown in Figure 4.5. Notice the excellent agreement with the results shown in Figure 4.4.

A major advantage of the present method is that the computational requirements for a problem can often be reduced by using a relatively small number of generalized degrees of freedom. For this example, very good estimates for the transverse tip deflection are obtained using just a single generalized degree of freedom. The computational advantages of the present method are made even more apparent in the next example.

4.5.3 Example 3

The third example deals with the motion of a plate rotating about a fixed axis which is aligned with its cantilevered edge. The dimensions for the plate are shown in Figure 4.6 and correspond to those used in an earlier study by Banerjee and Dickens [50]. The density and Poisson's ratio of the material are taken as those of steel and the

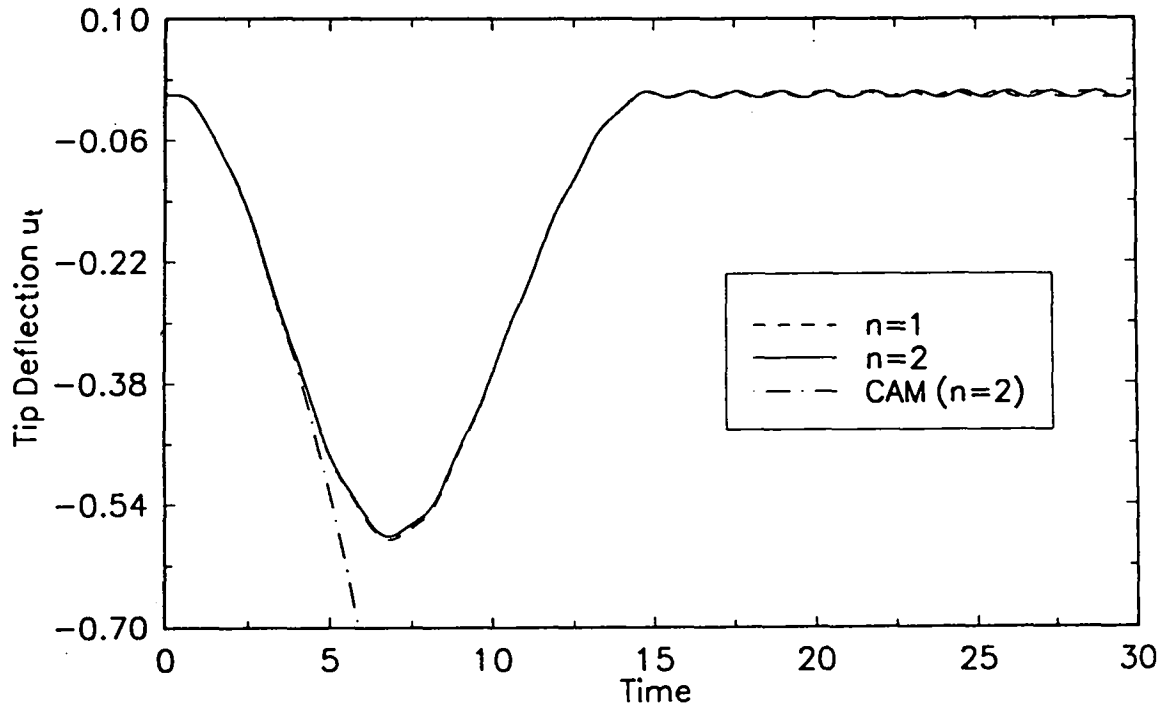

Figure 4.4. Tip deflection of cantilevered beam for spin-up maneuver with $\Omega = 6$ and $T = 15$.

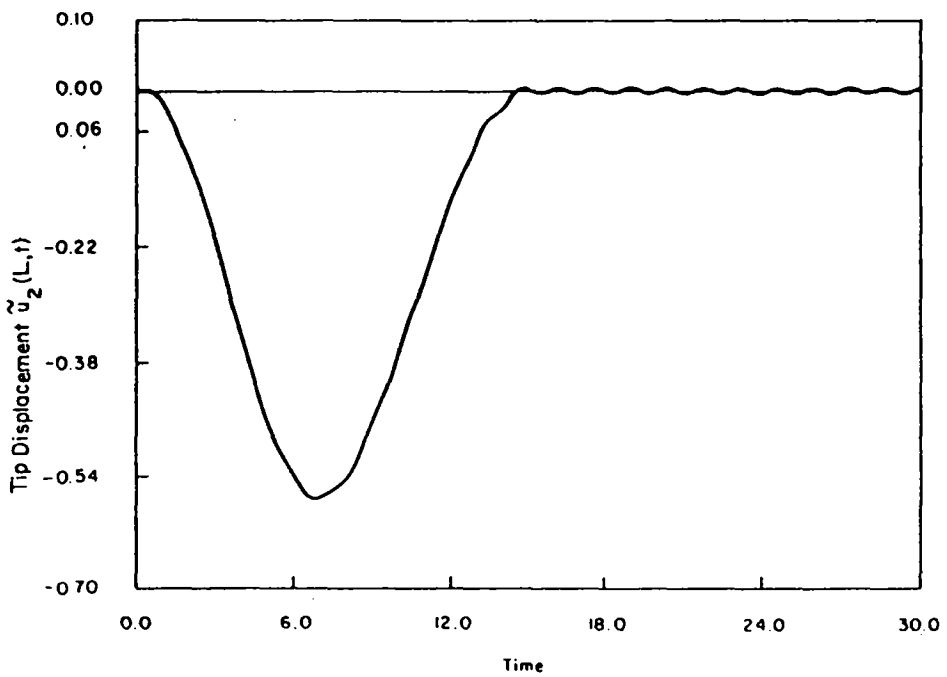

Figure 4.5. Tip deflection of cantilevered beam for spin-up maneuver with $\Omega = 6$ and $T = 15$. Results are taken from Ref. 42.

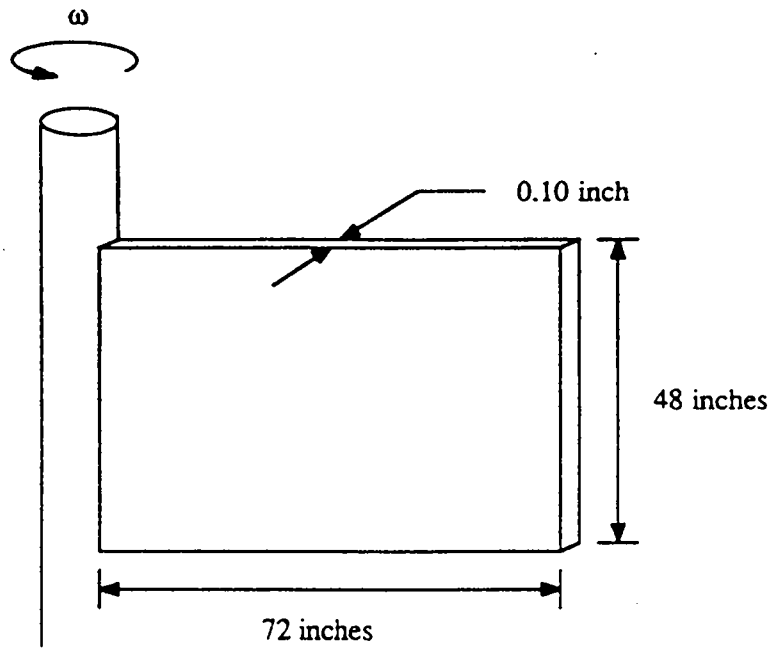

Figure 4.6. Sketch of the system for Example 3.

elastic modulus is chosen to yield a first natural frequency of 0.75 rad/sec. The spin rate of a rotating frame attached to the fixed edge of the plate is assumed to be a specified function of time given by Eq. (4.79).

An ABAQUS model of the plate was constructed using an 8×6 mesh of S4R5 shell elements. The first three linear modes of vibration for the plate were calculated using ABAQUS and are shown in Figure 4.7. Procedures outlined earlier were then used to determine the quadratic modes and nodal masses. The effects of rotational inertia were neglected.

A simulation was performed for a spin-up maneuver with $\Omega = 1.25$ rad/sec and $T = 30$ sec in an attempt to verify the present approach. The maximum transverse deflection of a corner of the plate was determined to be in excess of 10 inches. A plot for the same problem taken from Ref. 50 and shown in Figure 4.8 indicates, however, a maximum deflection of only about 0.3 inch.

Close examination of Figure 4.8 shows that there are very small residual oscillations during the part of the spin-up maneuver in which $\dot{\omega} = 0$. Interestingly, these oscillations appear to have a frequency much closer to 0.75 Hz than to 0.75 rad/sec. This observation motivated the conjecture that perhaps the results in Figure 4.8 are for a cantilevered plate with a first natural frequency of 0.75 Hz rather than 0.75 rad/sec.

To test this conjecture, the original value of the elastic modulus was increased by a factor of $(2\pi)^2$. Simulation results for the stiffer plate shown in Figure 4.9 are in excellent

Mode 1

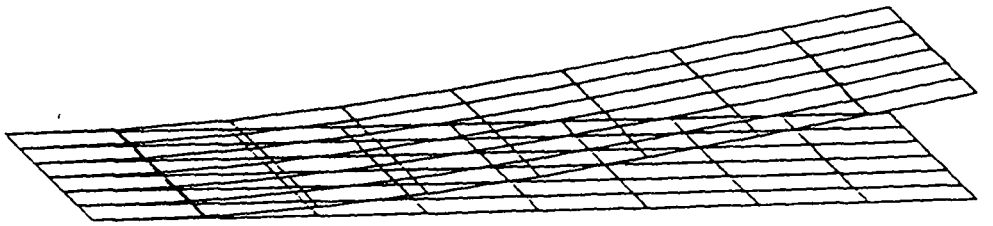

Mode 2

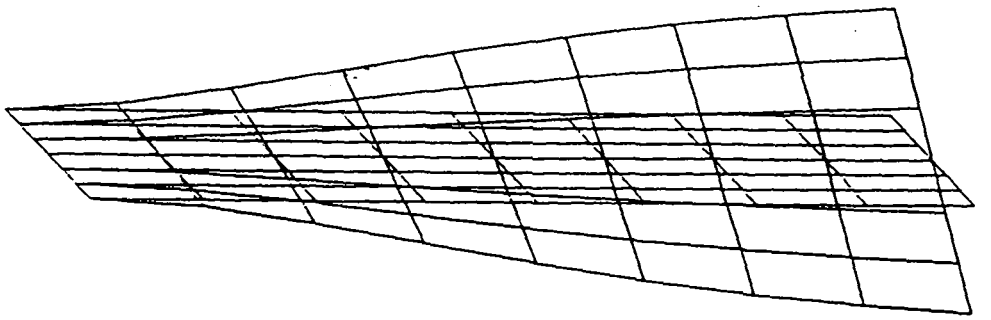

Mode 3

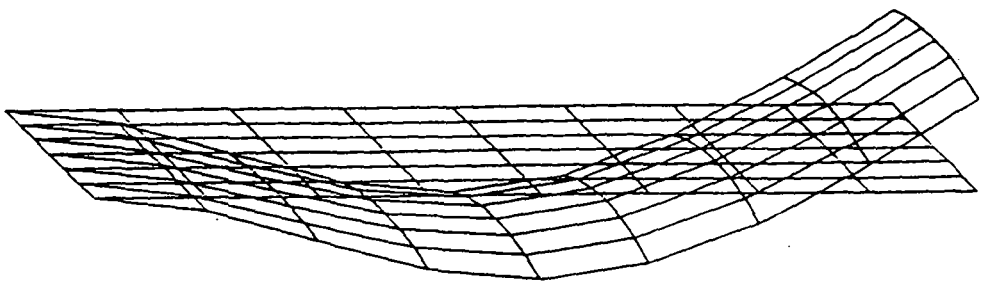

Figure 4.7. First three mode shapes of cantilevered plate. Both the undeformed and deformed shapes are shown.

agreement with those in Figure 4.8. Different sign conventions are adopted in the two figures; both indicate the corner deflection lags the motion of the rotating frame during the period $0 < t < 30$ sec. Notice that the results based upon a CAM approach are also in reasonable agreement.

Simulations were also performed using the original value of the elastic modulus for a spin-up maneuver with $\Omega = 0.8$ rad/sec and $T = 50$ sec. This example examines the situation where the steady value of the spin rate rate exceeds the first natural frequency of the nonrotating plate. Plots of the transverse corner deflection are shown in Figure 4.10 for both one mode and three mode approximations. The second mode is antisymmetric (see Fig. 4.7) and therefore is not excited. Results are also shown in the figure for the CAM approach. As in the cantilevered beam example, the results based upon the CAM approach exhibit physically unrealistic behavior.

For purposes of comparison, ABAQUS was used directly to simulate the motion for the above spin-up maneuver. The same model of the plate used earlier was employed in a geometrically nonlinear dynamic analysis using the convergence parameters reported in Figure 4.11. The corner tip deflection was obtained by projecting the ABAQUS results onto a coordinate system fixed in the rotating reference frame. The ABAQUS results are in excellent agreement with those shown in Figure 4.10.

Two different values of the parameter HAFTOL were used to obtain the results shown in Figure 4.11. This parameter affects the accuracy of the solution by controlling the automatic time incrementation scheme used by ABAQUS. Smaller values of this parameter generally result in more accurate solutions.

The cpu times on a VAX 8550 for HAFTOL=3000 and HAFTOL=300 were 2.7 hours and 8.2 hours, respectively. In contrast, the cpu time required by the present approach to numerically integrate the equations of motion was only 3.5 seconds[4]. The differences in the computational requirements for ABAQUS and the present approach are clearly significant.

The above example demonstrates that simulation of large angle motions with a commercial code may not always be practical. A great deal of computing resources were required to obtain the results in Figure 4.11 even though the total rotation of the plate was only about three quarters of one revolution.

4.5.4 Example 4

The final example examines the motion of the plate used in Example 3 when all four edges are free. In contrast to the previous three examples, the motion here is completely unrestrained. In addition, the analysis employs a Buckens reference frame as opposed

[4]The total cpu time to form the equations of motion for $n = 3$ was around 5 minutes.

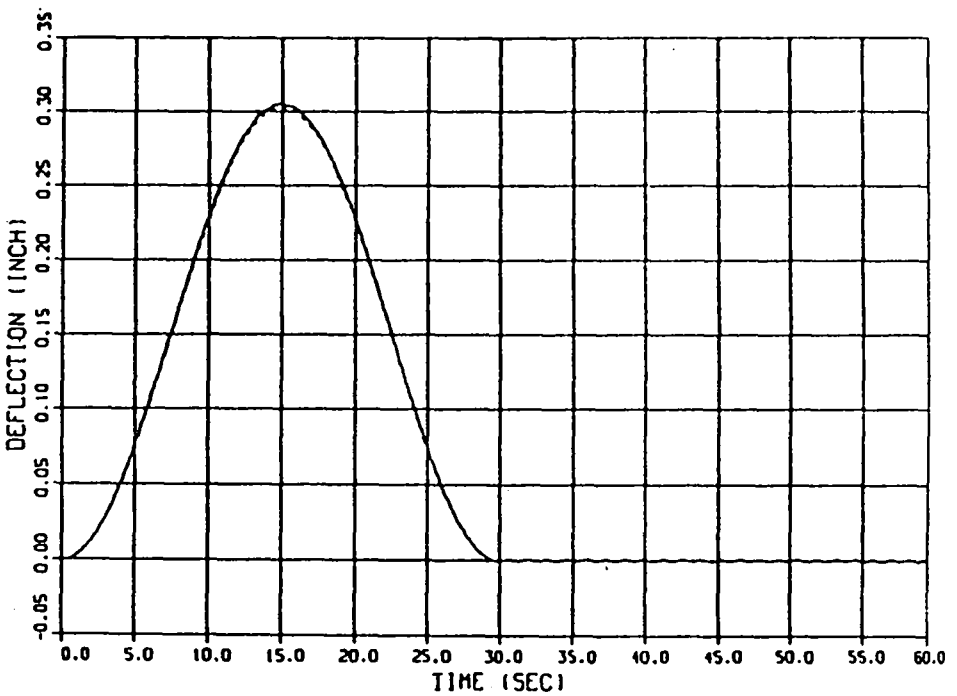

Figure 4.8. Corner deflection of cantilevered plate for spin-up maneuver with $\Omega = 1.25$ rad/sec and $T = 30$ sec. Results are taken from Ref. 50.

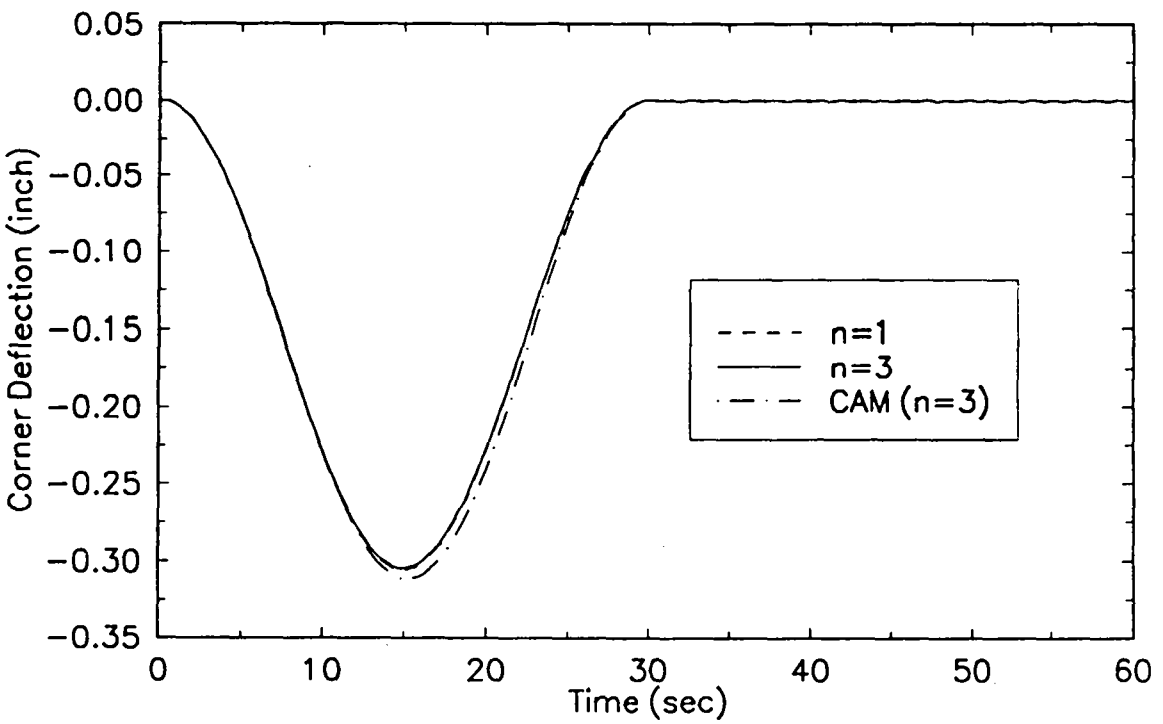

Figure 4.9. Corner deflection of cantilevered plate for spin-up maneuver with $\Omega = 1.25$ rad/sec and $T = 30$ sec. First natural frequency of plate is 0.75 Hz.

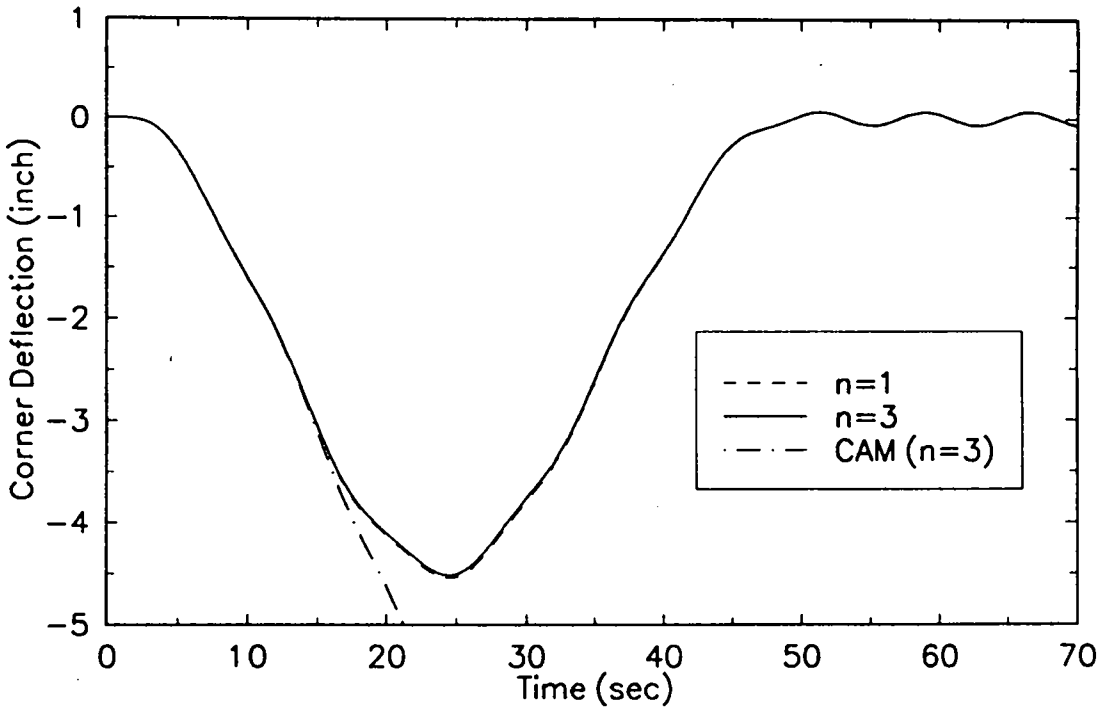

Figure 4.10. Corner deflection of cantilevered plate for spin-up maneuver with $\Omega = 0.8$ rad/sec and $T = 50$ sec. First natural frequency of plate is 0.75 rad/sec.

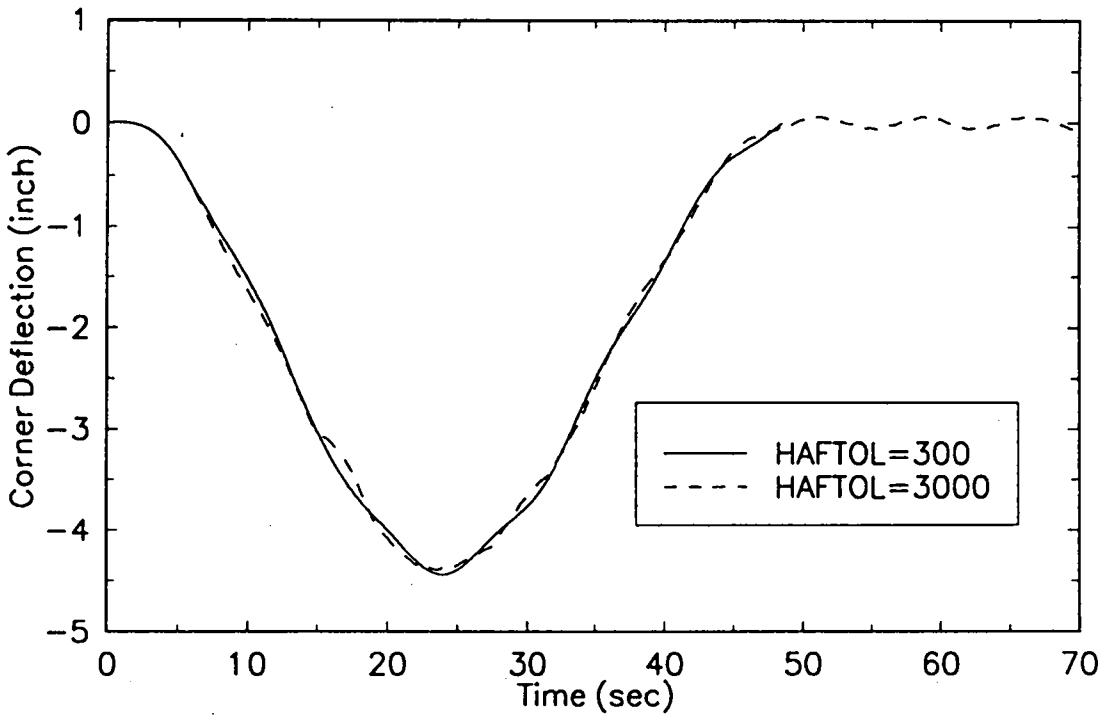

Figure 4.11. Corner deflection of cantilevered plate for spin-up maneuver with $\Omega = 0.8$ rad/sec and $T = 50$. Results obtained using ABAQUS with parameters PTOL=1×10^{-4} and MTOL=8×10^{-4}.

to a locally attached frame. The first three flexible modes of vibration calculated using ABAQUS are shown in Figure 4.12.

The orientation of the Buckens frame is chosen such that $\mathbf{b}_1$ (see Fig. 2.1) is perpendicular to the plane of the undeformed plate. The initial angle between the angular momentum vector and $\mathbf{b}_1$ is 5 degrees for the motion under consideration. Moreover, the plate is initially deformed into the shape of its first flexible mode.

Plots of corner deflection relative to the Buckens frame are shown in Figures 4.13 and 4.14 for nominal spin rates of 1 rad/sec and 4 rad/sec (see Eq. (2.29)). The results shown in the two figures were obtained from numerical integration of Eqs. (2.35-2.39). The first mode remains uncoupled from the others even for nonzero values of the spin rate. As such, the response shown in the two figures is entirely from the first mode.

Comparing the two sets of results in Figure 4.13 shows that the CAM approach predicts a plate vibration frequency lower than that of the present approach. The differences are even more pronounced in Figure 4.14 when the spin rate is increased by a factor of four. It is clear from comparison of the two figures that the present approach predicts the expected increase in the frequency of vibration with increased spin rate. Quite the opposite is observed for the results based on the CAM approach which fails to account for the stiffening effect.

4.6 Summary

A new method for modeling rotating flexible structures is developed and investigated in this chapter. The method is similar to conventional assumed mode approaches with the addition that quadratic terms are retained in the kinematics of deformation. Retention of these terms is shown to account for the geometric stiffening effects which occur in rotating structures.

Reciprocal relations are established between the deformation modes by using an argument based upon conservation of energy. Expressions are also developed for the strain energy and kinetic energy of a structure in terms of a set of generalized degrees of freedom. These expressions can be used together with results from Chapter 2 to form the equations of motion.

Computational techniques are developed for the practical implementation of the method. The techniques make use of finite element analysis results, and thus are applicable to a wide variety of structures. It is shown that all of the terms appearing in the equations of motion can be determined by utilizing a finite element analysis code capable of nonlinear static and linear dynamic analysis.

Motion studies of specific problems are provided to demonstrate the validity of the new method. Excellent agreement is found both with results from the literature and ones

Mode 1

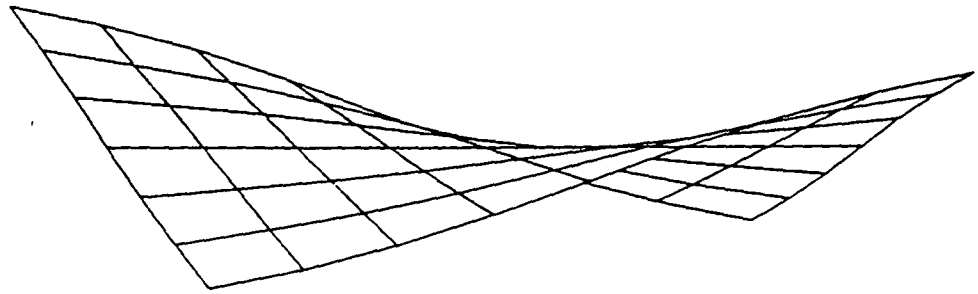

Mode 2

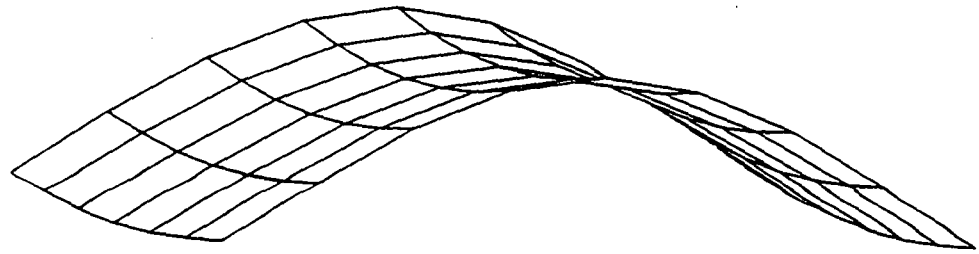

Mode 3

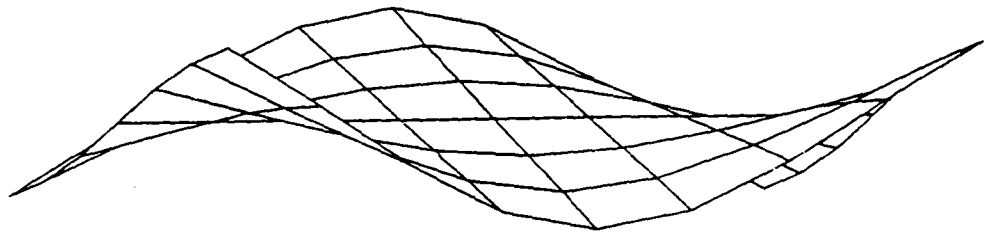

Figure 4.12. First three mode shapes of unrestrained plate.

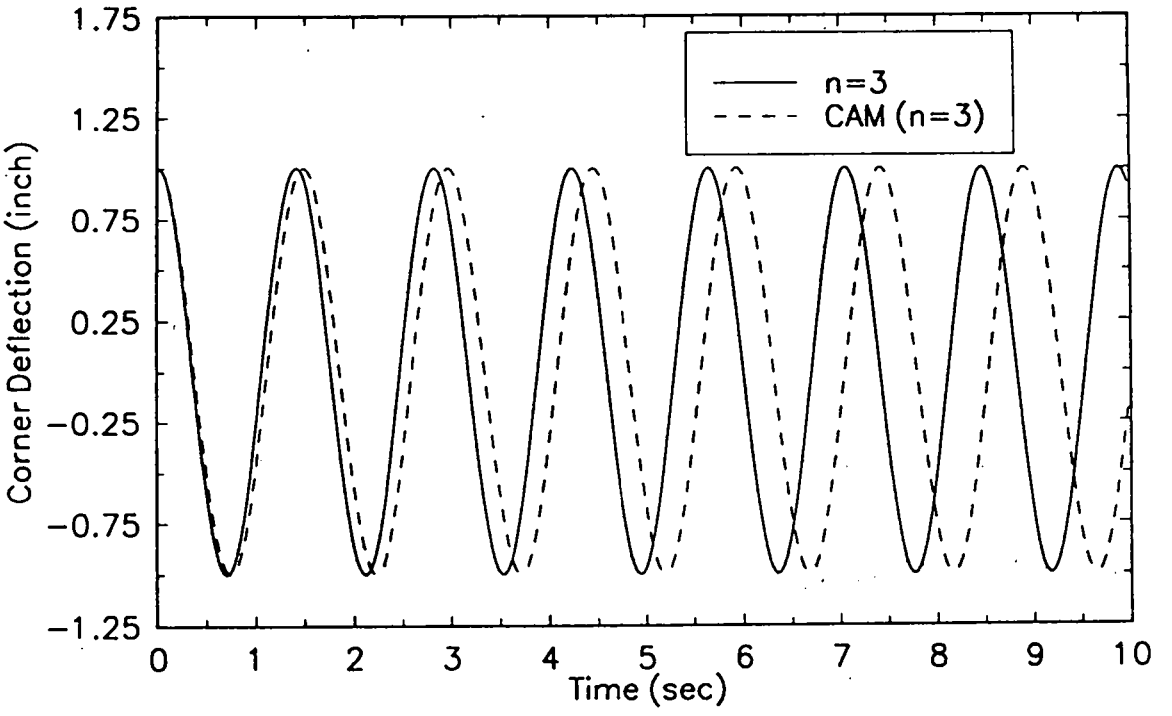

Figure 4.13. Corner deflection of unrestrained plate for a nominal spin rate of 1 rad/sec.

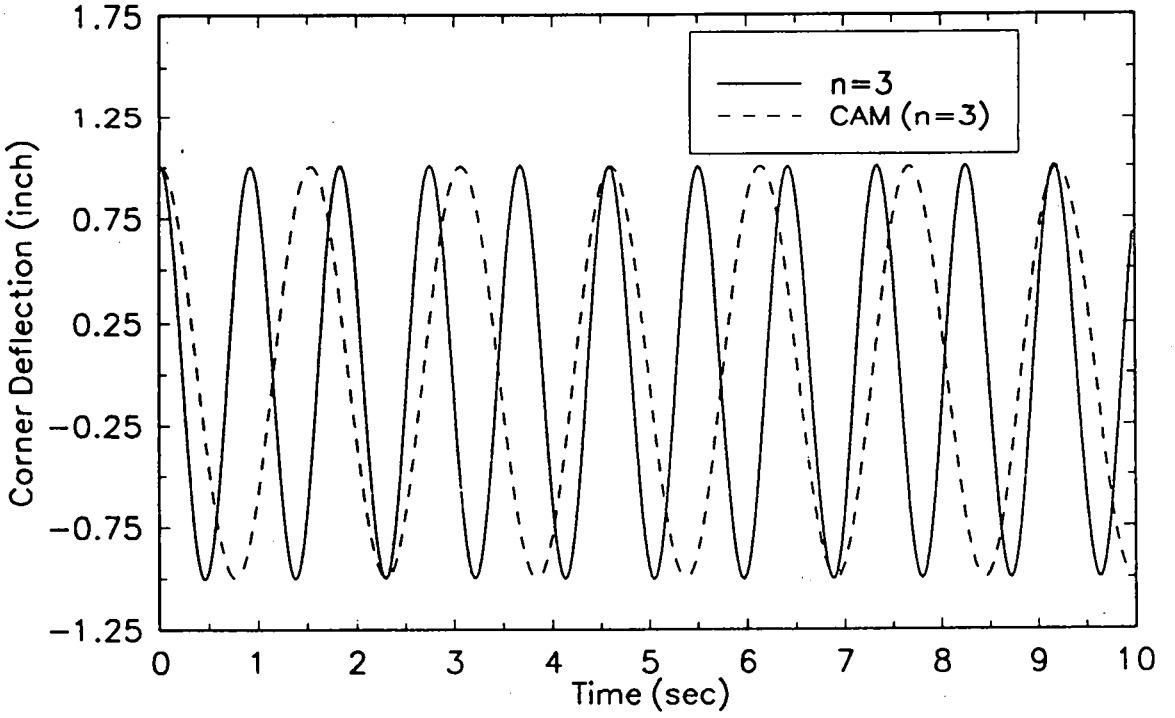

Figure 4.14. Corner deflection of unrestrained plate for a nominal spin rate of 4 rad/sec.

obtained from a commercial finite element analysis code capable of geometric nonlinear dynamic analysis. The computational advantages of the new method are demonstrated.

5. Conclusions

5.1 Summary of Results

5.1.1 Equations of Motion

Equations of motion are developed in Chapter 2 for rotating flexible structures that are undamped and free of applied forces and moments. Central to the development is the use of a floating reference frame which follows the overall rigid body motion of the structure. Within this frame, elastic deformations are expressed as functions of n generalized degrees of freedom. A nonlinear transformation of variables is devised which permits the expression of the equations of motion as a Hamiltonian system with $n + 1$ degrees of freedom. This result is shown later to provide the basis for the analysis of spin stability. Application of the transformation is illustrated for a problem involving the torque-free motion of a rigid body.

5.1.2 Stability Analysis

The nonlinear stability of undamped flexible structures free of applied forces and moments is investigated in Chapter 3 for spin about the minor axis. The equivalence established between the equations of motion and a Hamiltonian system is used as an avenue for the study of spin stability. It is shown that a motion which is spin stable in the linear approximation may be unstable when nonlinear terms are included. For linearly stable systems, the existence of at least one low-order resonance relation among the characteristic frequencies is typically required for instability. Stability criteria are developed in detail for systems satisfying a single resonance relation of order four or less. General guidelines are also provided for determining the stability of systems possessing multiple resonance relations. These criteria are applied to the stability analysis of an example problem and confirmed by numerical integration of the equations of motion.

5.1.3 Modeling

A new method for modeling rotating flexible structures is developed and investigated in Chapter 4. The method is similar to conventional assumed mode approaches with the addition that quadratic terms are retained in the kinematics of deformation. Retention of these terms is shown to account for the geometric stiffening effects which occur in rotating structures.

Reciprocal relations are established between the deformation modes using an argument based upon conservation of energy. Expressions are also developed for the strain

energy and kinetic energy of a structure in terms of a set of generalized degrees of freedom. These expressions can be used together with results from Chapter 2 to form the equations of motion for a structure.

Computational techniques are developed for the practical implementation of the method. The techniques make use of finite element analysis results, and thus are applicable to a wide variety of structures. It is shown that all of the terms appearing in the equations of motion can be determined using a finite element analysis code capable of nonlinear static and linear dynamic analysis. Motion studies of specific problems are provided to demonstrate the validity of the new method. Excellent agreement is found both with results from the literature and ones obtained from a commercial finite element analysis code. The computational advantages of the new method are demonstrated.

5.2 Contributions

A significant contribution is made to the current understanding of the stability of rotating flexible structures. In particular, a method of stability analysis is developed for undamped structures spinning about the axis of minimum moment of inertia. Previous work in the literature has dealt almost exclusively with the stability analysis of spin about the axis of maximum moment of inertia.

A contribution is made towards a practical means for the motion simulation of rotating flexible structures. A new method of modeling is presented which can be implemented efficiently and is applicable to a wide variety of different structures. The method provides a practical alternative to the use of commercial codes which may require excessive amounts of computer time.

A new transformation of variables is developed which allows the governing equations of motion for rotating flexible structures to be expressed as a Hamiltonian system. Although primarily of theoretical interest, the transfomation does have application to the stability analysis of rotating systems.

References

[1] M. Kaplan, *Modern Spacecraft Dynamics and Control.* New York: John Wiley & Sons, 1976.

[2] R. Bracewell and O. Garriot, "Rotation of Artificial Earth Satellites," *Nature*, vol. 182, no. 4638, pp. 760–762, 1958.

[3] W. Thomson and G. Reiter, "Attitude Drift of Space Vehicles," *The Journal of the Astronautical Sciences*, vol. 7, no. 2, pp. 29–34, 1960.

[4] R. Pringle, "On the Stability of a Body with Connected Moving Parts," *AIAA Journal*, vol. 4, no. 8, pp. 1395–1404, 1966.

[5] L. Meirovitch and H. Nelson, "On the High-Spin Motion of a Satellite Containing Elastic Parts," *Journal of Spacecraft and Rockets*, vol. 3, no. 11, pp. 1597–1602, 1966.

[6] L. Dokuchaev, "Plotting the Regions of Stable Rotation of a Space Vehicle with Elastic Rods," *Cosmic Research*, vol. 7, no. 4, pp. 484–494, 1969.

[7] P. Hughes and J. Fung, "Liapunov Stability of Spinning Satellites with Long Flexible Appendages," *Celestial Mechanics*, vol. 4, pp. 295–308, 1971.

[8] K. Kaza and R. Kvaternik, "Nonlinear Flap-Lag-Axial Equations of a Rotating Beam," *AIAA Journal*, vol. 15, no. 6, pp. 871–874, 1977.

[9] H. Nelson and L. Meirovitch, "Stability of a Nonsymmetrical Satellite with Elastically Connected Moving Parts," *The Journal of the Astronautical Sciences*, vol. 13, no. 6, pp. 226–234, 1966.

[10] L. Meirovitch, "Stability of a Spinning Body Containing Elastic Parts via Liapunov's Direct Method," *AIAA Journal*, vol. 8, no. 7, pp. 1193–1200, 1970.

[11] L. Meirovitch, "A Method for the Liapunov Stability Analysis of Force-Free Dynamical Systems," *AIAA Journal*, vol. 9, no. 9, pp. 1695–1701, 1971.

[12] L. Meirovitch and R. Calico, "Stability of Motion of Force-Free Spinning Satellites with Flexible Appendages," *Journal of Spacecraft and Rockets*, vol. 9, no. 4, pp. 237–245, 1972.

[13] L. Meirovitch and R. Calico, "A Comparative Study of Stability Methods for Flexible Satellites," *AIAA Journal*, vol. 11, no. 1, pp. 91–98, 1973.

[14] D. Teixeira-Filho and T. Kane, "Spin Stability of Torque-Free Systems–Part I," *AIAA Journal*, vol. 11, no. 6, pp. 862–867, 1973.

[15] D. Teixeira-Filho and T. Kane, "Spin Stability of Torque-Free Systems–Part II," *AIAA Journal*, vol. 11, no. 6, pp. 868–870, 1973.

[16] D. Levinson and T. Kane, "Spin Stability of a Satellite Equipped with Four Booms," *Journal of Spacecraft and Rockets*, vol. 13, no. 4, pp. 208–213, 1976.

[17] V. Rumiantsev, "Steady-Motion Stability of Free Systems," *Cosmic Research*, vol. 6, no. 5, pp. 533–537, 1968.

[18] V. Rumiantsev, "On the Motion and Stability of an Elastic Body with a Cavity Containing Fluid," *Journal of Applied Mathematics and Mechanics*, vol. 33, no. 6, pp. 927–937, 1969.

[19] V. Rubanovskii, "On the Stability of Certain Motions of a Rigid Body with Elastic Rods and Liquid," *Journal of Applied Mathematics and Mechanics*, vol. 36, no. 1, pp. 38–53, 1972.

[20] D. Brown and A. Schlack, "Stability of a Spinning Body Containing an Elastic Membrane via Liapunov's Direct Method," *AIAA Journal*, vol. 10, no. 10, pp. 1286–1290, 1972.

[21] F. Barbera and P. Likins, "Liapunov Stability Analysis of Spinning Flexible Spacecraft," *AIAA Journal*, vol. 11, no. 4, pp. 457–466, 1973.

[22] L. Meirovitch, "Liapunov Stability Analysis of Hybrid Dynamical Systems in the Neighborhood of Nontrivial Equilibrium," *AIAA Journal*, vol. 12, no. 7, pp. 889–898, 1974.

[23] P. Willems, "Stability Analysis of Dynamic Systems with Couplings and Integrals of Motion," *Journal of Applied Mathematics and Mechanics*, vol. 38, no. 4, pp. 565–573, 1974.

[24] J. Samin and P. Willems, "On the Attitude Dynamics of Spinning Deformable Systems," *AIAA Journal*, vol. 13, no. 6, pp. 812–817, 1975.

[25] D. Holm, J. Marsden, T. Ratiu, and W. A., "Stabilty of Rigid Body Motion using the Energy-Casimir Method," *Contemporary Mathematics*, vol. 28, pp. 15–23, 1984.

[26] P. Krishnaprasad and J. Marsden, "Hamiltonian Structures and Stability for Rigid Bodies with Flexible Attachments," *Archives for Rational Mechanics and Analysis*, vol. 98, no. 1, pp. 71–93, 1987.

[27] J. Baillieul and M. Levi, "Rotational Elastic Dynamics," *Physica D*, vol. 27, pp. 43–62, 1987.

[28] J. Simo, T. Posbergh, and J. Marsden, "Stability of Coupled Rigid Body and Geometrically Exact Rods: Block Diagonlization and the Energy-Momentum Method," *Physics Reports*, vol. 193, no. 6, pp. 279–360, 1990.

[29] A. Bloch, "Stability Analysis of a Rotating Flexible System," *Acta Applicandae Mathematicae*, vol. 15, pp. 211–234, 1989.

[30] Y. Liu, "The Stability of the Permanent Rotation of a Free Multibody System," *Acta Mechanica*, vol. 79, pp. 43–51, 1989.

[31] B. de Veubeke, "The Dynamics of Flexible Bodies," *International Journal of Engineering Sciences*, vol. 14, pp. 895–913, 1976.

[32] J. Canavin and P. Likins, "Floating Reference Frames for Flexible Spacecraft," *Journal of Spacecraft and Rockets*, vol. 14, no. 12, pp. 724–732, 1977.

[33] R. Cavin and A. Dusto, "Hamilton's Principle: Finite-Element Methods and Flexible Body Dynamics," *AIAA Journal*, vol. 15, no. 12, pp. 1684–1690, 1977.

[34] T. McDonough, "Formulation of the Global Equations of Motion of a Deformable Body," *AIAA Journal*, vol. 14, no. 5, pp. 656–660, 1976.

[35] P. Likins, "Modal Method for Analysis of Free Rotations of Spacecraft," *AIAA Journal*, vol. 5, no. 7, pp. 1304–1308, 1967.

[36] R. Laskin, P. Likins, and R. Longman, "Dynamical Equations of a Free-Free Beam Subject to Large Overall Motions," *The Journal of the Astronautical Sciences*, vol. 31, no. 4, pp. 507–527, 1983.

[37] T. Kane and D. Levinson, *Dynamics: Theory and Applications*. New York: McGraw-Hill, 1985.

[38] T. Kane, R. Ryan, and A. Banerjee, "Dynamics of a Cantilevered Beam Attached to a Moving Base," *Journal of Guidance, Control, and Dynamics*, vol. 10, no. 2, pp. 139–151, 1987.

[39] T. Kane, R. Ryan, and A. Banerjee, "Reply by Authors to K.W. London," *Journal of Guidance, Control, and Dynamics*, vol. 12, no. 2, pp. 286–287, 1989.

[40] E. Christensen and S. Lee, "Nonlinear Finite Element Modeling of the Dynamics of Unrestrained Flexible Structures," *Computers and Structures*, vol. 23, no. 6, pp. 819–829, 1986.

[41] J. Simo and L. Vu-Quoc, "On the Dynamics of Flexible Beams Under Large Overall Motions–The Plane Case: Part I," *Journal of Applied Mechanics*, vol. 53, pp. 849–854, 1986.

[42] J. Simo and L. Vu-Quoc, "On the Dynamics of Flexible Beams Under Large Overall Motions–The Plane Case: Part II," *Journal of Applied Mechanics*, vol. 53, pp. 855–863, 1986.

[43] J. Simo and L. Vu-Quoc, "On the Dynamics in Space of Rods Undergoing Large Motions–A Geometrically Exact Approach," *Computer Methods in Applied Mechanics and Engineering*, vol. 66, pp. 125–161, 1988.

[44] H. Yoo, R. Ryan, and R. Scott, "Use of Assumed Modes in Equations Governing Large-Displacement Elastodynamic Plate Behavior," in *Proceedings of the 1988 American Control Conference*, (Atlanta, Georgia), pp. 170–176, June 1988.

[45] B. Chang and A. Shabana, "Total Lagrangian Formulation for the Large Displacement Analysis of Rectangular Plates," *International Journal for Numerical Methods in Engineering*, vol. 29, pp. 73–103, 1990.

[46] V. Omprakash and V. Ramamurti, "Coupled Free Vibration Characteristics of Rotating Tuned Bladed Disk Systems," *Journal of Sound and Vibration*, vol. 140, no. 3, pp. 413–435, 1990.

[47] A. Banerjee and T. Kane, "Dynamics of a Plate in Large Overall Motion," *Journal of Applied Mechanics*, vol. 56, pp. 887–892, 1989.

[48] L. Peterson, "Nonlinear Finite Element Simulation of the Large Angle Motion of Flexible Bodies," in *Proceedings of the AIAA/ASME/ASCE/AHS 30th Structures, Structural Dynamics and Materials Conference*, (Mobile, Alabama), April 1989.

[49] T. Zeiler and C. Buttrill, "Dynamic Analysis of an Unrestrained, Rotating Structure Through Nonlinear Simulation," in *Proceedings of the AIAA/ASME/ ASCE/AHS 27th Structures, Structural Dynamics and Materials Conference*, (Washington, D.C.), pp. 167–177, April 1988.

[50] K. Banerjee and J. Dickens, "Dynamics of an Arbitrary Flexible Body in Large Rotation and Translation," *Journal of Guidance, Control, and Dynamics*, vol. 13, no. 2, pp. 221–227, 1990.

[51] D. Segalman and C. Dohrmann, "Dynamics of Rotating Flexible Structures by a Method of Quadratic Modes," Tech. Rep. SAND90–2737, Sandia National Laboratories, Albuquerque, New Mexico, December 1990.

[52] E. Whittaker, *A Treatise on the Analytical Dynamics of Particles and Rigid Bodies.* London: Cambridge University Press, 1937.

[53] T. Kane, P. Likins, and D. Levinson, *Spacecraft Dynamics.* New York: McGraw-Hill, 1983.

[54] V. Arnold, ed., *Dynamical Systems III.* New York: Springer-Verlag, 1988.

[55] A. Giorgilli, "A Computer Program for Integrals of Motion," *Computer Physics Communications*, vol. 16, pp. 331–343, 1979.

[56] L. Meirovitch, *Methods of Analytical Dynamics.* New York: McGraw-Hill, 1970.

[57] F. Gustavson, "On Constructing Formal Integrals of a Hamiltonian System Near an Equilibrium Point," *The Astronomical Journal*, vol. 71, no. 8, pp. 670–686, 1966.

[58] A. Lichtenberg and M. Lieberman, *Regular and Stochastic Motion.* New York: Springer-Verlag, 1983.

[59] M. Hénon and C. Heiles, "The Applicability of the Third Integral of Motion: Some Numerical Experiments," *The Astronomical Journal*, vol. 69, no. 1, pp. 73–79, 1964.

[60] C. Siegel and J. Moser, *Lectures on Celestial Mechanics.* New York: Springer-Verlag, 1971.

[61] A. Bruno, "On the Question of Stability in a Hamiltonian System," in *Dynamical Systems and Ergodic Theory*, vol. 23, pp. 361–365, Polish Scientific Publishers Warszawa, 1989.

[62] A. Celletti and A. Giorgilli, "On the Stability of the Lagrangian Points in the Spatial Restricted Problem of Three Bodies," *Celestial Mechanics and Dynamical Astronomy*, vol. 50, pp. 31–58, 1991.

[63] A. Sokol'skii, "On the Stability of an Autonomous Hamiltonian System with Two Degrees of Freedom in the Case of Equal Frequencies," *Journal of Applied Mathematics and Mechanics*, vol. 38, no. 5, pp. 741–749, 1974.

[64] L. Khazin, "On the Stability of Hamiltonian Systems in the Presence of Resonances," *Journal of Applied Mathematics and Mechanics*, vol. 35, no. 3, pp. 384–391, 1971.

[65] A. Markeev, "Stability of a Canonical system with two Degrees of Freedom in the Presence of Resonance," *Journal of Applied Mathematics and Mechanics*, vol. 32, no. 4, pp. 766–772, 1968.

[66] Hibbitt, Karlsson, and Sorenson, Inc., *ABAQUS User's Manual.*

Appendix A
Example System

The system used in the examples of Chapter 3 is shown in Figure A.1 and described below. A particle of mass m is connected to a carrier body, B, of mass M by a spring. Unit vectors $\mathbf{b}_1$, $\mathbf{b}_2$, $\mathbf{b}_3$ fixed in B are parallel to the central principal axes of B. The position of the particle relative to the mass center of B is given by

$$\mathbf{p} = (h - lx_2)\mathbf{b}_1 \tag{A.1}$$

where x_2 is a generalized coordinate which is zero when the spring is unstretched. The constant l in Eq. (A.1) is a given characteristic length, e.g., the dimension h if $h \neq 0$.

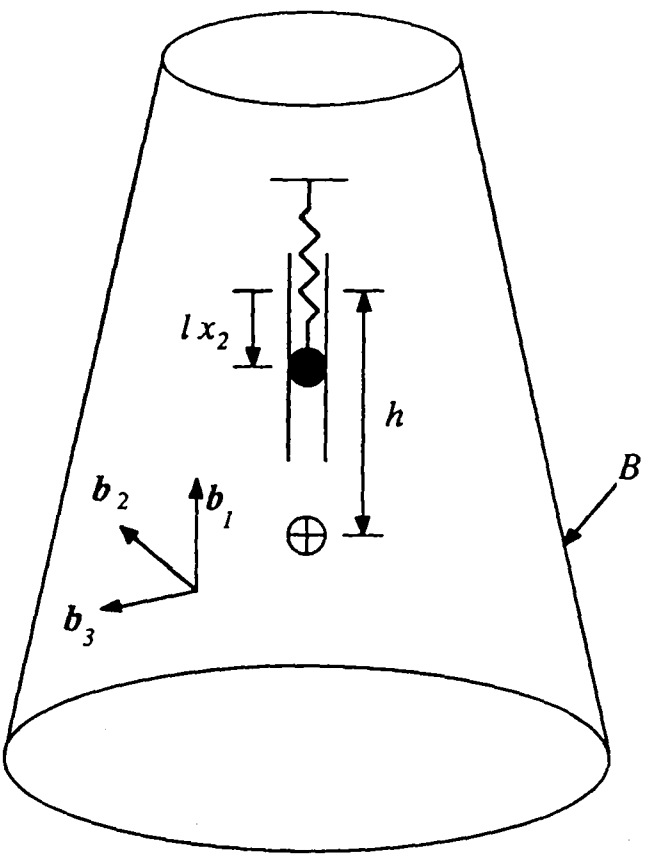

Figure A.1. Sketch of the system used in the examples of Chapter 3.

The central principal moments of inertia of B are denoted by I_1, I_2 and I_3. The angular velocity of B in an inertial frame is expressed as

$$\boldsymbol{\omega} = \omega_1 \mathbf{b}_1 + \omega_2 \mathbf{b}_2 + \omega_3 \mathbf{b}_3 \tag{A.2}$$

The tension in the spring connecting the particle to B is given by

$$f = k(lx_2) + k_3(lx_2)^3 \tag{A.3}$$

It can be shown that the kinetic energy, T, and strain energy, U, of the system are given by

$$T = \frac{1}{2}\left\{I_1\omega_1^2 + [I_2 + \hat{m}l^2(\beta - x_2)^2]\omega_2^2 + [I_3 + \hat{m}l^2(\beta - x_2)^2]\omega_3^2 + \hat{m}l^2\dot{x}_2^2\right\} \tag{A.4}$$

and

$$U = \frac{1}{2}kl^2x_2^2 + \frac{1}{4}k_3l^4x_2^4 \tag{A.5}$$

where

$$\alpha = \frac{m}{M+m} \tag{A.6}$$

$$\beta = h/l \tag{A.7}$$

$$\hat{m} = m(1-\alpha) \tag{A.8}$$

Applying the procedure given in 2.2, one obtains

$$\begin{aligned} G = \frac{1}{2}\Bigg\{1 + \left(\frac{I_1/\bar{I}_2}{1 + \frac{\hat{m}l^2}{\bar{I}_2}f(x_2)} - 1\right)m_2^2 + \frac{I_1}{\hat{m}l^2}y_2^2 + \\ \left(\frac{I_1/\bar{I}_3}{1 + \frac{\hat{m}l^2}{\bar{I}_3}f(x_2)} - 1\right)m_3^2 + \frac{kl^2}{I_1\Omega^2}x_2^2 + 2a_5x_2^4\Bigg\} \end{aligned} \tag{A.9}$$

and

$$\begin{aligned} H = \frac{1}{2}\Bigg\{1 + \left(\frac{I_1/\bar{I}_2}{1 + \frac{\hat{m}l^2}{\bar{I}_2}f(x_2)} - 1\right)y_1^2\left(1 - \frac{x_1^2+y_1^2}{4}\right) + \frac{I_1}{\hat{m}l^2}y_2^2 + \\ \left(\frac{I_1/\bar{I}_3}{1 + \frac{\hat{m}l^2}{\bar{I}_3}f(x_2)} - 1\right)x_1^2\left(1 - \frac{x_1^2+y_1^2}{4}\right) + \frac{kl^2}{I_1\Omega^2}x_2^2 + 2a_5x_2^4\Bigg\} \end{aligned} \tag{A.10}$$

where

$$\bar{I}_2 = I_2 + \hat{m}l^2\beta^2 \tag{A.11}$$

$$\bar{I}_3 = I_3 + \hat{m}l^2\beta^2 \tag{A.12}$$

$$a_5 = k_3l^4/4 \tag{A.13}$$

$$f(x_2) = -2\beta x_2 + x_2^2 \tag{A.14}$$

As an aside, it is noted that the Hamiltonian given by Eq. (A.10) is integrable if $\bar{I}_2 = \bar{I}_3$ since $H = H(x_1^2 + y_1^2, x_2, y_2)$.

Distribution:

Professor Henry Busby (2)
Department of Mechanical Engineering
The Ohio State University
Columbus, OH 43210

Professor Gary Kinzel
Department of Mechanical Engineering
The Ohio State University
Columbus, OH 43210

Professor Chia-Hsiang Menq
Department of Mechanical Engineering
The Ohio State University
Columbus, OH 43210

Professor Rajendra Singh
Department of Mechanical Engineering
The Ohio State University
Columbus, OH 43210

Professor Anthony Bloch
Mathematics Department
The Ohio State University
Columbus, OH 43210

Gary Gray
University of Wisconsin Madison
Department of Engineering Mechanics
1415 Johnson Drive
Madison, WI 53706

Sandia Internal:

1425 J. H. Biffle
1434 D. R. Martinez
1434 C. R. Dohrmann (15)
1434 D. W. Lobitz
1434 J. R. Red-Horse
1434 D. J. Segalman
1561 H. S. Morgan
1561 J. G. Arguello
1562 R. K. Thomas
1562 F. J. Mello
6214 P. S. Veers
9811 R. D. Robinett
7141 Technical Library (5)
7151 Technical Publications
7613-2 Doc. Processing for DOE/OSTI (10)
8523-2 Central Technical Files

THIS PAGE INTENTIONALLY LEFT BLANK